Development of a Minimally Invasive Sliding Hip Screw

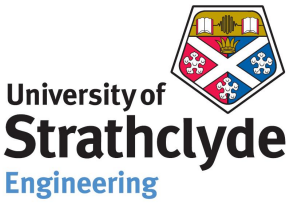

Daniel Gilroy

Department of Biomedical Engineering

University of Strathclyde

A thesis submitted for the degree of

Engineering Doctorate in Medical Devices

November 2015

Declaration

This thesis is the result of the authors original research. It has been composed by the author and has not been previously submitted for examination which has led to the award of a degree.

Date: 27/11/15

Signed: 

Abstract

Extracapsular proximal femoral fractures are becoming an increasingly common injury as both the population and average life expectancy increase. Currently sliding hip screws (SHS) are used to treat these fractures; however the surgery to implant these devices causes significant soft tissue damage. This results in long healing times which puts a large financial burden on the health service. Development of an SHS which can be implanted through a minimally invasive technique may reduce healing time for the patients as well as the cost of treating these patients. This study details the development of a new device the minimally invasive Sliding hip screw (MISHS).

A finite element (FE) model was developed in order to allow both the current device to be studied and for new designs to be evaluated. Mechanical testing was carried out on the current device in order to validate the model. The results showed that the model behaved similarly to the mechanical test and therefore valid conclusions could be drawn from it.

A design process was carried out to evaluate each of the proposed designs, three suitable designs were found and each of these were modelled in order to determine which one should be taken to the prototyping stage.

Three prototypes of the chosen design were manufactured for mechanical testing. Both static and cyclic fatigue tests were carried out in order to evaluate the performance of the new design. The results show that the MISHS performed similarly to the SHS in testing. With further development the MISHS has the potential to significantly improve the treatment of extracapsular proximal femoral fractures.

Acknowledgements

I would like to acknowledge both my supervisors, Dr Philip Riches and Dr Marcus Wheel for the help which they have given me throughout this project and my surgical advisor, Odhrán Murray, whose idea initiated this project an whose expertise and knowledge were invaluable resources throughout.

I would also like to thank James Ure and Alan Jappy who gave me advise throughout the development of the finite element model.

Contents

List of Figures

List of Tables

Acronyms

AP anteroposterior.

CAD computer-aided design.

CNC computerized numerical control.

DCS dynamic condylar screw.

DHS dynamic hip screw.

EDM electrical discharge machining.

FE finite element.

FEA finite element analysis.

HPC high-performance computing.

IM intramedullary.

IMHS intramedullary hip screw.

IMN intramedullary nail.

MI minimally invasive.

MIDHS minimally invasive dynamic hip screw.

MISHS minimally invasive sliding hip screw.

MISS minimally invasive sliding screw.

ML mediolateral.

PCCP percutaneous compression plate.

PCF polyurethane cellular foam.

PFN proximal femoral nail.

SFRE short fibre re-enforced epoxy.

SHS sliding hip screw.

SR strain ratio.

Notation

E Young's Modulus.

I Second moment of area.

k Stiffness of Beam.

L Length of beam.

ν Poisson's Ratio.

P Load.

σ Stress.

w Displacement of beam in 3-point bending.

The SI system of units was adopted for this thesis.

1

Introduction

As the average life expectancy of the population has increased, the incidence of intertrochanteric hip fracture has also increased significantly, with the number of fractures expected to reach 4.5 million worldwide by 2050 (Gullberg et al., 1997). These fractures carry a high risk of mortality and morbidity and have high healthcare costs (Haentjens et al., 2005). In younger active patients it is desirable to avoid a hip arthroplasty; repair of the fracture is therefore the preferred option with these patients when possible. There are several methods used to fix the femoral head to the femur, the SHS is one such device which is commonly used for extracapsular hip fractures and has been shown to produce excellent results (Willoughby, 2005; Chirodian et al., 2005). The insertion of a SHS requires a large incision to be made, between 100-150mm long beginning at the greater trochanter and continuing distally down the lateral side of the thigh (Wong et al., 2009). This causes substantial damage to the soft tissue and significant blood loss which can result in lengthy hospital stays and reduce the chance of returning to pre-fracture levels of activity.

In recent years there has been a trend towards developing MI surgery techniques in orthopaedics. MI surgery has been shown to reduce blood loss and soft tissue damage improving the patient's recovery time (DiGioia et al., 2003; Hata et al., 2001). A clinical trial has shown that a MI technique for fixation of an SHS reduced blood loss and pain in patients compared to the standard surgical technique (Wong et al., 2009). With this in mind it is our aim to develop a minimally invasive sliding hip screw (MISHS), that is specialised for MI surgery, this would ease the surgical process and allow MI surgery to become more common thus reducing the cost to the healthcare system.

2

Literature Review

This chapter aims to provide the background information that must be understood in order to design and develop an new orthopaedic implant. It will first discuss the anatomy of the femur and classification of proximal femoral fractures. The fracture healing process will then be discussed along with the history of treatment methods and the development of the sliding hip screw (SHS) device, this will give an understanding of why the current devices are designed the way they are and which features must be maintained in any new design. It will then cover the current devices used for treatment, including comparative clinical studies and real world usage statistics taken from national registers. It will also discuss the advantages of minimally invasive (MI) surgical techniques and previous attempts to design MI devices for the treatment of proximal femoral fractures. It is important to show that the SHS is an effective treatment, which justifies the development of a new device, and why previously designed MI devices have not been commonly used, which will aid in development of the device. Finally the finite element (FE) modelling of bone and implants will be discussed, finite element analysis (FEA) will be used to model new designs and compare them to the current device, it is important to understand the issues with modelling implants in bone.

2.1 Anatomy

2.1.1 Bone Structure

Bone is a complex biological material and can be described at varying levels of complexity. The macrostructure of a long bone can be seen in Figure 2.1. The bone can

be divided into 3 regions, the proximal and distal epiphyses at either end and the shaft known as the diaphysis, the structure of bone varies between these areas. The diaphysis is constructed of cortical (compact) bone which forms a hollow cylinder the centre of which is known as the medullary cavity, this cavity contains the bone marrow. The epiphyses consist of cancellous (spongy bone) covered in a layer of cortical bone. There are two tissues which line the bones surfaces, the periosteum lines the bones outer surface and the endosteum lines the medullary cavity.

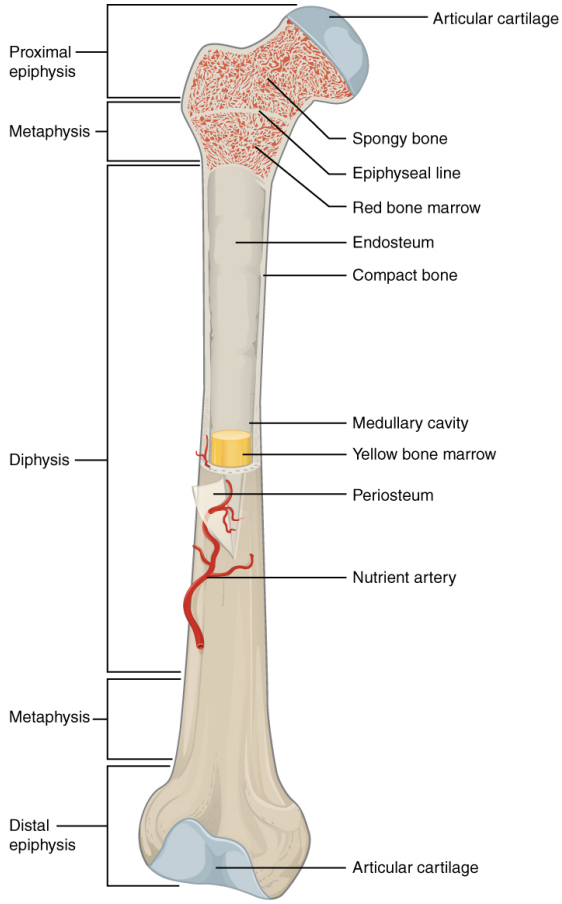

by OpenStax College 2013 – Anatomy & Physiology, Connexions Web site. http://cnx.org/content/col11496/1.6/ – CC BY 3.0

Figure 2.1: Macro structure of long bones.

The micro structure of the two bone types, compact and cancellous vary significantly. Cancellous bone is constructed from a series of interconnected struts known as trabeculae (Figure 2.2). The trabeculae form a mesh-like structure which is aligned in

such a way that it efficiently transfers the load from the joint surface to the diaphysis.

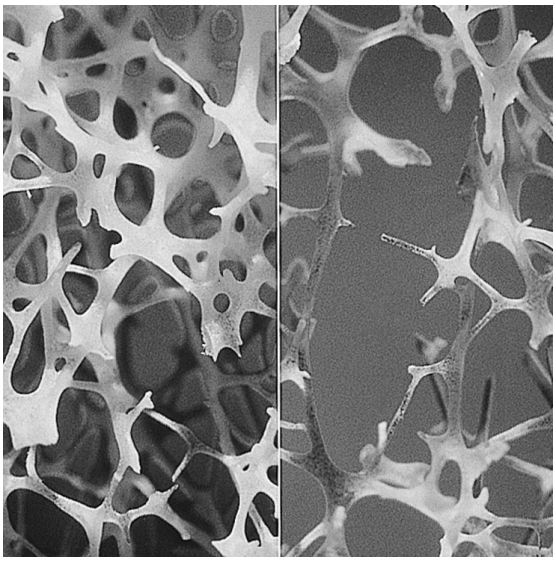

by Gtirouflet 2012 – https://commons.wikimedia.org – CC BY-SA 3.0

Figure 2.2: Trabeculae in the structure of cancellous bone.

Cortical bone is constructed from structures known as osteons (Figure 2.3). Osteons are constructed from a series of concentric lamellae centred around the haversian canal which contains a capillary.

There are three main types of bone cells, osteoblasts which produce bone, osteoclasts which break down bone and osteocytes which form a network of cells throughout bone. Osteoblasts that become trapped in bone transform into osteocytes.

2.1.2 Hip Joint

The acetabulofemoral or hip joint is a synovial joint between the femoral head and acetabulum of the pelvis. The joint allows motion in three axes and is stabilized by three extracapsular ligaments, the iliofemoral, ischiofemoral, and pubofemoral, which prevent hyperextension, excessive medial rotation, and excessive abduction and medial rotation respectively. An intra capsular ligament, the ligamentum teres, is also present in the joint. It has been suggested that the ligamentum teres has little mechanical function past childhood (Tan and Wong, 1990).

Movement of the joint is actuated by a complex system of muscles shown if Figures 2.4 to 2.6

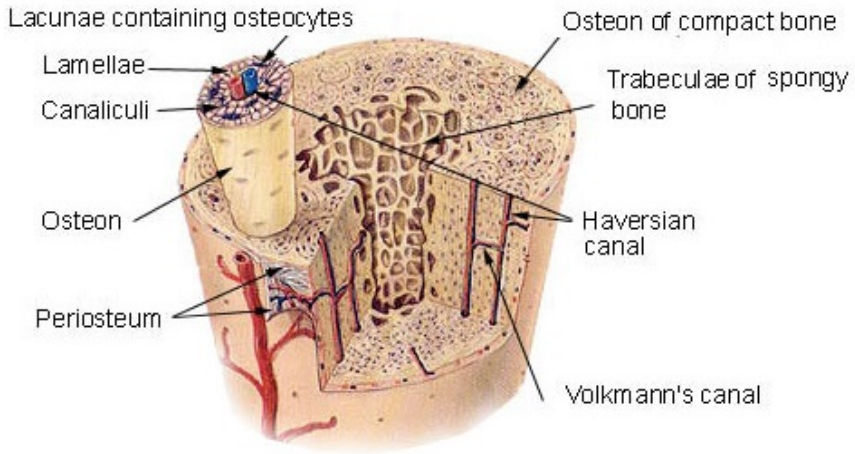

Taken from http://training.seer.cancer.gov, public domain

Figure 2.3: Structure of bone.

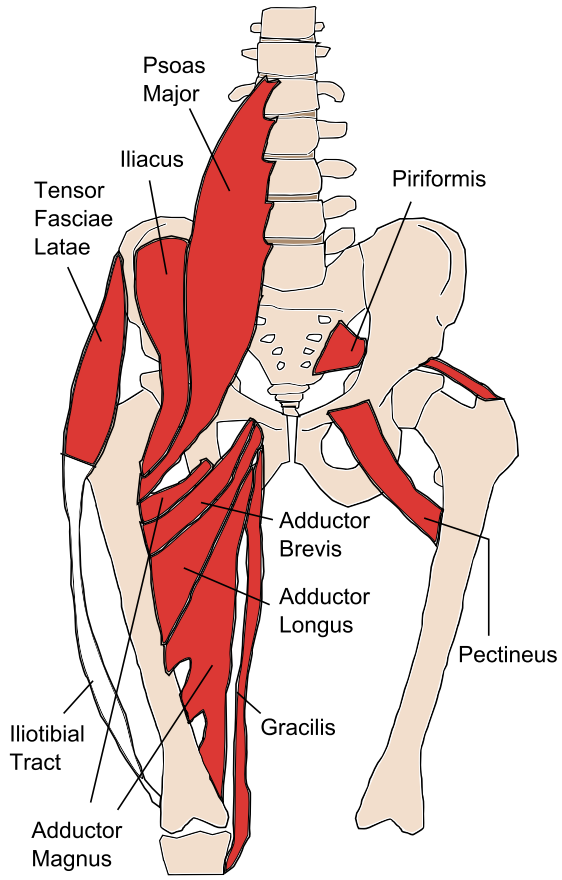

Figure 2.4: Anterior view of the muscles of the hip joint.

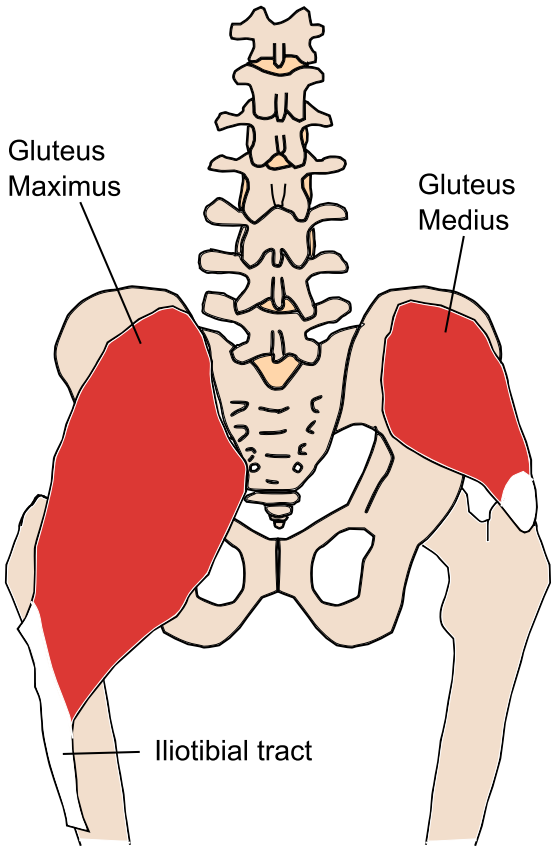

Figure 2.5: Posterior view of the muscles of the hip joint.

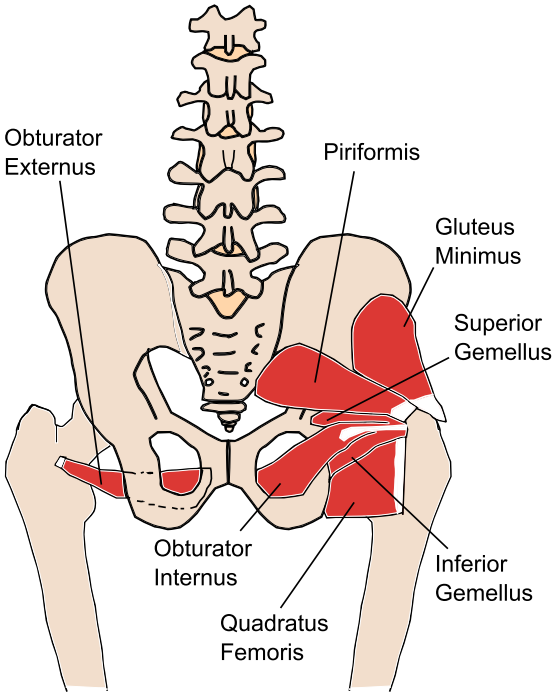

Figure 2.6: Posterior view of the muscles of the hip joint.

2.1.3 Femur

A posterior view of the proximal end of the femur is shown in Figure 2.7. The articular surface of the hip joint is located on the femoral head at the superior medial end of the femur. The head connects to the trochanteric region via the femoral neck. The trochanteric region contains two protrusions, the greater trochanter on the superior lateral side, which is the insertion point for both the gluteus medius and minimus, and the lesser trochanter, located on the inferior medial posterior side, which is the insertion point for the iliopsoas.

The linea aspera is a ridge that runs vertically on the posterior side of the femoral shaft, the origin of the short head of the biceps femoris is located on the lower half of the linea aspera,the insertion points of the pectineous, adductor longus and adductor magnus are also located on the linea aspera. The linea aspera diverges at the proximal end to form the gluteal tuberosity on the lateral side and the pectineal line on the medial which continues superiorly to join the lesser trochanter. The gluteal tuberosity is the insertion point for the gluteus maximus, which also connects to the iliotibial tract. The pectineal line is the insertion point for the adductor brevis.

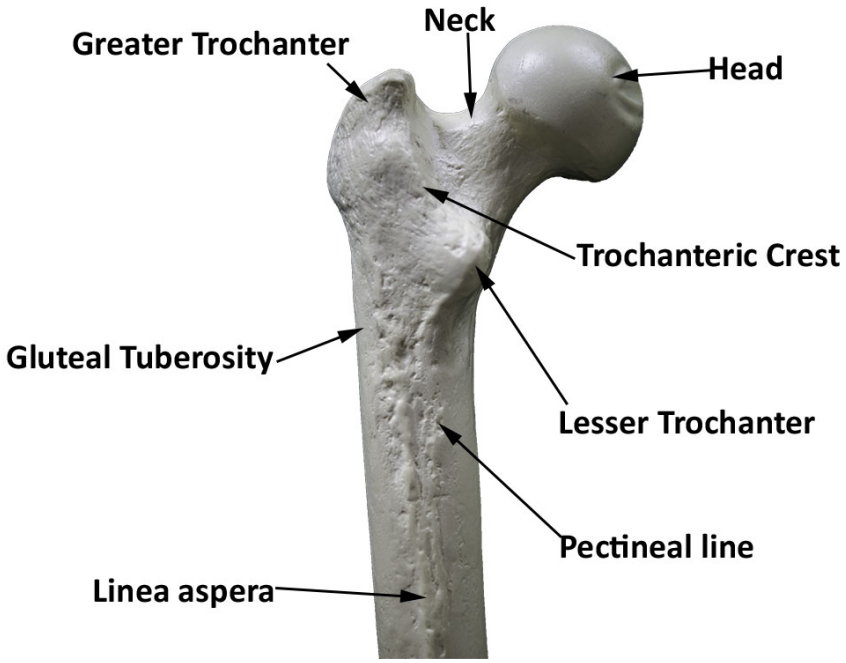

Figure 2.7: Anatomy of the proximal femur.

2.2 Hip Fractures

2.2.1 Classification

Hip fracture is a term generally used to describe any fracture of the proximal end of the femur, these can generally be grouped into two categories, intracapsular and extracapsular. Intracapsular proximal femoral fractures are within the the joint capsule, these include fractures of the femoral head and articular surface. Extracapsular proximal femoral fractures are outwith the joint capsule, these include fractures of the femoral neck and fractures of the trochanteric area, including pertrochanteric and intertrochanteric fractures.

Figure 2.8 shows the AO classification of extracapsular proximal femoral fractures. This thesis will use the AO classification to describe fractures, however many older papers use the Jensen (1980a) modification Evans (1949) classification and this may lead to some confusion during this review. Figure 2.9 shows the Evans classification of intertrochanteric fractures. It can be seen that Evans' definition of an intertrochanteric fracture is defined in AO classification system as a pertrochanteric fracture. Also what is defined as an intertrochanteric fracture in the AO classification is often called a reverse

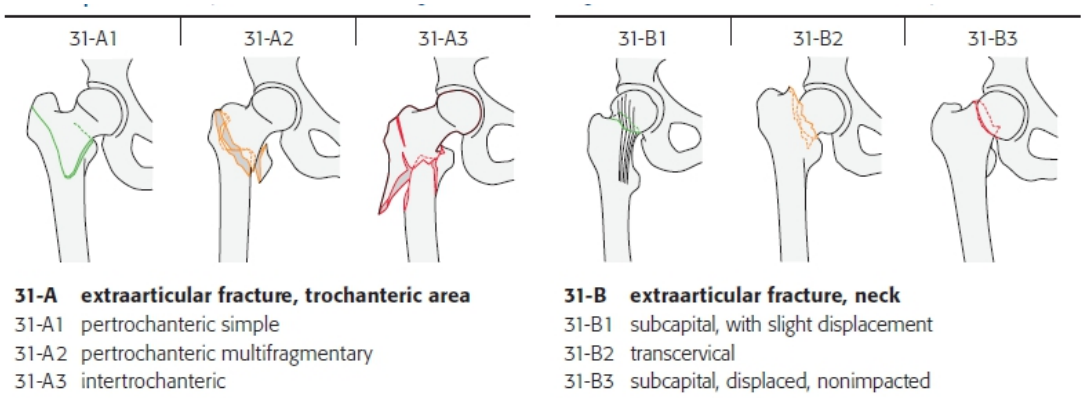

Figure 2.8: AO classification of extracapsular proximal femoral fractures (Source: AO Surgery Reference, www.aosurgery.org).

oblique fracture by those using the Evans classification. Therefore to avoid confusion all references to fracture classification have been expressed in the AO classification system when discussed in the literature review.

2.2.2 Occurrence

As the average life expectancy of the population has increased, the incidence of hip fracture has also increased significantly, with the number of fractures expected to reach 4.5 million worldwide by 2050 (Gullberg et al., 1997). These fractures carry a high risk of mortality and morbidity and have high healthcare costs (Haentjens et al., 2005).

2.3 Principles of Bone Healing

There are two different types of bone healing known as primary and secondary bone healing.

2.3.1 Secondary Bone Healing

Secondary bone healing, is the healing process seen in nature, it occurs when the fragments are not rigidly fixed and therefore movement can occur between them. After a fracture has occurred damage to the bones blood vessels causes haematoma and haemorrhage to occur. This leads to a thrombosis forming at the fracture ends and the

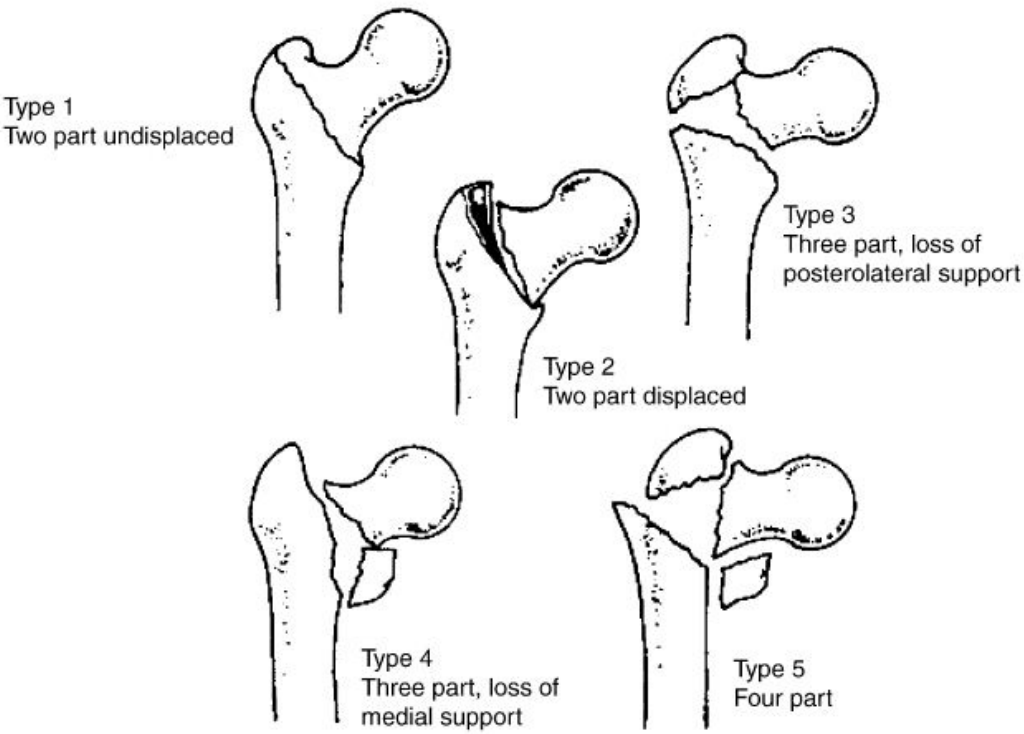

Reprinted from Injury, 36(6) , Chirodian et al., Sliding hip screw fixation of trochanteric hip fractures: Outcome of 1024 procedures, pp.793-800 , Copyright (2005), with permission from Elsevier.

Figure 2.9: Evans classification of intertrochanteric fractures, taken from Chirodian et al. (2005).

initiation of the inflammatory response at the site of the fracture. Granulation tissue is then formed between the fracture fragments and around the fracture site. Collagen fibrils and fibrocartilage begin to be produced at the fracture site providing more stability between the fragments; this structure is known as the procallus. Osteoclasts then begin to absorb the necrotic bone at the fracture surface. The next stage in the healing is the formation of the callus, chondroblasts and osteoblasts produce extracellular matrix of cartilage and woven bone. Osteoprogenitor cells produce osteoid, a substance consisting of mainly hydroxyapatite, which adds rigidity to the callus. When sufficient stability has been gained mineralization of the callus occurs. The healing process then enters the remodelling stage which involves the replacement of the callus with new bone. Mineralized cartilage in the callus is replaced with woven bone which is in turn replaced with lamellar bone. The callus between the fragment ends is replaced with secondary osteons which align parallel to the stress in the bone. The modelling stage then occurs over the next one or more years, during this process cells reshape the bone, this process can occur at the same time as the remodelling phase (Greenbaum and Kanat, 1993). The stages of secondary fracture healing can be seen in Figure 2.10 below.

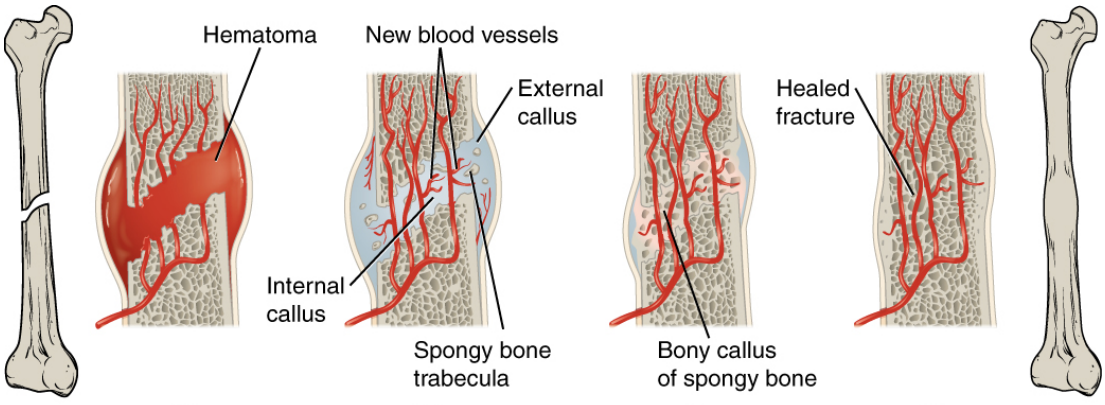

by OpenStax College 2013 – Anatomy & Physiology, Connexions Web site. http://cnx.org/content/col11496/1.6/ – CC BY 3.0

Figure 2.10: Stages in secondary bone healing.

2.3.2 Primary Bone Healing

Primary bone healing occurs when the fragments are held rigidly so that there is no movement at the fracture site. Primary bone healing was therefore not observed until surgeons began to employ internal fixation devices in the treatment of fractures. Primary bone healing does not involve the formation of a callus as seen in secondary bone healing, the bone is healed through a process known as haversian remodelling, which is the same process which continuously remodels healthy bone. There are two separate processes that are described as primary bone healing, contact healing and gap healing. Contact healing occurs when two fragments are held in contact with no motion at the fracture site. A structure known as a cutting cone, which is a complex of osteoclasts, begins to protrude from the haversian canal on one fragment. The cutting cone is closely followed by osteoblasts, as the osteoclasts tunnel into the opposing fragment the osteoblasts produce new bone behind them. Several cutting cones operate simultaneously eventually joining the two bone fragments. Gap healing occurs when there is a small gap between fragments. The gap is filled with haematoma after the fracture, capillaries grow and osteoblasts move into the gap. Woven bone is produced in the fracture site and is later remodelled into the same alignment as the surrounding bone (Greenbaum and Kanat, 1993).

2.3.3 The Effect of Fracture Stability on Bone Healing

It has been suggested that strain at the fracture site stimulates the healing process and that it is therefore advantageous to allow strain across the fracture providing it is less that the level required to rupture the tissues which form between the bone fragments during the healing process.

Claes et al. (1995) studied the effect of fracture instability on fracture healing in sheep. An external fixation device was developed which allowed the authors to vary the allowable axial displacement of the fracture and also to measure the displacement which occurs throughout the healing process. Claes et al. found that when fracture displacement was allowed the callus produced was significantly larger than when the fractures were fully fixed. This can be explained as the body producing more callus tissue in an attempt to stabilise the fracture. It was also observed after 8 weeks that significantly more calcification had occurred in the tissue between the fragments of the

dynamic group compared to the group with fixed fractures. This would suggest that the healing process was occurring more rapidly in the dynamic group.

Grundnes and Reikers (1993) carried out a study on rats which showed that when fixed rigidly fractures heal without the formation of a callus which is the process of primary healing. When the fractures were fixed with axial instability or both axial and rotational instability the fractures heal through secondary healing forming a callus. They also showed that although both groups with instability formed similarly sized calluses, the group with only axial instability was almost twice as strong as the group with axial and rotational instability and also the rigidly fixed group. This would suggest that axial instability allows the fracture to heal better than if it was rigidly fixed and that the shear forces caused by rotational instability are detrimental to the healing process.

2.4 History of Treatment

Treatment of extracapsular hip fractures has developed significantly over the past 70 years. Prior to the 1940s it was considered standard to treat patients conservatively with non operative treatment involving traction. Over time it became apparent, that in order to reduce the rates of mortality and morbidity, it was important to allow the patients to regain mobility as soon as possible and internal fixation was developed to facilitate this. Conservative treatment was the standard treatment for extracapsular hip fractures for many years; there are various different methods of treatment involving different forms of traction and splints. One such method was described by Murray and Frew (1949), the patient was placed in traction for approximately 8.3 weeks for an pertrochanteric fracture, they began exercises around 4.6 weeks and remained in bed for an average of 9.5 weeks after which they were allowed to walk with crutches. Reported mortality rates for conservative vary significantly from 44% reported by Morris (1941) to 10% by Murray and Frew (1949), the latter of which is lower than most internal fixation trials at that time. It is argued by Murray and Frew (1949) that without significant improvement in mortality or function internal fixation was not worth the risk. It was also claimed by Bartels (1939) that internal fixation may lead to coxa vara deformity if the implant was to bend or break. Despite some success with conservative treatments and concerns over the risks of internal fixation, clinical trials involving

implants continued to be carried out. Early fixation devices included nails, screws and wires, a few of which were studied by Cleveland et al. (1947) who conclude that threaded wires do not securely hold the fracture, a simple nail "may secure a good result, but is apt to prove ineffective" (Cleveland et al., 1947) and that screws produce good fixation but can lead to formation of coxa vara deformity. This later point was also made by Putti (1940) who showed how a lag screw without fixation to the femoral shaft can lead to displacement of the femoral shaft as shown in Figure 2.11 below.

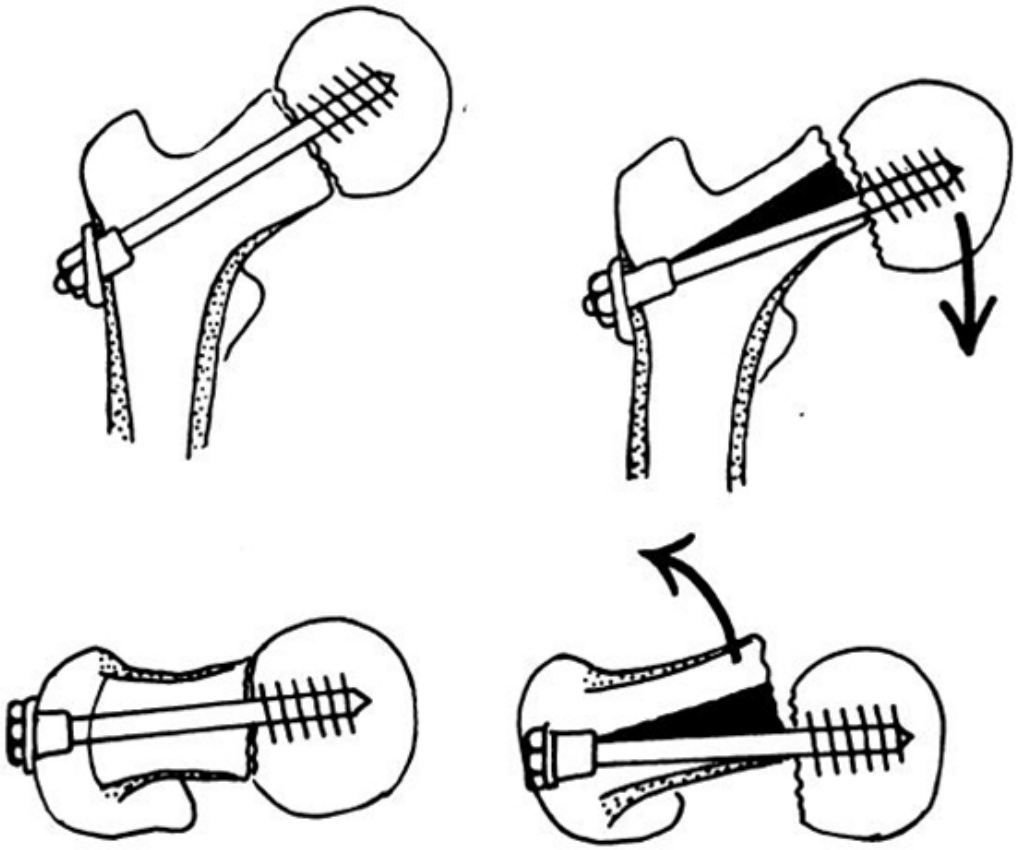

Figure 2.11: Displacement of the femoral head which may occur when a fracture is fixed with a lag screw with no fixation to the femoral shaft (Putti, 1940).

To overcome the problems associated with these simple internal fixation devices more complex implants involving femoral shaft fixation were designed. One of the earliest of these designs was the nail-plate an example of which, the Jewett nail, can be seen in Figure 2.12. There are two types of nail-plate devices, single piece implants

like the Jewett and two piece implants such as the McLaughlin nail-plate in which the nail and plate are separate parts connected by a screw.

Reprinted from Journal of Bone and Joint Surgery (American), 23(4) , Jewett, One-Piece Angle Nail for Trochanteric Fractures, pp.803-810, Copyright (1941), with permission from Wolters Kluwer.

Figure 2.12: Jewett one piece nail-plate device (Jewett, 1941).

In their 1947 paper Cleveland et al. (1947) advocate the use of a single piece nail-plate, claiming that a two piece device would be more likely to break; using the Jewett nail-plate their clinical trial had a mortality rate of 12.6%. However in 1950 Arden and Walley (1950) carried out a trial using a two piece device, the McKee nail-plate, claiming that the surgical procedure was easier than the insertion of a single piece nail and that the flexibility in the joint would decrease the chance of the nail breaking, this trial had a mortality rate of 12.5%. Although both studies had a relatively low mortality rate for the time they both resulted in complications involving broken and bent nails as well as cases of nails penetrating the femoral head. These complications caused coxa vara deformity and pain in many cases. It is suggested that this is due to

reabsorption of bone at the fracture site which leads to "telescoping", as the femoral head, unsupported at the fracture site, is driven onto the nail which breaks through into the acetabulum (Cleveland et al., 1947). In cases where reabsorption occurs but telescoping does not occur the nail is left to support the bending load over the area where no bone is present, this could lead to bending or breaking of the nail. Due to this problem it became apparent that a mechanism to maintain contact between the two fragments must be developed.

One of the first sliding nail devices was developed by Pugh (1955) to overcome the problem of maintain contact between the fragments (Figure 2.13). As the nail is not fixed rigidly to the plate, much of the force applied during weight bearing is supported by the bone at the fracture surfaces, this leads to good contact between the fracture surfaces being maintained at all times. With contact being maintained the load is supported by the bone thus the nail will not break. Pugh's initial trial resulted in no cases of bent nails or penetration of the nail into the joint (Pugh, 1955) and further clinical trials have shown the Pugh nail to be more successful than the simple nail, 22.3% non union with Smith-Petersen nail against 10% with Pugh Nail reported by Fielding et al. (1974).

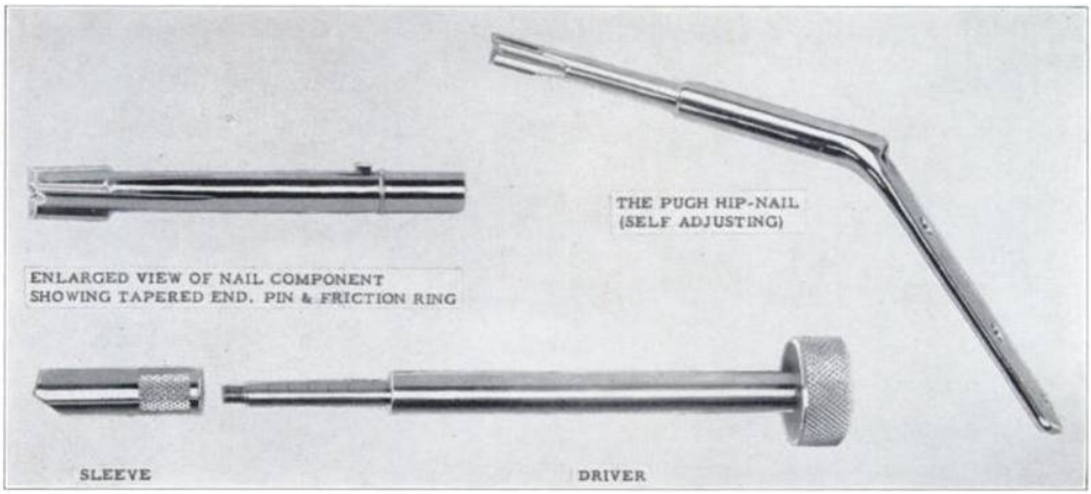

Reprinted from Journal of Bone and Joint Surgery (American), 37(4) , Pugh, A Self-Adjusting Nail-Plate for Fractures About the Hip Joint, pp.1085-1093, Copyright (1955), with permission from Wolters Kluwer.

Figure 2.13: Pugh sliding nail-plate along with some of the tooling used to implant it (Pugh, 1955).

Ernst Pohl developed an alternative to the nail-plate around the same time which Pugh was developing the sliding nail. Pohl's design differed from Pugh's in only one feature; the nail was replaced with a lag screw which he believed would give more secure fixation to the femoral head than a nail. Pohl's gliding screw-plate can be seen in Figure 2.14 below. In their study Schumpelick and Jantzen state:

> "We required the patient to stand once a day, beginning with the first postoperative day, to achieve impaction. Exercises in bed begun on the second to the fourth day and ambulation with full weight-bearing is begun as soon as the patient can tolerate it" (Schumpelick and Jantzen, 1955)

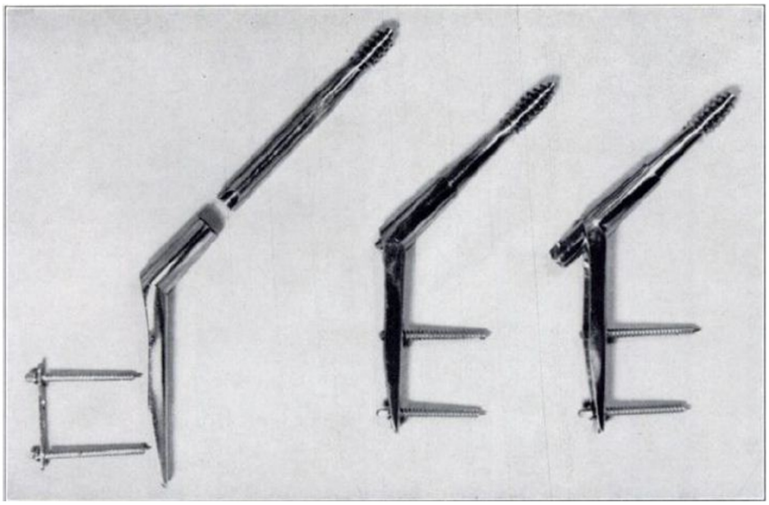

Reprinted from Journal of Bone and Joint Surgery (American), 37(4) , Schumpelick & Jantzen, A New Principle in the Operative Treatment of Trochanteric Fractures of the Femur, pp.693-698 Copyright (1955), with permission from Wolters Kluwer.

Figure 2.14: Pohl gliding screw plate with the screw in various positions (Schumpelick and Jantzen, 1955).

This is a dramatic improvement of in time to get the patient out of bed; patients implanted with the Pugh nail were permitted to walk with no weight bearing on the injured side after two weeks and were not allowed full weight bearing until x-rays showed union of the fracture (Fielding et al., 1974). Union occurred in all cases in Schumpelick and Jantzen study and there were two cases of coxa vara deformity although with only 28 patients significant conclusions cannot be drawn from this, it was claimed that the

two cases of coxa vara were caused by poor screw placement (Schumpelick and Jantzen, 1955). The device which Pohl developed is the basis of what was later to become known as the dynamic hip screw (DHS) or sliding hip screw (SHS) which is one of the most commonly used devices in the treatment of extracapsular hip fractures today.

There have also been attempts to modify the sliding screw device to produce compression on the joint without the need for weight bearing. Charnley et al. (1957) produced a compression hip screw which can be seen in Figure 2.15, this devices provides constant compaction which reduces any shearing between the fragments by stopping them rotating. They claim that eliminating any shearing motion is essential to the prevention of avascular necrosis in fractures of the femoral neck. It is suggested that the Pohl screw cannot stop this rotation of femoral neck fractures and is therefore not suitable for their treatment, however it is stated that they believe the Pohl screw "is likely to be highly satisfactory in trochanteric fractures" (Charnley et al., 1957). The Charnley screw also provides a method with which a doctor can accurately assess the risk of avascular necrosis in the femoral head. As necrosis occurs the screw loses its grip on the femoral head and is pulled out by the spring, as the threads are a known distance apart they can be used as a ruler to measure the distance of screw extrusion in an x-ray. If the screw is being extruded relatively rapidly then avascular necrosis has occurred and action must be taken.

The nail-plates and SHS devices discussed in this chapter are all part of a group known as extramedullary fracture fixation devices: devices which are mounted to the outer surface of bone in order to maintain alignment between the bone fragments. However the extramedullary method was not the only technique developed for internal fixation of fractures. The intramedullary (IM) technique was first developed in Kiel, Germany during the second world war by Gerhard Küntscher and Richard Maatz. The intramedullary (IM) technique was developed, independently from the extramedullary technique, as an alternative to conservative treatment. Rather than screwing plates to the external surface of the bone, fragments are secured in place by inserting a nail into the medullary cavity. Küntscher and Maatz developed IM techniques for the treatment of a number of long bone fractures as described in Kuntscher and Maatz (1945).

IM nails for the treatment of proximal femoral fractures fall into two groups: retro grade or condylocephalic nails which are inserted from the distal end of the femur up towards the proximal end, and ante grade or cephalocondylic nails which are inserted

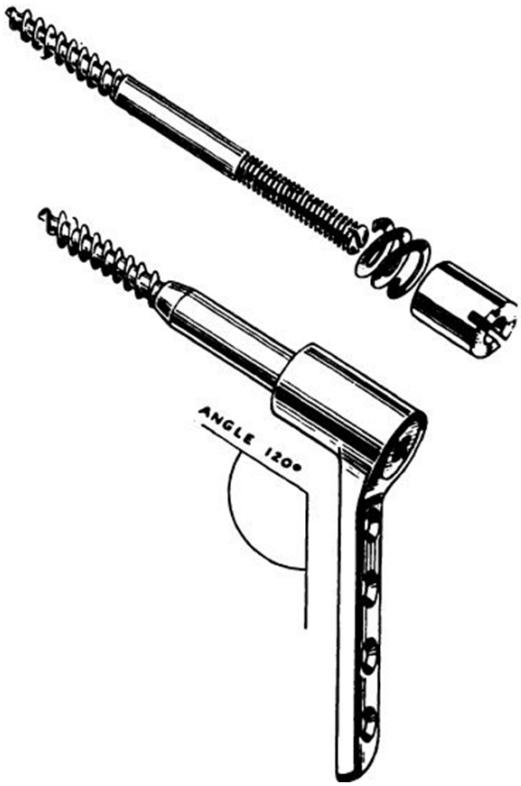

Figure 2.15: Charnley compression screw with exploded detail of components (Charnley et al., 1957).

from the proximal end of the femur downwards. The Küntscher Y-nail is an example of a cephalocondylic nail and is the predecessor to modern day intramedullary nails (IMNs) such as the proximal femoral nail as can be seen in 2.16. Several versions of cephalocondylic nails are available including models with multiple screws for rotational stability or a sliding mechanism like the SHS.

The ender nail is an example of a condylocephalic nail, it is a bent flexible rod which is inserted up from the distal end of the femur across the fracture site and into the femoral head. Several nails are usually inserted to secure the fracture, Figure 2.17 shows the ender nail in use. The ender nail is no longer considered a suitable treatment for proximal femoral fractures in adults.

2.5 Current alternative devices

Although the SHS is seen as the standard device for fixing extracapsular hip fractures there are several alternative devices that many claim are more effective.

2.5.1 Extramedullary devices

Extramedullary devices are a group of implants which include the SHS and nail-plate. These devices have a plate which is fixed to the outside of the bone with screws. Most of the current extramedullary implants are adaptations of the standard SHS. One such device is the percutaneous compression plate (PCCP) developed by Gotfried (2000) (Figure 2.18). The PCCP is also designed to be inserted using MI techniques. The need for MI techniques will be discussed later in this chapter.

Another similar device is the minimally invasive sliding screw (MISS) was developed in France (Figure 2.19), this device functions similarly to a standard SHS however the barrel of the side plate is a separate component allowing the device to be inserted through a small in incision.

The Medoff sliding plate is a more complex design which incorporates a sliding mechanism into the plate section of the devices as well as the the screw. It has been claimed that the Medoff plate has less chance of failing in unstable fractures compared to the SHS (Olsson et al., 1998).

by Bullenwächter 2011 – https://commons.wikimedia.org/ – CC BY 3.0

Figure 2.16: Proximal femoral nail used to treat a fractured femur.

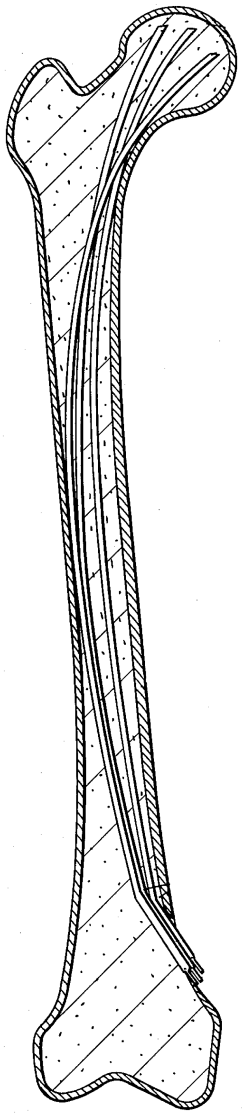

Figure 2.17: Ender nails inserted into fractured femur (Ender and Ender, 1977)

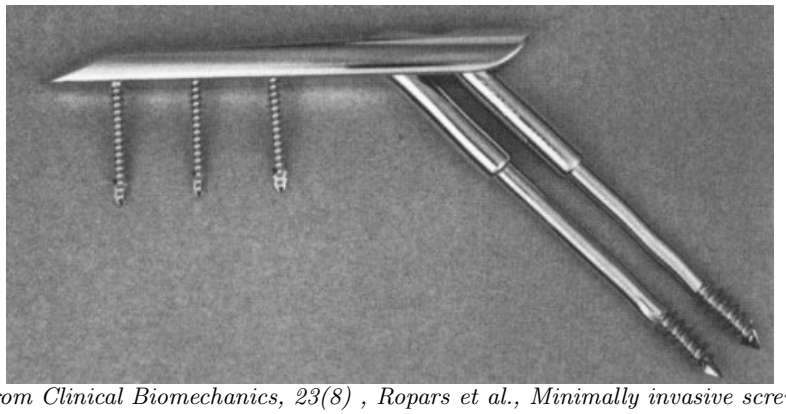

Reprinted from Clinical Biomechanics, 23(8) , Ropars et al., Minimally invasive screw plates for surgery of unstable intertrochanteric femoral fractures: A biomechanical comparative study, pp.1012-1017 , Copyright (2008), with permission from Elsevier.

Figure 2.18: PCCP a MI alternative to the SHS (Ropars et al., 2008).

Reprinted from Clinical Biomechanics, 23(8) , Ropars et al., Minimally invasive screw plates for surgery of unstable intertrochanteric femoral fractures: A biomechanical comparative study, pp.1012-1017 , Copyright (2008), with permission from Elsevier.

Figure 2.19: The minimally invasive sliding screw (MISS) (Ropars et al., 2008)

2.5.2 Intramedullary devices

Cephalocondylic IM nails which are inserted from the proximal end of the femur downwards, are the most commonly used alternative to the SHS. The claimed advantage of IM over extramedullary implants is that, as they are inserted in the centre of the bone, the moment arm is shorter and therefore the bending moment on the screw will be smaller. They are recommended for use in subtrochanteric fractures by NICE in the UK, the Australia and New Zealand Hip Fracture Registry and the Canadian Bone and Joint Health Network (NICE, 2014; ANZHFR, 2014; Waddell et al., 2010). The American American Academy of Orthopaedic Surgery (AAOS, 2014) recommends the use of either the IMN or the SHS for treatment of unstable fractures while it recommends only the IMN for stable fractures. The difference between the US recommendations and the recommendations from the Commonwealth countries appears to come down to cost. The Australia and New Zealand guidelines state that the could not recommend either approach over the other on clinical grounds, but that a significant cost difference lead them to recommend the SHS.

IM nails can also be regarded as MI devices. The implantation procedure does not require a large incision down the lateral side of the thigh, rather two smaller incisions are made. However despite it's MI advantage over the SHS, the IM has not managed to replace the SHS as the most common treatment stable proximal femoral fractures in countries including the UK, Norway and the Republic of Ireland (Royal College of Physicians, 2014; Health service Bergen, 2010; IHFD, 2014).

2.6 Minimally Invasive Surgery

In recent years there has been a trend towards developing minimally invasive (MI) surgery techniques in orthopaedics. MI surgery has been shown to reduce blood loss and soft tissue damage improving the patient's recovery time (DiGioia et al., 2003; Hata et al., 2001).

2.6.1 Minimally Invasive Sliding Hip Screw Insertion

Procedures have been developed to insert a standard SHS in a MI manner, one such procedure is described by Wong et al. (2009). A 2.5 cm incision is made through which the bone is drilled and the lag screw inserted. The side plate is then inserted into

the incision with the barrel positioned laterally, this position can be seen below in Figure 2.20, the plate is then rotated and guided into position using a fluoroscope for guidance. The study found that patients who underwent the MI surgery had less blood loss, tissue damage and pain than those who underwent conventional surgery; they also had a short rehabilitation period (Wong et al., 2009).

It is however mentioned in this paper that one patient who was due to have the MI surgery was transferred to the standard group due to the need for a longer plate. This would suggest that this method is not suitable for long plated implants. As long plated implants require larger incisions, MI techniques are more important when implanting them than when implanting standard plates. Therefore the success of the technique demonstrated in this study does not reduce the need for a minimally invasive sliding hip screw (MISHS) to be developed.

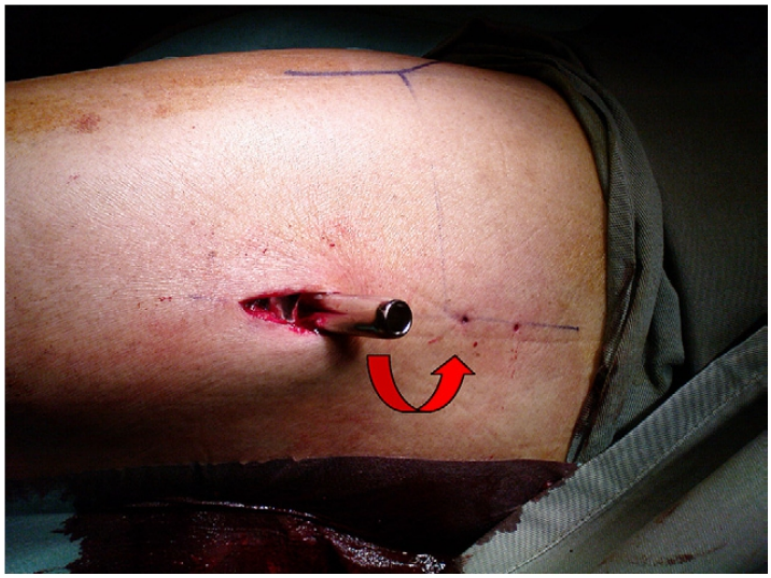

Reprinted from Injury, 40(4) , Wong et al., A double-blind, prospective, randomised, controlled clinical trial of minimally invasive dynamic hip screw fixation of intertrochanteric fractures, pp.422-427 , Copyright (2009), with permission from Elsevier.

Figure 2.20: MI technique for inserting a standard SHS (Wong et al., 2009).

2.6.2 Other Minimally Invasive Extramedullary Devices

Several attempts have been made to create devices for the treatment of extracapsular hip fractures which can be easily inserted using MI techniques. Two such devices,

previously mentioned in Section 2.5.1, the PCCP developed by Gotfried (2000) (Figure 2.18)and the MISS (Figure 2.19), were tested by Ropars et al. who concluded that both have a similar biomechanical performance to the standard SHS (Ropars et al., 2008). However it was also suggested that the double screw is more resistant to sliding than a single screw which could lead to failure of the fracture to impact, in the study it was recorded that the fracture impacted less for with the PCCP than with the MISS. A possible problem with the MISS device is that it does not appear to contain a device to prevent the rotation of the neck screw. While the screw itself appears to have some flats which would prevent it rotating inside the barrel, the barrel itself does not seem to have a mechanism to prevent if from turning inside the plate when they are assembled. This could result in the flats on the screw being ineffective as the entire barrel rotates within the plate, and may lead to instability of the fracture.

A clinical study comparing the PCCP to the SHS was carried out by Brandt et al., who found that the two devices performed similarly for bone healing and stability, however the follow up was short and the number of patients was small so the results are not conclusive. Blood loss, tissue damage and operation duration were all reduced through the use of the PCCP, however hospital stay was not significantly different between the two groups (Brandt et al., 2002).

A third device not previously mentioned is the Kyle implant described in Kyle (1984) with the surgical tooling described in Kitchens (2005). There are no clinical or biomechanical studies of these devices to be found in scientific literature, however it can be seen from the patent that as with he MISS device there is no anti-rotation device on the Kyle implant which could cause instability at the fracture site. Problems may also occur due to the design of the neck screw of the device, the screw consists of two components, the thread of the screw and the shaft, during implantation the shaft is screwed into the thread before the whole component is screwed into the bone. It is possible that rotation of the screw shaft may lead to it becoming detached from the thread and therefore the femoral head would no longer be attached to the shaft of the femur, this could result in failure of the device.

No patent could be found for the MISS device and no description of the implantation procedure could be found in literature. Patents for both the PCCP and the Kyle device show that the surgical procedures for implanting these devices are more complex than the current procedures. This is a potential reason why these devices have not been

widely adopted. The implantation of the current SHS device is a simple procedure, any changes to this procedure which would make the surgery longer or significantly more difficult to perform may lead to low adoption by surgeons. It is therefore important when designing a new MISHS device that the surgical procedure should differ as little as possible from the current device.

2.7 Clinical Performance of the SHS as a Treatment for Extracapsular Proximal Femoral Fractures

The SHS is now widely regarded as the standard treatment for extracapsular proximal femoral fractures. One reason for this is the short time which the patient must remain in bed. When treated with a SHS the patient is encouraged to begin weight bearing as soon as possible, often on the first postoperative day (Schumpelick and Jantzen, 1955; Jensen et al., 1978). Jensen suggested in his 1978 study that the early mobilization of patients may be the reason for the low mortality rate of 8.8% (Jensen et al., 1978) which he recorded.

The SHS has been shown to perform well with high incidence of good union and low occurrences of technical failure. In his study on the treatment of stable pertrochanteric fractures Jensen concluded that both the nail-plate and SHS were valid treatments, with technical failure rates of all devices studied between 4-6% (Jensen et al., 1980b). In a further study on the treatment of unstable pertrochanteric fractures the recorded technical failure rates were, McLaughlin nail-plate (53%), Jewett nail-plate (48%), SHS (6%) and Ender nail (32%); Jensen thus concluded that the SHS was the only valid treatment for unstable pertrochanteric fractures (Jensen et al., 1980a).

In their clinical trial Esser et al. found that after 6 months 88% of patients treated with a SHS who were mobile before their fracture had regained their mobility, compared to only 61% of patients treated with the Jewett nail-plate (Esser et al., 1986).

Heyse-Moore et al. reported in their paper that for patients with unstable pertrochanteric fractures, the percentage of patients who were allowed to either return home or to their preoperative accommodation within three weeks after treatment with a SHS was more than double those treated with a nail-plate. However for stable fractures the percentages were much closer although they were still higher for the SHS than the nail-plate.

In a more recent paper Chirodian et al. reported a failure rate of only 3.6% from their study of 1024 patients, more than half of which were due to screw cut out. After one year 49.3% of patients assessed had no pain, 26% hand occasional slight pain, 17.5% had pain when starting movement, 4.1% had pain during activity and only 1% had constant but bearable pain. Of the 523 surviving patients who lived at home pre-fracture 83% were living at home 1 year after fracture while 10% were in a residential home, 6% were in a Nursing home and 1% were in hospital. Mortality after one year was 31.5%, this is relatively high but it is suggested that it may be due to the average age of the patients being 81.7 years. It is also noted that the survival rate was highest in patients with greatest mobility, which supports the argument that allowing patients to regain mobility quicker is beneficial. In this study 85% of surviving patients returned to pre-fracture levels of mobility, with 45.5% of patients who walked without any aids before fracture returning to this state (Chirodian et al., 2005).

As mentioned previously screw cut out is one of the most common causes of SHS failure. Baumgaertner et al. suggested that the chance of screw cut out is related to the position of the screw within the femoral head (Baumgaertner et al., 1995). They found that there was a correlation between a measurement known as the tip-apex distance, which measured the distance between the tip of the screw and the apex of the femoral head, and the risk of screw cut out occurring. They found that the greater the tip-apex distance the greater the risk of cut out occurring, with no cut out occurring in patients with a tip-apex distance of 25 mm or less. This would suggest that the technical failure rate of SHS could be reduced when performed by experienced surgeons who specialize in the procedure.

Parker and Handoll (2009a,b, 2010) have published several papers with the Cochrane collaboration reviewing the randomized clinical data for the SHS versus alternative implants.

2.7.1 SHS versus other extramedullary devices

Parker and Handoll (2009b) reviews the randomized clinical data for extramedullary implants such as the SHS and nail-plate. The current update of the paper includes 14 studies published between 1986 and 2005.

SHS versus fixed nail-plate

Parker and Handoll conclude that there is insufficient randomized clinical data, from studies with good methodologies, comparing the SHS and fixed nail-plates to draw any definite conclusions. It is suggested that this may be because the majority of trials comparing these devices were carried out before randomized trials were widespread. It is stated that in the data available the risk of fixation failure is shown to be significantly higher with fixed nail-plates than with the SHS. It is recommended by the authors that the SHS should be used rather than the fixed nail-plate.

SHS versus Pugh nail

Only one study comparing these implants was included in the review. It indicated that there was no difference in the performance of the two implants. With only one case of cut out in the Pugh nail group and none in the SHS group, resistance to cut out being the main argument in favour of SHS over Pugh nail. However due to only the single randomized trial being present the authors are unable to confirm this conclusion.

SHS versus Medoff sliding plate

Parker and Handoll state that the Medoff plate has similar results to the SHS when used for stable fractures with no incidence of fixation failure. The studies reviewed show that the operative time and blood loss are larger for the Medoff plate however Parker and Handoll caution that this may be due to the larger Medoff plate being used and that when the four hole plate was used the differences between the operative time and blood loss compared to the SHS were smaller.

For unstable fractures the Medoff plate was shown to cause less failures than the SHS. However the number of incidence of cut out in the SHS is much higher in these studies than in others. The authors therefore state that no definite conclusions can be made without further studies.

SHS versus PCCP

Only two small studies were carried out comparing these implants. Both suggested intra-operative complications involved with the PCCP as well as reduced blood loss with the PCCP. There is not enough data for clear conclusions to be drawn.

From this review paper it can be seen that the is insufficient randomized clinical data to draw any conclusions. The large amount of data for non-randomized trials involving the SHS and nail-plate are probably enough to suggest that the SHS is the better of the two options as the fixation failure rate in the nail-plate is so high. However further trials are needed before it can be confirmed whether more advanced plates, such as the PCCP and the Medoff plate, perform better than the SHS.

2.7.2 SHS versus Condylocephalic Intramedullary Devices

Parker and Handoll (2009a) reviews randomized clinical data comparing condylocephalic and extramedullary implants. It contains eleven studies of which eight compared condylocephalic implants to the SHS. The authors conclude that while the condylocephalic implants involve shorter surgery and less tissue damage these advantages are out weighed by increased incidence of fracture, cut-out, and reoperation. They also found an increased rate of deformity and a poorer return to pre fracture levels of mobility in the groups treated with condylocephalic implants. It is suggested that the SHS should be used rather than condylocephalic implants to treat extracapsular fractures.

2.7.3 SHS versus Cephalocondylic Intramedullary Devices

Parker and Handoll (2010) systematically reviews the randomized clinical data from studies comparing cephalocondylic and extramedullary devices. Forty three papers were included in the review of which thirty seven compared the SHS with an cephalocondylic device.

Parker and Handoll found that there was no significant difference in the number of incidence of cut-out, non-union or wound infection between the two implants. However they found that there was a significant increased rate of intra-operative and later fractures to the femoral diaphysis around and below the implant in patients treated with the IM device. Femoral fractures were found to be the main reason for the increased re-operation rate in patients treated with the Gamma nail. There was insufficient evidence to determine whether the rate of these complications had reduced with the most recent designs of the Gamma nail as many of the papers that reviewed these implants did not report the intra-operative or later fracture rates.

Data for blood loss and operative time was contradictory and therefore no conclusions could be drawn as to which implant is better by these measures. Data for anatomical deformities showed no significant difference between implants and for long term outcomes such as mortality, mobility and pain were inconsistent or were not significantly different.

The data does however suggest that for transverse and reverse oblique fractures at the lower trochanter the IMN may be a superior device to the SHS.

This review therefore suggests that the SHS is superior to the cephalocondylic IMN for both stable and unstable extracapsular hip fracture due to the lower rate of complications associated with it.

Bhandari et al. (2009) hypothesised that the the rate of femoral fractures in patients treated with an IMN was decreasing. The authors carried out a meta-analysis of 20 papers, the found that when looking at all the data from 1991 to 2005 combined that patients treated with an IMN were significantly more likely to to suffer from a femoral fracture than those treated with an SHS. However when looking at data from 2000 to 2005 the increased risk was no longer significant. The authors suggest that this decrease in femoral fracture risk is most likely due to improved implant design and increased experience of surgeons and notes that evidence from earlier trials and meta-analysis should be interpreted with caution.

Matre et al. (2013) carried out a review of data from the the Norwegian Hip Fracture Register, from 2005 to 2010, to investigate whether patients with type 31-A1 fractures treated with an IMN had less pain and increased quality of life, and a lower reoperation rate than those treated with SHS devices. The authors found that after one year the reoperation rate for patients with an IMN was 4.8% compared with 2.4% for patients with an SHS and that after 3 years the rates were 7.1% and 4.5% respectively. The authors could not however find any significant difference between the quality of life or pain in the two groups of patients. This review therefore supports the conclusion of Parker and Handoll (2010) that the SHS is a superior device for the treatment of stable fractures and disagrees with the findings of Bhandari et al. (2009)

Audigé et al. (2003) carried out a meta-analysis of 17 randomised studies which compared the use of the SHS and IMN in the treatment of unstable extracapsular hip fractures. They found that although more complications occurred with the IMN devices

there was not clinically significant advantage to either device. This conclusion differs from that of Parker and Handoll (2010).

A non-systematic review by Schipper et al. (2004) looked at 18 randomized clinical trials comparing two different fracture fixation devices. They concluded that IM devices could not be recommended for the treatment of stable trochanteric fractures and that the IM devices were biomechanically superior to the SHS for treatment of unstable fractures but clinical advantages had yet to be demonstrated on evidence base.

These studies show that although there is still some disagreement over the effectiveness of the IMN, the SHS is an effective treatment, with rates of complication either equal to (Bhandari et al., 2009) or lower than (Parker and Handoll, 2010; Matre et al., 2013; Audigé et al., 2003; Schipper et al., 2004) those for the IMN.

From these studies it can be seen that the SHS performs very well in the treatment of extracapsular proximal femoral fractures, with failure rates lower than other devices. It is possible to allow patients to safely regain mobility only days after surgery. This in turn increases there chance of regain pre-fracture levels of mobility and therefore of returning to a similar life style without need of further care.

2.8 Current Treatment Statistics

The Norwegian hip fracture registry reported that from 2005 until 2009 78% of all trochanteric fractures were treated with some form of SHS or compression hip screw, while 18.73% were treated wit an IMN (Health service Bergen, 2010). In the UK the national hip fracture database reported in 2013 that 84.2% of trochanteric fractures were treated with an SHS while 11.9% were treated with nails (Royal College of Physicians, 2013), while in 2014 it reported that the numbers were 84% and 13.1% respectively (Royal College of Physicians, 2014). The Irish Hip Fracture Database reported that 54% of patients with intertrochanteric fractures were treated with the SHS while 36% were treated with an IMN. This is in accordance with NICE CG 124 guidelines (NICE, 2014) which suggests that an extramedullary device should be used in preference to an IMN in patients with type 31-A1 and 31-A2 fractures according to the AO classification.

For subtrochanteric fractures the UK registry shows that 21% of patients are treated with SHS devices while 74.1% are treated with IM. These statistics differ from those

given in the Norwegian registry which show 62.4% of patients being treated with hip screws and 34.3% with nails.

These statistics show that the SHS is a much more commonly used device that the IMN for the treatment of trochanteric fractures in the UK, Norway and the Republic of Ireland. Due to a lack of accessible fracture registries in many countries, obtaining data on the use of each device globally has been difficult. Canada, Australia and New Zealand have all issued guidelines which agree suggest the use of SHS over IMN for stable fractures (ANZHFR, 2014; Waddell et al., 2010) and it may therefore be safe to assume that the use of the SHS is more common in these countries. The Australia and New Zealand guiltiness however, state that they could find no clinical reason to prefer the SHS, but that the decision was made due to a significant cost difference. The guidelines given in the US (AAOS, 2014) state that they cannot recommend one device over the other, it may be the case therefore that the IMN has become more prevalent in the US, due to the privatised health system which is less focused on reducing cost and may allow surgeons more freedom to select the device which they prefer.

While the IMN is a viable MI alternative to the SHS, the fact that the SHS is the recommended and most common treatment for stable fractures in many countries including the UK suggests that there may be a reasonable market for a MISHS. For this reason it was decided that a MI device which would fit with the UK standard practice for the treatment of stable fractures was worth developing and could improve treatment in this country.

2.9 Mechanical Testing of the Femur and Fracture Fixation Devices

There is one published standard (ASTM, 2011), which could be found, which recommended a method by which angled fracture fixation device could be tested. However this standard only specifies a method for testing an implant outside of bone and gives no recommendation as to how stiff an implant should be. In order to produce a new implant it is necessary not only to be able to compare the stiffness of the device against current designs but to also compare its performance when implanted in bone.

Several people have carried out mechanical testing on both the femur and fracture fixation devices with the aim to discover how strong and stiff a device must be to safely

allow weight bearing and to evaluate which device is best. Jensen carried out several such experiments in his series of papers on unstable trochanteric fractures (Jensen et al., 1978; Jensen, 1978a,b, 1980b,c,d)

Jensen first tried to quantify the stress in the femur using a photo elastic technique (Jensen, 1978b), this led to the conclusion that to reduce the stress in an implant, nail-plates with a large angle which placed the nail steeply into the femur should be used (Jensen, 1978a). This is a logical conclusion given that a larger angle nail-plate provides a smaller moment arm and therefore a reduced bending moment occurs. However a steeper angle is likely to create a higher stress at the nail tip leading to increased chance of the nail breaking through the bone.

Early attempts at mechanically testing devices assumed that they would be required to take the full load at the hip which was estimated by Paul (1967, 1976) to be approximately 3-5 times body weight while walking. Jensen concluded that the McLaughlin nail-plate was not strong enough to support the forces during walking, and also concluded that the larger angled versions of the Jewett nail, which should be subject to a smaller bending moment, were also too weak due to their design which caused the plate to be weaker than the smaller angled versions (Jensen, 1980b). It was concluded that the smaller angled Jewett nails were sufficiently strong to bear the force while walking.

However devices may not be required to take the full load at walking Harrington and Johnston (1973) suggest that metal failure may not be the most important factor in the performance of an implant. The mechanical test carried out by Jensen does not take into account the strength of the bone around the nail. It has been shown in clinical trials that the Jewett nail, deemed strong enough by Jensen, often failed due to cutting out of the nail from the bone. It can therefore be suggested that in situations where the entire load is transferred through the nail, the bone is likely to fail if the nail does not and therefore an implant cannot be evaluated on strength alone but by its ability to maintain contact of the fragments and to transfer load through the bone.

More recent attempts at mechanically testing implants have included bone and have tried to replicate the loading much more accurately. Krischak et al. (2007) carried out an experiment to compare the stability of two devices the SHS implanted with an additional stabilizing screw and PCCP. The devices were implanted into cadaver specimens and fitted to a test rig which simulated vertical compressive loading and loading from the iliotibial tract (Figure 2.21). The specimen was loaded cyclically and

the displacement between the two fragments was measured using an ultrasonic motion analysis sensor. The study found that the PCCP allowed higher displacements than the SHS and therefore that the SHS provided more stability to an unstable fracture.

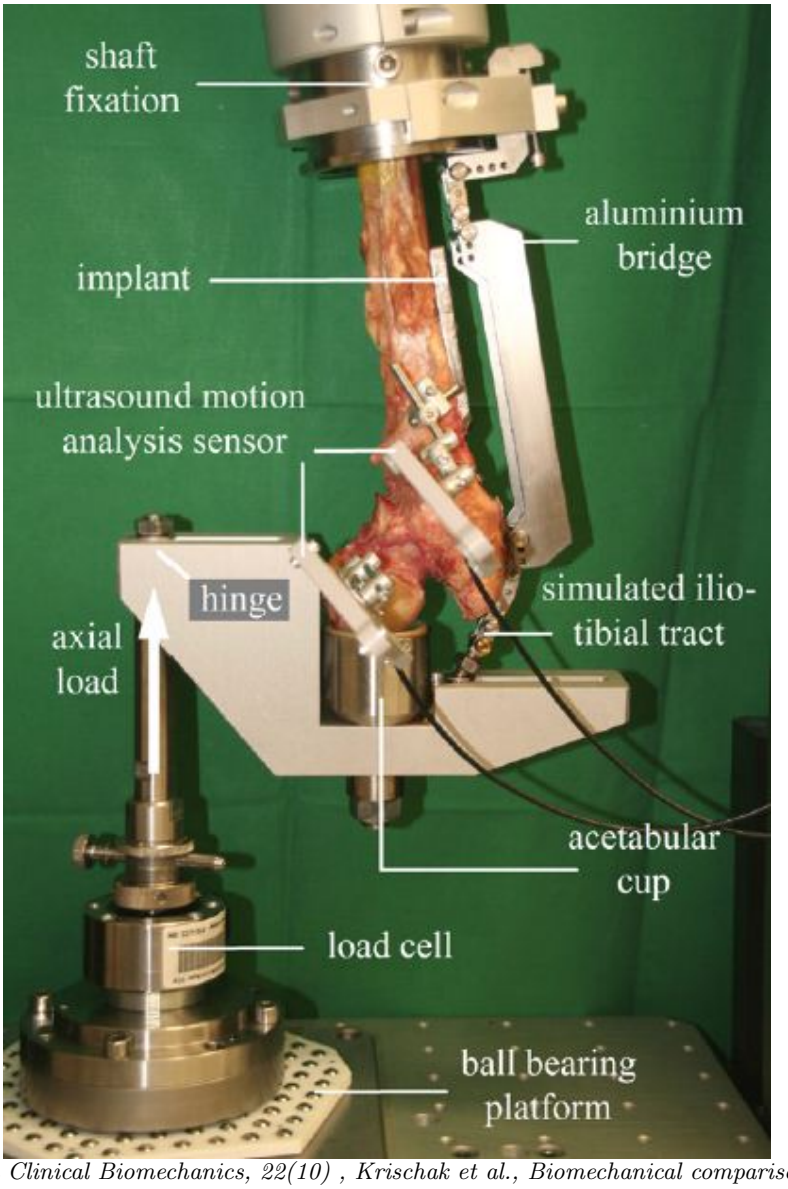

Reprinted from Clinical Biomechanics, 22(10) , Krischak et al., Biomechanical comparison of two side plate fixation techniques in an unstable intertrochanteric osteotomy model: Sliding Hip Screw and Percutaneous Compression Plate, pp.1112-1118 , Copyright (2007), with permission from Elsevier.

Figure 2.21: Set-up used for mechanical testing of an SHS used by Krischak et al. (2007).

2.10 Finite Element Modelling

It is both expensive and time consuming to manufacture prototypes of implant designs and test their mechanical performance in a laboratory. It was therefore decided that during this project designs would be modelled using FEA, this would allow several designs to be assessed, the most suitable design could then be selected for manufacturing and testing. The modelling of implants in bone is a complex task with many possible problems to overcome.

2.10.1 Material Models of Bone

Bone is a complex biological material and cannot be easily modelled in engineering terms without making many assumptions. Some of the common bone models are discussed below.

2.10.1.1 Linear Elastic

This is the simplest model which can be applied to bone, however is also the one which is furthest from the real behaviour of bone. It assumes that bone behaves like a simple engineering material, such as steel, and can be described by the Young's modulus and Poisson's ratio alone. When using a linear elastic model there is no time dependant response from the material, the model is therefore useful for static analyses however it may not give accurate results when used in a dynamic simulation. This model is useful when carrying out analyses on complex geometries, as it is much less computationally intensive than non-linear models.

2.10.1.2 Viscoelastic

A more accurate model than linear elastic is viscoelastic. This model takes into account the time dependant response of bone to a force thus giving more accurate results in dynamic analyses than the linear elastic model. However this model will lead to a much more computationally intensive analysis. It is also much harder to develop a viscoelastic model for bone than a linear elastic model and therefore several models exist. Careful thought must therefore be given to choosing which model to use and to answering the question whether a bad viscoelastic model is much better than a good linear elastic model.

2.10.1.3 Isotropy of Constitutive Behaviour

Within the above models there are different variations available. Isotropic material models assume that the material properties are the same in all directions. This is the simplest model and is again useful when modelling complex geometries. The opposite of isotropic is anisotropic, this is a material with different properties in different directions. Anisotropic models are a more accurate representation of bone when compared to isotropic models, however it is difficult to quantify the coefficients for these models. Orthotropic models are a specific type of anisotropic model, in which the material properties vary between two or three orthogonal axes. An example of an orthotropic material is wood which which has different properties axially, radially and circumferentially. It has been suggested that cortical bone, especially in long bones, could be described with an orthotropic model.

2.10.2 Modelling SHS Implants in Bone

2.10.2.1 Models Which Exclude the Fracture Site

There are a limited number of studies which have attempted to model the SHS in a femur with a extracapsular fracture. One of the most difficult problems to overcome where creating such a model is how to model the fracture site itself. Several studies have attempted to overcome this problem by removing the fracture from the model either by removing the femoral head completely from the model or leaving the head fully connected to the femoral shaft.

Peleg et al. (2006) carried out mechanical testing and produced a model in order to compare two different designs of SHS. The model consisted of the device implanted in a femoral shaft with the head removed and was loaded by applying a moment and force to the proximal end of the femur. This loading model assumes that all load is transferred across the fracture site and no load is transferred directly between the screw and the plate. However as discussed Section 2.4, Putti (1940) showed that screws inserted without plates would migrate through the bone under loading, it must therefore be assumed that load is transferred between the screw and the plate in order for the plate to prevent this migration of the screw. As the primary purpose of the plate is to maintain alignment of the screw it is essential that when modelling the plate the forces transmitted between the screw and the plate are included.

Limited results were presented from the model and conclusions were drawn only from the mechanical test, no attempt was made to validate the model with the results from the test. The results from the mechanical test were deemed successful against criteria set out in the British Standard "Orthopaedic joint prostheses. Method for determination of endurance properties of stemmed femoral components of hip joint prostheses without application of torsion" (British Standards Institute, 1990a) which was withdrawn in 1998 and has no relevance to fracture fixation devices and is therefore not a suitable criteria for the test to be measured against.

Taheri et al. (2011) carried out a study comparing the performance of SHS devices manufactured from two different materials: titanium and stainless steel. A 3D FE model of a proximal femur implanted with an SHS was built. The model included frictional contact between the plate, screws and femur. The threads of the screws were simplified to cylinders and tied to the femur. No fracture was included in the model as it was intended to analyse the performance of the devices post fracture healing. The author found that the lower stiffness of the titanium implant lead to reduced stresses within the femur and therefore recommended that titanium implants should be preferred over stainless steel. However the author does not take into consideration the mechanical requirements of the implant prior to fracture healing. The author states:

> "For internal-fixation implants, tt[*sic*] is necessary to choose a material similar to the mechanical characteristics of bone to reduce stress and increase the strength and stability of the fractured femur."

While it might correctly be claimed that choosing an implant material closer to the properties of bone will reduce the stress within the femur, it cannot be said that reducing the stiffness of the implant will increase the stability of the fracture. The stability of the fracture is reliant on the implants ability to maintain the alignment of the bone fragments and therefore a lower stiffness will in some way reduce fracture stability. The authors recommendation that titanium implants should be preferred over stainless steel, is not based upon how the implants perform the task for which they were intended, that is to aid the healing of the fracture, but rather how they perform after that task is completed. The current statistics show that the rate of re-operations due to fracture of the bone around the implant after surgery is 0.2% (Matre et al., 2013), this number includes all those fractures which occur after surgery and is not limited to

those which occur after the fracture heals. This suggests that there may be no need to reduce the stress in the bone after the fracture is healed. It is for this reason that the implant manufacturers continue to manufacture SHS devices from stainless steel, contrary to the recommendations of the author of this paper.

A second paper by Taheri et al. (2012) investigated the stress distributions in femurs implanted with SHS devices and loaded under different conditions. The authors again chose to model femurs without fractures, the model also contained no contact conditions between the plate and the bone with all components in the model being bonded together. The exclusion of contact conditions from the model could significantly change the stress patterns within the model. The author states in their conclusion that the main objective of the model was to determine stress distributions and does not discuss the lack of contact as limitation of the model.

Oken et al. (2011) carried out a study to investigate the performance of different fracture fixation including the SHS. FE models were built and mechanical testing was carried out using simple artificial femur model. Each model contains a femur implanted with a device and does not include a fracture, instead the author compares the performance of each device by looking at the stress which occurs on an imaginary line which represented the fracture. This method was taken from a paper by Keyak et al. (2001), however the method was intended to model the occurrence of fractures not the behaviour of fractures which already exist, the author does not discuss the suitability of this method for modelling the performance fracture fixation devices. The mechanical tests were carried out in simplified artificial femurs which did contain fractures. Load cells were placed at the fracture site to measure the normal load transferred across the fracture. The author acknowledges that the load recorded by the load cells cannot be directly compared to the stress at the fracture line in the model, however states that the intent was to see "concordance" between the results. The study shows that the use of the SHS implant results in higher stress at the fracture line and higher load in the mechanical test that other devices. The author concludes that the lower stress and load of the other devices may make them more suitable for use. While it may be possible to claim that the lower stress in the model is an indication that one device is more suitable than another, the claim that a lower load recorded across the fracture site is desirable, is more questionable. The load measured by the author in the mechanical

test is only the normal force between the bone fragments. Sliding fracture fixation devices such as the SHS were designed to allow the bone fragments to remain in contact and as such provide no resistance to force in the normal direction at the fracture site. It could therefore be said, contrary to the opinion of the author, that and increase load at the fracture site is more desirable. A decreased load at the fracture site indicates that there is either no sliding mechanism or that it is resisting sliding. As discussed in Section 2.4, the sliding mechanism is an important feature to prevent bending of the screw and penetration of the screw into the joint.

2.10.2.2 Models Which Include the Fracture Site

Several studies have been carried out which model the behaviour of the SHS including the fracture site. The studies contain a variety of methods for modelling the fracture site and there appears to be no consensus for which is best.

Peleg et al. (2010) carried out a study which investigate the use of FEA in patient specific modelling in order to select the most suitable implant. The study included both mechanical testing and FEA of proximal femurs implanted with hip screws. The implant used in this model included a static screw rather than a sliding mechanism. The author noted that during the mechanical test there was a gap between the bone fragments at all times. Therefore a gap was included in the model and no contact conditions were included between the fragments. The paper therefore does not provide any method for modelling the fracture site when a sliding implant is used. The author suggests that the suitability of implants could be measured by calculating the strain ratio (SR), between the maximum principle strains in the intact and implanted femurs. Although this measurement is not suitable to determine whether an implant is sufficiently stiff and strong enough to be used for the treatment of fractures. It may be a useful to compare the SRs of the current device and any new designs which have been deemed to be suitable stiff and strong.

Sim et al. (1995) carried out a study which aimed to analyse the stress in a fracture femur after stabilisation with the a SHS and a cephalocondylic nail. The authors produced a 2D FE model of femur and implant. The bone was assumed to be linear elastic isotropic, the Young's modulus was not considered uniform throughout the femur therefore different values were assigned to various regions of the femur. Sim et al. (1995) assumed three different conditions at the fracture site to represent three stages of

healing. Frictionless contact was assumed between the two bone fragments to represent the fracture before healing has began, a low stiffness layer was created between the fragments to model the callus which forms between the fracture during the healing process and the fragments were joined to represent the fracture after it has healed. The results for this study are not clearly presented in the paper, however it is stated that the stress in the implant does not exceed the maximum admissible value.

The conditions used to model the fracture site in this study are not explained or justified. The frictionless contact condition does not accurately model the condition between the two surfaces, as fracture is unlikely to produce to smooth bone fragments. However the frictionless contact can be considered as the worst case scenario where the implant will take the majority of the load, although this is no accurate, it is safe to assume that if the implant does not fail with this condition it will not fail in any other with the same geometry. The frictionless condition does not however give an useful information about the stress within the femur, as only a fraction of the load is is being transferred across the fracture site. The condition where the fracture is modelled with a layer of low stiffness material may also not be an accurate model. The results will vary greatly with changes in either the thickness or stiffness of the fracture layer, as these values do no appear to have been decided on scientifically the results form these analyses cannot be considered valid.

Rooppakhun et al. (2010) carried out a study in which the utilized a 3D FE model to analyse the performance of an SHS. The fracture conditions in this study were similar to those used by Sim et al. (1995). Rooppakhun et al. (2010) used an intermediary layer of material at the fracture site during all stages of healing, changing the material properties to vary the conditions. As with Sim et al. (1995) the properties and geometry of the intermediary layer do not appear to have been decided on scientifically, the material properties are referenced, however these values do not appear in the referenced paper.

Papers by Goffin et al. (2014) and Hrubina et al. (2013) both described FE models which used friction to model the behaviour of fractures. However the coefficients of friction used by Goffin et al. were referenced from Eberle et al. (2010) which took the values from unpublished experiments, while coefficients used by Hrubina et al. are not referenced. The use of frictional contact between fracture fragments may be a suitable way to model the fracture site, however a published source of frictional coefficients must be found. Where there is a lack of published coefficient of friction values it may be

necessary use frictionless contact, as was used by Sim et al. (1995), and consider this a worst case scenario.

Hrubina's model also utilised complex material models, it is stated that elasto-plastic models were used for both the implant and the bone. However in reality the material model used for the bone, which was taken from Baca et al. (2007), was not an elasto-plastic model, instead heterogeneous linear elastic isotropic and anisotropic models were used for the cancellous and cortical components respectively. The elasto-plastic model used for the implant is not specified, however the yield stress (690 MPa) and strength (860 MPa) are significantly higher than the values usually given for stainless steel (approximately 215 MPa and 505 MPa respectively.)

2.11 Use of Artificial Bones in Bio-mechanical Testing

Over the last few decades several generations of artificial femurs have been developed with the aim of providing an alternative test medium to cadaveric specimens. It has been suggested that artificial bones can both simplify and reduce the cost of testing as well as providing specimens that are more consistent than cadaveric specimens.

Sawbones® 4th generation composite bones are the most recent design of artificial bones. The consist of both a cortical component manufactured from short fibre reenforced epoxy (SFRE) and a cancellous component manufactured from polyurethane cellular foam (PCF).

Studies by Heiner (2008) and Gardner et al. (2010) compared the structural performance of both artificial femurs and tibia against human bone. Both studies compared the flexural rigidity of the bones in both the anteroposterior (AP) and mediolateral (ML) planes as well as torsional and axial stiffness. In their analysis Gardner et al. (2010) included the data from Heiner (2008) as well as data for human bones from earlier studies (Cristofolini et al., 1996; Cristofolini and Viceconti, 2000). It was found that for both the femur and tibia, the AP and ML flexural rigidities fall within the average range found for biologically healthy specimens from adults below 80. The results also showed that the axial stiffness of the artificial femurs was lower than that of the human femur and that the torsional stiffness of both the femur and tibia fell within the range of the data from human bones.

Gardner et al. (2010) also investigated the ultimate bending, axial and torsional strengths of the artificial bones. It was found that for bending and torsional there was not enough published data on the ultimate strength of cadaveric bone to allow a comparison, however for axial loading of the femur it was shown that the artificial femur is more than twice as strong as the cadaveric samples. It was suggested by the author that this may be due to the artificial femur having a proportionally smaller neck length than the average cadvaeric specimen.

Heiner (2008) included strain gauge data in their investigation. Stain gauges were placed at 5 positions on the medial side of the shaft at the distal end of the femur. The readings for the 4th generation femur were between 11 and 54% higher than those from the human specimens, however the range of the readings was considerable and as such it is difficult to draw any conclusions from the data. The spread of data could be due to the difficulty in accurately mounting strain gauges to the bone, bones are complex shapes with no flat edges which can be used as datums. Any miss alignment in gauges will result in drastically different readings and as such comparison between gauges on different femurs can be incredibly difficult.

These studies show that the 4th generation composite femurs replicate the stiffness of human bone relatively well, however the strength of the artificial bone appears to be too high. While the studies have shown that the overall stiffness's of the bones are similar, the lack of good strain gauge data prevents us from confirming whether the artificial bones are capable of replicating the stress and strain distribution throughout the bone.

Sawbones® 4th generation composite bones have come to be used in a range of studies where analysis of fracture fixation devices is to be carried out including: Wu and Tai (2009), Clyde et al. (2013) and Bariteau et al. (2014). While it has not been proven that are an model human bone completely accurately, the results from the studies discussed in this section along with their wide use in biomechanical studies show that they are suitable to be used in this study.

2.12 Design Methodology

A design methodology is a framework that can be used to help guide the product design process and provide a method by which designs can be quantitatively assessed to ensure

the final product meets the design requirements. A number of design methodologies exist, each of which will have its own strengths and weaknesses. For this study I choose to use the Total Design methodology created by Stuart Pugh (Pugh, 1991). I had successful utilised this methodology on a number of previous projects and felt that it's philosophy of looking at the design process as a whole, rather than focusing on the technical design, made it ideally suited for this project. Pugh's method centres around a six stage process know as the design core:

- Market
- Product Design Specification
- Conceptual Design
- Detailed Design
- Manufacturing
- Sales

These stages are iterative and the designer is encouraged to me back and forth between the stages as many times as is necessary to develop a successful product. At the market stage research is carried out, the purpose of this stage is to gather all the information that is needed to generate the product design specification in the following stage. At the product design specification stage a list of requirements is drawn up, these requirements will be used later to evaluate any designs which are created. Ultimately a design must meet the specification in order to be deemed suitable to manufacture. At the conceptual design stage several concepts are generated, these are then compared against the specification and each other in a design matrix. If no design is found which successfully meets all the necessary specifications, then the process is repeated until a suitable design is created. At the detailed design stage the chosen design is refined and completed, the product is then taken to the manufacturing stage where the process, by which it will be manufactured, is designed. It may be necessary to iterate between the detailed design and manufacturing stage several time as decisions made in the detailed design can have a significant effect on how the product is manufactured. Finally the sales looks at how the product will be sold, how much it will cost to manufacture and

how much it will be sold for, at this point it may be necessary to return to previous stages in order to reduce the overall cost of production and ensure that the product can be sold for a suitable price.

Within the medical device industry there are codes which state how a manufacturer should control the design process, two prominent examples are FDA 21 CFR 820.30 and BS EN ISO 13485, both of which are very similar:

- The manufacture is required to document the design and development plan, this will define what the stages of the design process are, when verification will take places and who will be responsible, and which methods will be used to ensure traceability.
- They are required to define suitable design inputs including: performance requirements, relevant standards, appropriate information from previous designs.
- Design outputs must also be defined these must meet the requirements of the inputs and contain acceptance criteria.
- A design verification process is required through which the design outputs will be checked against the design inputs to ensure the design is acceptable. Design validation must be carried out to ensure the product is suitable for its intended purpose, this may include clinical or performance evaluations of initial batches of products.
- The manufactures must define a process by which the design is correctly transferred into product specifications at manufacture.
- A process by which design changes are reviewed, verified, validated and approved must be defined.
- The manufacturers must maintain a design history file which will contain records which show that the design process correctly followed that which was set out in the design and development plan.

While on the surface the processes set out in these two standards may appear to be design methodologies, they are not. These standards do not define how a design should be evaluated, only that it should happen and that it must be properly documented. The

stages in Pugh's method provide a framework for some of the requirements which these standards set out. The market and product design specification stages can fulfil the requirements to produces design inputs and outputs, the conceptual design stage and matrix method of comparing designs provides a method for verification of the design. The design transfer process may fit within then manufacturing stage of Total Design, at which the methods for manufacturing the product is designed. The validation process does not fit directly into Pugh's method, however in reality this validation is not part of the design process itself, but rather it is a final check to ensure that the finished product works as intended. While the Total Design method could have been used within the process set out in the standards, the requirements to define and document the design process—as set out in the FDA and ISO standards—were not followed during this project. The design process is instead documented in this thesis.

2.13 Summary of Findings

This review of the literature identified several important facts which were key to the research which was carried out.

Firstly, the study into the history of treatment of extracapsular proximal femoral fractures helped to identify the key design features of the SHS which should be incorporated into any new design:

- Sliding Screw - Maintains contact at fracture site and helps to prevent penetration of the screw into the joint capsule
- Flats on screw - Prevent Rotation of the screw within the barrel, providing stability to the femoral head.
- Lateral Plate - Transfers load from the femoral head to the shaft preventing migration of the screw.

These features were developed over decades in response specific problems which occurred with previous devices. It is important that any future device either maintains these features or incorporates alternative methods for preventing these issues.

Secondly the literature investigated the current use of MI surgical techniques in the treatment of extracapsular proximal femoral fractures. It was found that several

attempts had been made to develop an MI version of the SHS but that no device had come into general use. The reason for the lack of adoption cannot be stated with absolute certainty, however it appears that all of these devices either do not contain all of the key features of the current devices identified in this literature review or have significantly more complex implantation procedures than the current device. This identifies the need for any new device to have a simple implantation procedure, as similar as possible to the current method.

Thirdly the literature review identified alternative devices to the SHS which are currently in use. Clinical studies comparing these devices and meta-analyses of these studies were reviewed. It was found that there was some disagreement as to whether the SHS was a more effective treatment than the IMN, the studies did however show that the SHS was an effective treatment. Data from both the Norwegian and British hip registers was also reviewed, it was found that the SHS was the most common treatment for extracapsular proximal femoral fractures in both countries. This shows that the SHS is an effective treatment that is more widely used than newer alternative devices. It can therefore be said that development of a new version of this device, which maintains the existing features and advantages while improving in other areas, is a significant opportunity which should be pursued.

Finally the literature review discussed the current use of FEA to model the SHS in a femur. It was hoped that this review would identify a method which could be used to model new designs in order to aid the development of a new device. However it was found that may of the models were not suitable for use as they were not validated or contained assumptions which brought into question the validity of their results. This meant that a new model would need to be designed and validated in order for the results to be used.

3

Aims and Objectives

This chapter discusses the aims and objectives of the research project which is detailed in this thesis. The aim of the project was:

> "To develop a SHS device, which is capable of being implanted using MI techniques, to be used for the treatment of extracapsular proximal femoral fractures."

In order to achieve the project aim it was necessary that the following objectives be met:

- Develop a FE model of the current SHS - This model would be used to compare and evaluate new designs. It was therefore important that it be designed in such a way that it could be easily used with different devices and that it could be validated against laboratory tests.
- Validate model through mechanical testing - In order for the results of the model to have any value the model had to be validated. This validation process would involve running a mechanical test which was similar to the model. The results of this test could then be compared against the results from the model
- Validation of Sawbones® artificial femur material - The mechanical testing carried out would involve the use of artificial femurs, it was necessary that the material properties of these femurs be investigated to ensure they could be modelled correctly.

- Generate conceptual designs for a MISHS - In order to create a new device it would first be necessary to set out design requirements, new concepts could then be generated and measured against these requirements. Once its was decided that a sufficient number of viable designs had been created, these designs could be taken to the next stage of development.

- FEA of MISHS designs - Once new designs were chosen FEA would be carried out in order to compare the performance of these designs both against each other and the current device. This would allow on design to be chosen to take to the next stage.

- Manufacture Prototype - Due to the both time and budget constraints only a single design was to be taken to the prototyping stage. Three full size working prototypes would be built in order to allow mechanical testing of the design.

- Mechanical testing of prototype - Finally the mechanical performance of the device would be tested in the lab and the results compared with similar tests performed on the current device. This would demonstrate that the device is capable of performing in a similar manner to the SHS.

The remainder of this thesis discusses the completion of these objectives and contains the following chapters. Chapter 4 details validation of a FE model of Sawbones® 4th generation composite femurs, which were utilised in place of cadvaeric samples during mechanical testing. Chapter 6 discusses the design process including concept generation and selection. Chapter 5 discusses the development of the FE model of the SHS, along with the validation of the model and FEA of the MISHS concepts. Chapter 8 details the manufacturing process for the MISHS prototype, the final mechanical tests on the prototypes are then discussed in Chapter 9.

4

Characterisation of Sawbones Artificial Cortical Bone

Sawbones® 4th Generation composite bones (Sawbones, Malmö, Sweden) are useful tools for the mechanical testing of orthopaedic devices and validation of finite element models. In order for us to utilise these artificial bones to validate complex models containing orthopaedic implants, it was first essential to ensure that we could accurately model the artificial femur itself. To do so an FE model was created using a 3D model of the Sawbones® femur, the results from this model were then compared against results from a mechanical test to validate it. Initial pilot attempts to model the femur found that the model was behaving much stiffer than the mechanical test. It was thought that there were two possible reasons for this difference in results, the material properties of these products differ from those provided by Sawbones® (Tables 4.1 to 4.3) or the mesh was behaving in a stiff manner due to the use of linear tetrahedral elements.

Table 4.1: Material properties for the cortical component of the Sawbones® 4th Generation composite femur.(www.sawbones.com)

	Strength (MPa)	Young's Modulus (GPa)
Longitudinal Tensile	106	16
Compressive	157	16.7
Transverse Tensile	93	10

No evidence could be found which reported studies which used the material prop-

Table 4.2: Material properties for both the solid and cellular variations of cancellous component of the Sawbones® 4th Generation composite femur.(www.sawbones.com)

	Strength (MPa)	Young's Modulus (MPa)
Solid	6	155
Cellular	5.4	137

Table 4.3: The Poisson's Ratios for both the cortical and cancellous components of the Sawbones® 4th Generation composite femur.(www.sawbones.com)

	Poisson's Ratio
Cortical	0.26
Cancellous	0.3

erties given by Sawbones® in FE models of the femur. Data presented by Younge (2011) shows that while the cancellous component of these femurs is relatively close to these properties, the cortical component is significantly less stiff than suggested by the manufacturer. It was therefore decided that experiments would be carried out to characterise the material properties of the cortical component of the femur using samples from the femurs themselves. The data gained from these experiments would then be applied to a finite element model the results from which would be compared against the mechanical test. If any significant difference in results occurred the mesh would then be refined in an attempt to reduce any stiffening behaviour of a course mesh.

As the material properties in Table 4.1 show, short fibre re-enforced epoxy (SFRE) is an anisotropic material with different material properties in the transfers and longitudinal directions. The modelling of anisotropic materials presents difficulties particularly when using complex geometries. When modelling an anisotropic material it is necessary to define an orientation for the material properties, in a case such as a femur this is not simple as the orientation of the material is different throughout the bone. Another issue is the properties required to define the material, while an isotropic material can be defined by only the Young's modulus (E) and Poisson's ratio (ν), an anisotropic material requires the Young's moduli, Poisson's ratios and shear moduli (G) for each of the three principle directions (X_1, X_2, X_3 Figure 4.1). Because the material can be regarded as a transversely isotropic material, that is the material properties are the

same in both transverse directions, some assumptions can be made which simplify the material property requirements (Equations (4.1) and (4.2)). Thus the material can be described with E_1, E_2, ν_{12}, ν_{23} and G_{12}. As test specimens were to be taken from the femur, there was a limit to the size and shape of specimen that could be obtained. It was only possible to obtain slender beams which were orientated so the length of the beam corresponded to the longitudinal axis of the femur. Therefore it was not possible to carry out experiments to accurately gain measurements for E_2, ν_{12}, ν_{23} or G_{12}. Due to the problems involved in both measuring anisotropic material properties and applying these to the complex geometry of the femur in a FE model it was decided that the model should be created using a isotropic linear elastic model. The Poisson's ratio 0.26, as provided by the manufacturer (Table 4.3), was assumed to be correct and the Young's modulus was calculated from bending tests on specimens taken from the femurs.

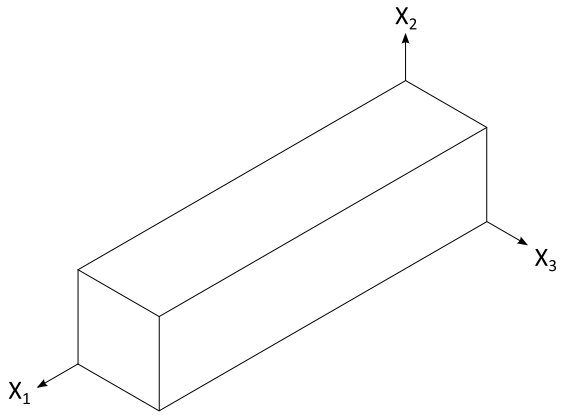

Figure 4.1: Principle directions of material.

$$E_3 = E_2, \qquad G_{13} = G_{12}, \qquad \nu_{13} = \nu_{12} \tag{4.1}$$

$$G_{23} = \frac{E_2}{2(1+\nu_{23})} \tag{4.2}$$

4.1 Methods

4.1.1 Cortical Component

Five samples of the cortical component of a Sawbones® large 4th Generation Composite Femur(product number: 3406) were tested in three point bending using a Bose Electroforce 3200 (Bose Corp., Eden Prairie, MN, USA) fitted with a 450 N load cell. Samples of dimensions 3 mm × 5 mm × 50 mm were cut from the mid diaphysis of a single large femur. Samples were supported on two cylindrical supports (⌀4 mm) held 40 mm apart. Load was applied by displacing the sample downwards using a cylindrical nose positioned midway between the supports (Figure 4.2).

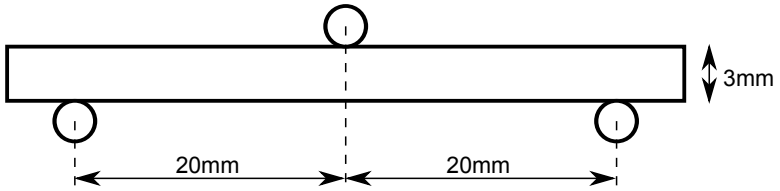

Figure 4.2: Configuration of three point bending test for femur sample.

The nose was displaced vertically downwards by 1mm at rate of 0.1 mm/s, the position was then held for 20 s before retraction at the same rate. The experimental procedure was repeated five times on each sample with 5 minutes between tests.

From Euler-Bernoulli beam theory Equation (4.3) was derived for 3-point bending, where w is the displacement of the beam, L is the length of the beam (distance between supports), P is the applied load, E is the Young's modulus and I is the second moment of area.

$$w_{L/2} = \frac{PL^3}{48EI} \tag{4.3}$$

$$k = \frac{P}{w_{L/2}} \tag{4.4}$$

$$E = \frac{kL^3}{48I} \tag{4.5}$$

The least squares method of linear regression was used to fit a linear relationship to each set of test results. The gradients of these curves were taken to equal the stiffness

(k), the mean value of stiffness was calculated for each sample and from this the Young's modulus of the sample was calculated using Equation (4.5). The mean of the Young's moduli of the samples was calculated along with the standard deviation and coefficient of variation, ANOVA was carried out to test for significant differences between samples.

4.1.2 Composite Femur

In order to evaluate the accuracy of the material properties found in the mechanical tests, a 3D finite element model of a the proximal end of a Sawbones® 4th generation composite femur was created. The results from this model were then compared to a mechanical test of a the same femur.

The mechanical test was carried out on a Sawbones® femur with a cancellous component constructed of polyurethane cellular foam (PCF). The femur was cut midway down the shaft with only the proximal end being used for testing. The femur was set in Isopon P38 polyester filler (U-POL, London, UK) and held in a custom made clamp. The femur was tested in an Electroplus E10000 Linear-Torsion Floor Instrument (Instron, Norwood, MA, USA) by displacing the femoral head downwards by 1 mm at a rate of 0.1 mm/s, load was recorded using a 10 kN load cell, the setup can be seen in Figure 4.3.

The model containing both cortical and cancellous components was obtained from www.biomedtown.org and imported into Abaqus. Both components were meshed with at total of 282338 linear tetrahedral elements and were connected using a tie constraint. A rigid body was added above the femoral head and meshed with shell elements. The femur was loaded by displacing the rigid body, by 1 mm, downwards onto the femoral head. Frictionless contact was defined between the femoral head and the rigid body. The femur was constrained at the mid shaft by applying a fully fixed boundary condition to the bottom surface of the model. The meshed model can be seen in Figure 4.4. For the cortical component a Young's Modulus of 10.7 GPa, as calculated from the bending test results (Table 4.4), was used and a Poisson's Ratio of 0.26 (Table 4.3). For the cancellous component the Young's Modulus used was 137 MPa and a Poisson's ratio of 0.3 (Tables 4.2 and 4.3).

The least squares method was then used to fit a linear relationship, between displacement and load, to the results from each experimental run and the FEA. The

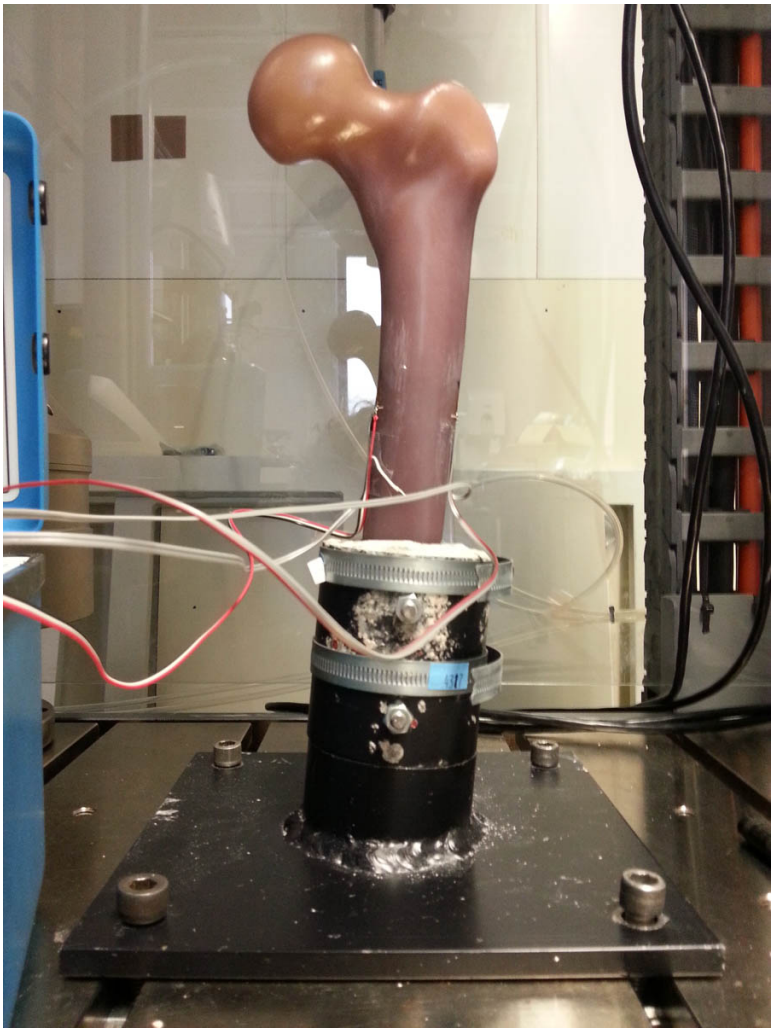

Figure 4.3: Proximal femur mechanical test setup.

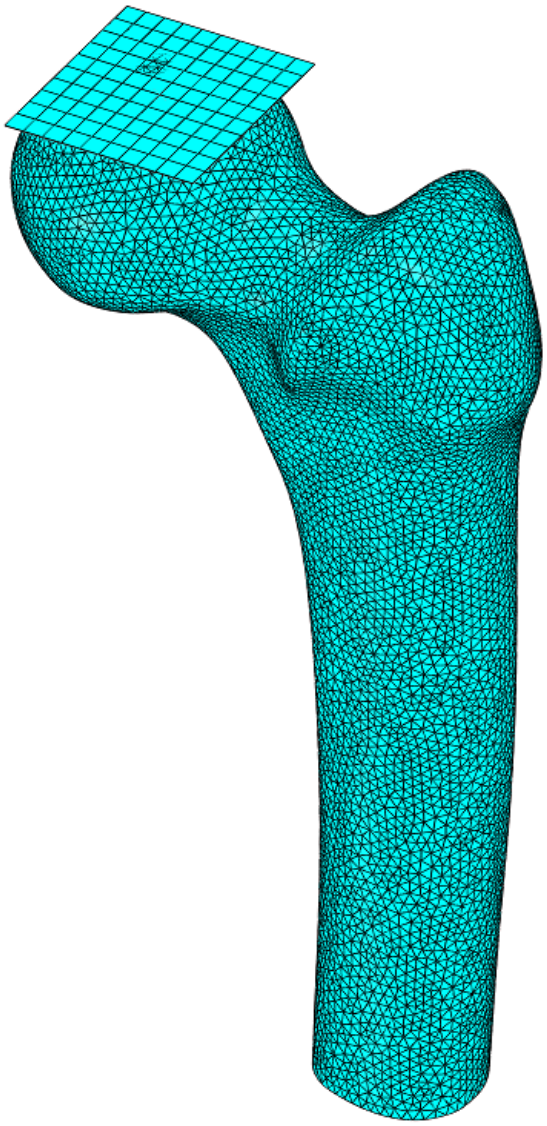

Figure 4.4: Proximal femur finite element mesh.

average experimental stiffness was calculated and compared to the stiffness calculated from the FEA results.

4.1.3 Cancellous Component Sensitivity Study

Although Younge (2011) found that the cancellous component of the femurs had similar properties to those given by Sawbones®, the study was carried out on blocks of PCF rather than samples taken from femurs and therefore we cannot be certain that the materials are identical in their properties. It was not possible to take samples of a suitable size and shape from the femurs and as such no tests could be performed on this material. In order to confirm that the material properties given by Sawbones® and confirmed by Younge were valid for use in this modelling, a sensitivity study was carried out to investigate how a change in cancellous material properties would affect the overall stiffness of the model.

The model was run a further two times as described in 4.1.2, however the Young's modulus of the cortical components was set to 68.5 MPa and 274 MPa, half and double the original value.

The change in stiffness of the overall model was then compared for each value of Young's modulus.

4.2 Results

4.2.1 Cortical Component

Table 4.4 shows the mean stiffness for each sample, the standard deviation of the stiffness and the calculated Young's modulus. It can be seen that the Young's modulus varies significantly between the samples ($p < 0.001$). The mean value of the modulus is 10.7 GPa with a standard deviation of 0.528 GPa and a coefficient of variation of 4.93%. The Young's modulus calculated was significantly lower than 16 GPa ($p < 0.0001$) and higher than 10 GPa ($p < 0.01$)

4.2.2 Composite Femur

The force-displacement curves for both the mechanical test and FEA of the composite femur are shown in Figure 4.5. The average stiffness of the four mechanical test runs

Table 4.4: 3-point bending test results from cortical component of femur.

	Mean Stiffness (N/mm)	S.D.	E (GPa)
Sample 1	93.3	0.202	11.1
Sample 2	89.5	0.315	10.6
Sample 3	93.3	0.259	11.1
Sample 4	85.2	0.414	10.7
Sample 5	82.8	0.248	9.81
		Mean	10.7
		S.D.	0.528

was calculated to be 1520 N/mm with a standard deviation of 18 N/mm. The stiffness of the FE model, using the Young's modulus 10.7 GPa, was found to be 1593 N/mm, thus the the FE model had a stiffness 4.8% higher than that of the mechanical test. The FEA results closely matched those of the mechanical test, it was therefore deemed unnecessary to refine the mesh.

4.2.3 Cancellous Component Sensitivity Study

The force displacement curves for each of the models can be seen in Figure 4.6. The results show that halving the Young's modulus of the cancellous component decreases the stiffness of the model by 3%, while doubling it increases the stiffness by 5%.

4.3 Discussion

From Table 4.4 it can be seen that the Young's modulus of the cortical component of the femur varies between samples. These results highlight two important issues. Firstly the material properties here are significantly lower than those provided by the manufacturer (Table 4.1). Secondly the material properties show significant variation from samples taken from the same product.

One potential cause of the variability in material properties may be the orientation of fibres within the epoxy. Figures 4.7 and 4.8 are images taken from a longitudinal section of the femoral shaft. From Figure 4.7 which was taken near edge of the sample it can be seen that the fibres are mostly aligned with the femoral shaft, however in

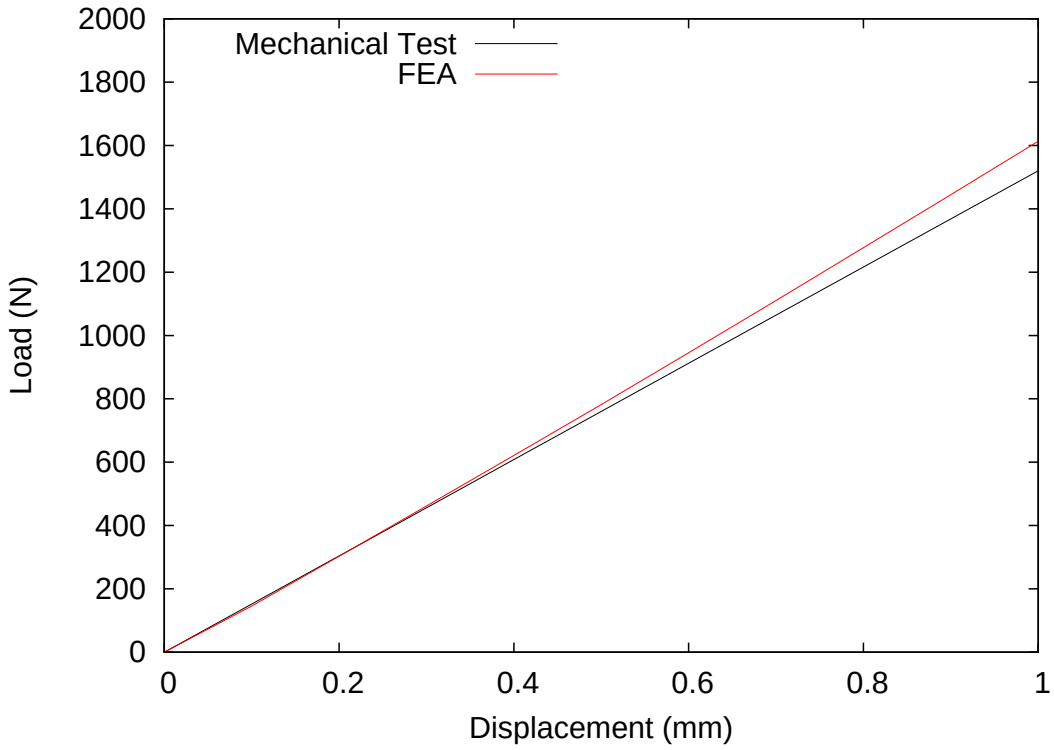

Figure 4.5: Force-displacement curve for both mechanical testing and FEA of the composite femur.

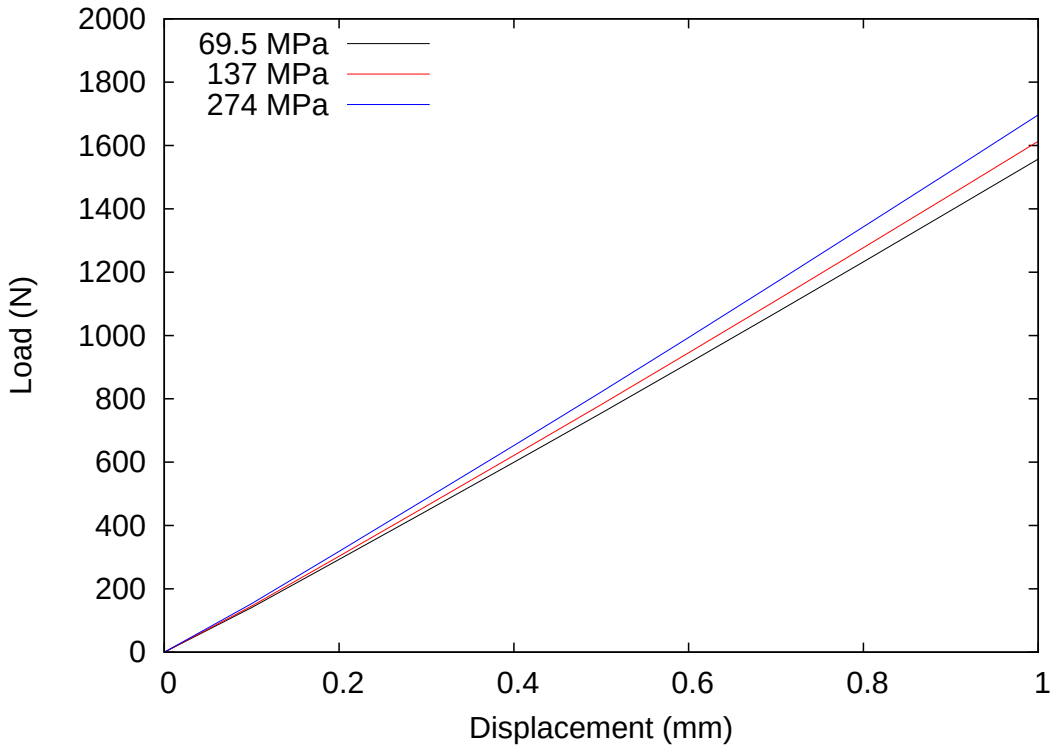

Figure 4.6: Force-displacement curve for each model in the Cancellous Component Sensitivity Study.

Figure 4.8 which was taken in the middle of the sample the fibres are more randomly orientated. It is possible that the manufacturing process will cause different areas of the femur to have a greater or lesser proportion of randomly orientated fibres. This could account for the variation in material properties found in this study.

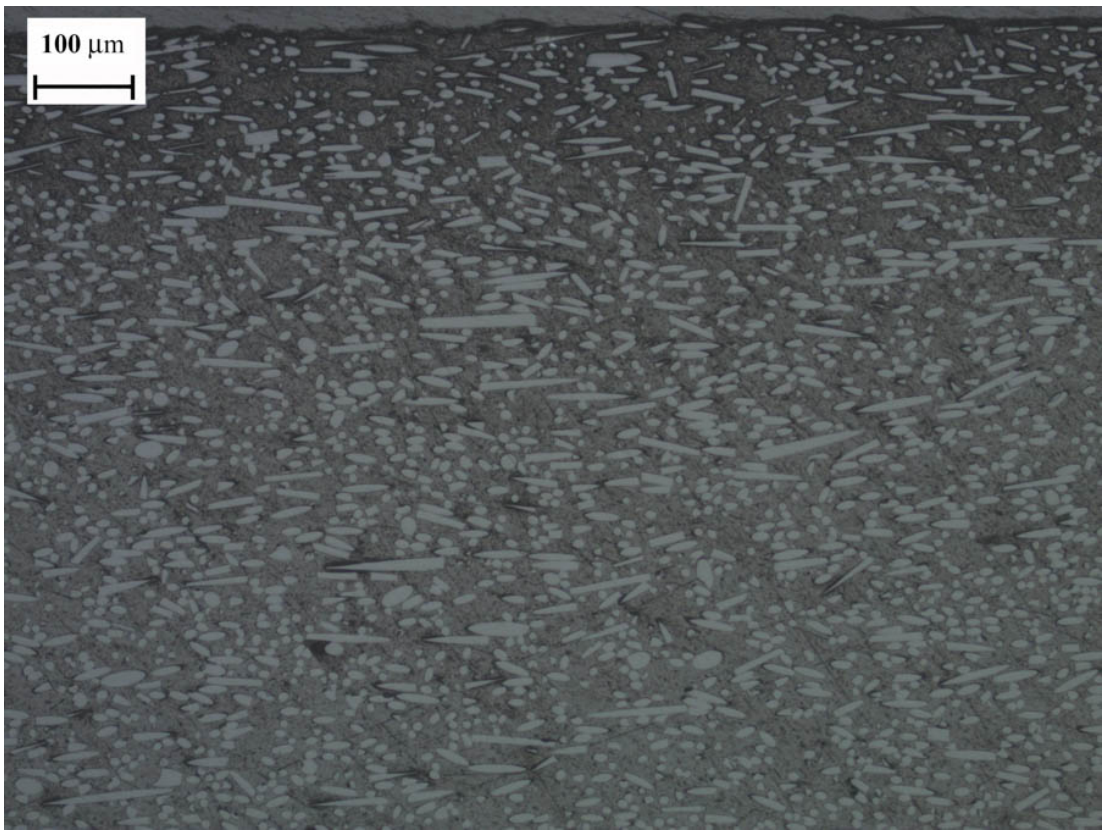

Figure 4.7: Sawbones® femur longitudinal section sample edge.

Another potential source of error could come from the the experimental procedure. Small variation in sample size may have caused some variation in results. The samples were measured using a micrometer to minimise any size discrepancies so the effects of these should be small. The orientation of the samples may have differed slightly. The samples were cut so that the long axis of the sample was parallel to the shaft of the femur. However small variations in the angle that the samples were cut may have lead to the fibres in the samples having slightly different orientations, this may have caused some variation in results. The position of the sample on the testing rig may also have caused some variation. Any rotation of the sample on the testing rig can cause

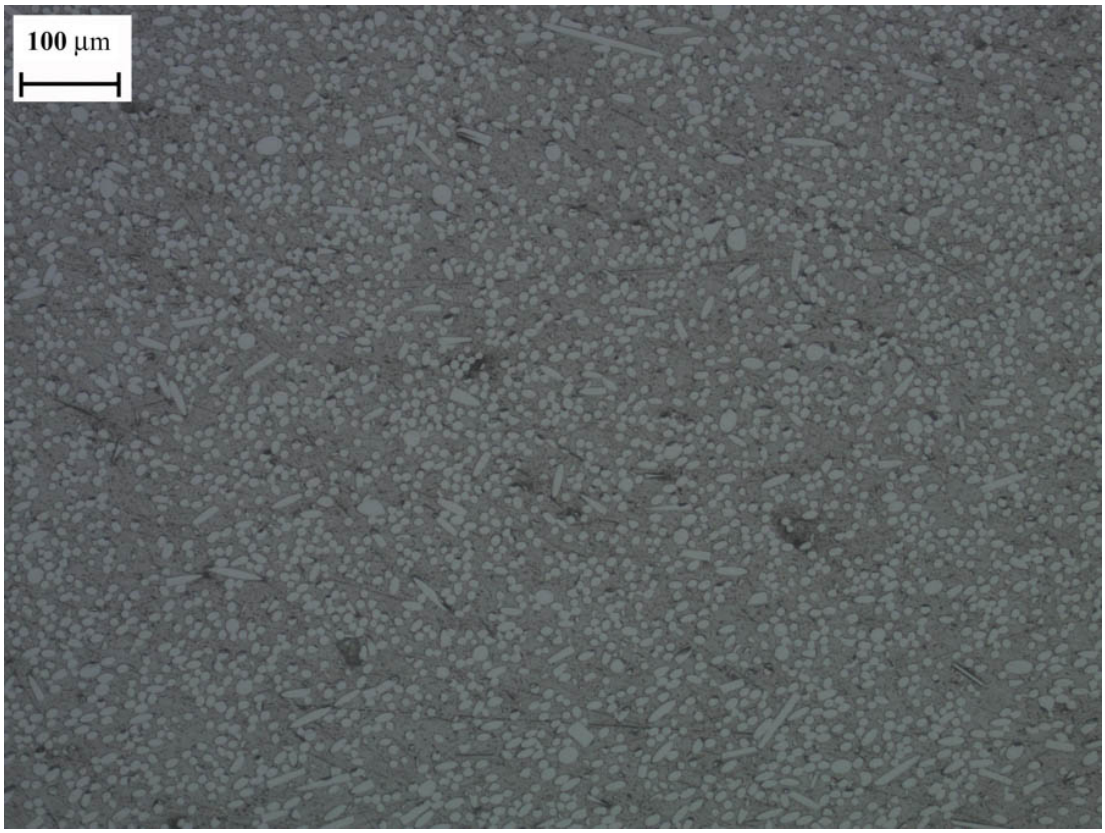

Figure 4.8: Sawbones® femur longitudinal section sample middle.

the effective length of the sample to become longer and therefore affect the results. When placed on the rig the samples were pushed up against the rubber bands which held cylindrical supports, this helped to ensure consistent placement of the samples, however potential for these bands to move during testing existed and therefore the possibility that sample placement could have affected the results cannot be completely disregarded.

It is not clear why the Young's modulus found in this study is significantly different from the properties listed by the manufacturer. Sawbones® state that the material properties where obtained from tests conforming to ASTM D638 (i.e. ASTM's standard test method for tensile properties of plastics), it does not give any citation to a published report. However a study by Chong et al. (2007) investigated the material properties of the 4th generation composite femurs, the testing carried out conformed to ASTM D638-03 (ASTM, 2003). Two of the authors on this paper were employees of Pacific Research Laboratories the parent company of Sawbones®. It may therefore be the case that this paper is the source of the material properties given on the Sawbones® website. The study found that the Young's modulus of the SFRE was 15.8 GPa, this value is similar to that given by Sawbones®. The authors also found that the Young's modulus of human cortical bone in the longitudinal direction was 17.5 GPa and that the modulus of the previous third generation composite femur was 11.3 GPa, it was therefore concluded that the 4th generation was a significant improvement over the 3rd.

However in order to carry out tests in accordance with the ASTM D638, relatively large dog bone samples had to be created and therefore the samples could not be taken from the Sawbones® directly. The specimens where manufactured by injection moulding to the required shape. This is the same process process which is used to manufacture the bones themselves and it was assumed that the material properties would be the same. It was also stated by the author that short fibre in the material would be randomly orientated and therefore that the material could have isotropic apparent mechanical properties. However as has been shown (Figures 4.7 and 4.8), the fibres in the samples taken from femurs are not randomly orientated throughout and that the fibres near the edge of the specimens tend to align longitudinally more often. The specimens manufactured in this study were 3.2 mm thick, in comparison the material on the femoral shafts is as high as 9 mm thick in places. It is therefore

possible that the thin test specimens have proportionally more longitudinally aligned fibres found at the edges compared to randomly aligned fibres in the middle, than the samples taken from the femur. This increase in longitudinally aligned fibres would lead to an increase in Young's modulus and therefore this may explain the differences in the test results.

It must also be said however that the experiments detailed in this chapter are three point bending tests and therefore assume that the compressive and tensile moduli are identical. Although this may not be the case, the purpose of this study was to obtain a values which could be used to model the SFRE as an isotropic material. While there is a potential that the material properties measured in these experiments are not accurate, particularly due to the assumed value of the Poisson's ratio. The results from the FEA closely replicate the results from the mechanical test of the femur. It can therefore be said that the linear elastic isotropic model of SFRE with a Young's modulus of 10.7 GPa and a Poisson's ration of 0.26 is suitable to be used in future FE models.

The results from the sensitivity study into the effect of varying the Young's modulus of the cancellous component show that making large changes to the material properties results in only a small change in stiffness. It can be assumed that and variations in material properties between the PCF blocks and the material used in the femurs is likely to be significantly smaller that the variation in material properties used in this study. It can therefore be said that using the material properties provided by the supplier is suitable and will give reasonable results for overall stiffness of the model.

It must be pointed out however that the sensitivity study does not assess the effects of the material properties on localised stresses and strains. Variations in material properties may therefore still play a significant role in models, particularly where contact occurs between this material and other components. Care should therefore be taken when interpreting the stress and strain results of any models using these material properties.

It should also be noted that while the results appear to show the cancellous component having very little effect on the overall model, these results only hold true for stiffness. The study did not look at the effect that the cancellous component has on the strength of the bone. It is possible that in small reduction in the stiffness of the cancellous component may lead to increased stresses in the cortical bone in the ends of the femur.

Therefore it can be said that the material properties found in this study are suitable to be used in a model where the overall stiffness of the model is the primary outcome. However it cannot be confirmed whether the local stresses and strains in the model will be valid and care should be taken when drawing conclusions, regarding stress and strain, from future models.

5

Testing and Finite Element Analyses of the Sliding Hip Screw

Finite element analysis (FEA) is a useful tool for evaluating new designs for devices before producing prototypes. It is however important to ensure that models are validated. This chapter details the development and validation of three FE models which will be used to compare the current SHS device to new designs.

The initial aim was to create a model that accurately replicated the behaviour of the implant in a fractured bone and to validate this model using cadaver specimens. The modelling of an implant in bone is a complex problem; many assumptions must be made about the material behaviour of the bone, the interaction between the bone and the implant, and the loading and boundary constraints which are applied. One of the most complex areas to model is the interaction between the bone fragments at the fracture site. The conditions at the fracture site vary throughout the healing process and experimental validation of the fracture model is very difficult.

Initially it was decided to model the fracture site using a layer of intermediary material between the bone fragments to represent the callus tissue formed at the fracture site during the healing process. It was intended that the properties of this intermediary material could be altered to reflect the variation in tissues properties during different stages of the healing process. This approach presented many issues: the material properties of the tissue at the fracture site were unknown, some studies had been carried out to measure these properties (Leong and Morgan, 2008; Markel et al., 1990) however the methods used in these studies do not provide accurate results for material properties

which could be used in a FE model. In their study Markel et al. (1990) carried out an indentation test on callus tissue in dogs, the authors report the indentation stiffness of the tissue at various intervals throughout healing and state that the indentation stiffness is an "appropriate measure of local material properties". However the authors make no attempt to translate the indentation stiffness into the Young's modulus, it is not clear whether the authors believe that the indentation stiffness is equal to the Young's modulus or whether they are simply saying that it can be used to calculate it. Leong and Morgan (2008) carried out a series of nano-indentation test on the callus tissue of rats. Again they reported only the indentation stiffness, however they acknowledge that they are unable to calculate the Young's modulus due to the difficulty in measuring the Poisson's ratio of the callus tissue, which is required to carry out the calculation.

Another issue which arises when modelling the tissue at the fracture site is its complex geometry and heterogeneity. Creating a uniform layer of material across the fracture site would not accurately represent the tissue. During the healing process several different tissues are present at the fracture site, any attempt to model these as a homogeneous layer of material would be a significant simplification of the problem. A previous study which used this method (Rooppakhun et al., 2010) did not cite a source for either the material properties or the geometry of the intermediate material. The geometry of the bone fragments presented another issue, bone fractures do not form in straight smooth lines, in order to produce an accurate model of the bone fracture a CT image of a fractured femur would be required, however each fracture is different and one fracture could not be said to be representative off all. Lastly validation of such a complex model would be extremely difficult, it is not possible to recreate a part healed femur from a cadaver sample and therefore a validation test could only be done with a femur which was part way through healing at the time of the patients death. It was decided that, due to the assumptions that would have to be made to model the callus and the difficult involved in validating the model, attempting to model the callus tissues was not a realistic aim.

Having decided not to model the callus tissue it was then decided to attempt to model the behaviour of the fracture pre-callus formation. This would negate the need for assumptions to be made about callus tissue properties and geometry and solve the issue of validating the tissue behaviour. It would not however solve the issue of fracture

surface geometry. To realistically model the behaviour of a fracture site, a femur would have to be fractured and an SHS implanted, the specimen would then need to be CT scanned to allow a FE model to be created of the exact fracture geometry. However the behaviour of the fracture site would be specific to its geometry and therefore the model many not be a useful tool for comparing the performance of different designs of implant. In order to avoid the use of CT, the model was instead created with a straight cut to to represent the fracture and friction applied to the contact between the fragments. This however could not accurately represent the behaviour of the fracture site. Friction is caused by micro scale geometry of contacting surfaces, and is modelled through a frictional coefficient which produces a frictional force proportional to the normal force as the two surfaces are moved across each other. However the behaviour of the fracture site would be defined not only by the micro scale geometry which produces friction but also by the macro scale geometry.

As the aim was to produced a model that could be used to compare new designs to the current device, it was decided that it was not necessary to attempt to model the behaviour of the device in the human body. Instead the model was developed to simulate mechanical testing which could be carried out in the laboratory, allowing the model to be properly validated. Although this would mean the model could not be considered to give validated results for how the device would operate in vivo, it could be used to model the performance of new designs an compare them to the results for the current device in the mechanical test.

As the model was not intended to exactly replicate the behaviour of the devices in vivo, it was decided that it was not necessary to use cadaver samples for validation at this stage. Instead artificial femurs produced by Sawbones® were used, these composite femurs consist of a cortical element manufactured from short fibre reinforced epoxy resin and a cancellous component produced from cellular rigid polyurethane foam. The use of these femurs simplified the implantation and testing procedure by removing the need for ethical approval and allowing the implantation to be carried out by a surgeon out with the university laboratory. As 3D models of the femurs were available, their use also negated any need to carry out CT scanning of specimens.

The fracture site would be created in the artificial femurs using a hack saw, it was initially decided that the fracture would be modelled using frictional contact. However it is stated in training notes produced by Simulia, the creators of Abaqus, that “friction

is a highly non-linear effect" and that "solutions are more difficult to obtain with frictional problems than they are with frictionless problems" They also recommend "do not use friction unless it is physically important to do so". The model which was created for this study is complex, with contact occurring between several components, some of which were complex geometries resulting in dense meshes and complex contact surfaces. The complexity of the model was such that the models had to be solved on the University's high-performance computing (HPC) facility and took around 24 hours to solve. It was understood that the addition of friction would significantly increase the time required to solve this model and that implementing friction within the model would require a large amount of work to be carried out in order to create a model which could be solved.

It was thought that friction may play an important role within the model and therefore it was decided that its addition to the model would be attempted. Friction was modelled using the penalty method, this is the default method available in Abaqus and is recommended for most situations. The alternative method: Lagrange, adds significant computational costs compared to the penalty method and can prevent convergence, it was therefore not chosen for this model. Several attempts were made to solve the model however each time it would not converge. The minimum allowable time steps were reduced several times in order to help the model solve. However smaller time steps result in a longer solution time and therefore each attempt to solve was taking increasing longer. After several weeks of attempting to solve the model without success it was decided that no more work should be carried out and that the model would be run without friction. As the purpose of these models was simply to compare designs in order to select one for prototyping, then the lack of friction would only cause significant problems if the results from the model differed significantly from the mechanical test and therefore the model could not be validated. In the event that this was the case it was decided that further attempts would be made to implement friction within the model. However in the case where the model without friction can be validated against the mechanical test then the model would be deemed sufficiently accurate to allow comparison between designs.

This chapter details the development and validation of the FE models which would be used to compare the new concepts to the current device.

5.1 FE methods

This section describes the methods common to all FE models detailed in this chapter.

5.1.1 Software

3D models were created using Autodesk Inventor Pro (Autodesk Inc.,San Rafael, CA, USA) mechanical computer-aided design (CAD) software. This software allowed both production of models for FEA and orthographic drawings for manufacturing of prototypes.

FEA was carried out using Abaqus (Dassault, Vélizy-Villacoublay, France) FE software. Models were imported from Inventor using the step file format, the analyses were then setup using Abaqus/CAE graphical user interface and solved with the Abaqus solver on the University HPC facility.

5.1.2 Material Models

It was known that the current device was likely to be manufactured from grade 316 stainless steel, in accordance with BS ISO 5832-1:2007 (British Standards Institute, 2007). The properties of this material can however vary between suppliers, it was therefore decided to assume the material properties shown in Table 5.1. The material properties for the Sawbones® were discussed previously in Chapter 4.

All components of the implant were modelled as grade 316 Stainless Steel with a linear elastic material model applied (for some models described in Chapter 7 a linear elastic perfectly plastic model was used). Both the cortical and cancellous components of the Sawbones® artificial femur were assumed to be linear elastic.

Table 5.1: Material Properties used in FE models.

Material	E(MPa)	ν	ρ(t/mm^3)	σ_{yield}(MPa)
Stainless Steel 316	200000	0.3	8.00E-09	241
Short-fibre-filled epoxy	10700	0.26	1.64E-09	
Rigid cellular foam	137	0.3	3.20E-10	

5.1.3 Elements

Due to the complex shape of the models it was necessary to mesh with tetrahedral elements, however, due to the use of contact, it was not possible to use the quadratic tetrahedral element. Therefore all components were meshed with 4-node linear tetrahedral elements (C3D4).

Linear tetrahedral elements are known to become stiff when used in coarse meshes (Cook et al., 2001, chap. 3). It was therefore essential to validate each component of the model to ensure that the mesh was suitable refined to provide accurate results.

Some of the models also contained a flat rigid body which was used to replicate the loading present in the mechanical test. These bodies were meshed with 4-node 3-D bilinear rigid quadrilateral elements (R3D4).

5.1.4 Meshing

The model meshes were created within Abaqus and seeded by defining the global element size for each part. Mesh convergence analysis is a method for generating the coarsest possible mesh that will produce accurate results. A model is first meshed with a relatively coarse mesh and the analysis is run, the mesh is then refined and the analysis run again, this process continues and each time the results are compared to the previous run, once the change in results is smaller than a defined value the mesh is said to have converged. Mesh convergence analysis is useful for creating a mesh that will produce accurate results while reducing the running time of the model. However the process itself requires a reasonable amount of time and computational power to run. It is therefore only useful in cases where the time saved through more efficient meshes is more than the time required to carry out the mesh convergence analysis.

As the models created in this study included several components that were to be run in only a few models it was decided that it would not be efficient to run a mesh convergence analysis. It was however still important to verify that the mesh would provide accurate results. As our aim with these models was to compare the overall stiffness of each device rather than to accurately model the stress within the devices, the accuracy of the mesh was verified by carrying out validation studies, to ensure that the stiffness of our models correspond to the stiffness of specimens in mechanical tests.

5.1.5 Contact

Contact in Abaqus can be applied in two ways, general contact or two surface contact. General contact allows the computer to automatically detect which surfaces are coming into contact while two surface contact requires the user to define pairs of surfaces, which will come into contact, before the analysis begins. General contact can increase the computation time required to solve the analysis however it can also greatly reduce the setup time for models containing multiple components. As several models each containing multiple parts were being created for this study, general contact was used in all models.

Frictionless tangential behaviour was applied to all contact conditions, this was chosen due to the better convergence rate of the frictionless condition as was discussed previously.

The contact behaviour in the normal direction was defined as "Hard", this condition allows any pressure to be transmitted across the contact pair when the surfaces are in contact and no pressure when they are not in contact. This differers from "soft" contact behaviour which allows some pressure to be transmitted across the contact pair as the surfaces come close to contact, usually using a linear or exponential relationship between contact separation and pressure.

Contact constraints were enforced using the penalty method which is the default method for surface to surface finite sliding problems. The penalty method allows the slave nodes to penetrate a small distance into the master surface, with the contact force being proportional to the penetration. The penalty method gives better convergence rates than alternatives, such as the Lagrange multiplier method, and is the preferred method when accurately modelling the load transferred across the contact pair is deemed more important than obtaining accurate pressure distribution at the contact site.

5.1.6 Solver

All models were solved using the Abaqus/Standard solver. This solver utilises the implicit method and is recommended by Dassault systems, for both linear and non-linear static analysis, over the alternative Abaqus/Explicit solver.

5.1.7 Results

A Python script was used to calculate the reaction force at the fixed surfaces of the models by summing the reaction force at each individual node. The reaction force data was then imported, along with applied displacement data, into Microsoft Excel, where the stiffness was calculated. Load displacement graphs were then plotted using GNUplot opensource plotting software.

5.2 Isolated Hip Screw Test

This model was created to compare the stiffness of the SHS device to new designs. It was also used to validate the model of the SHS in isolation before it was added to more complex models.

5.2.1 Methods

5.2.1.1 Mechanical Testing

The SHS was tested using a Rel 2061 universal testing machine produced by Zwick, Ulm, Germany, fitted with a FFL fatigue rated universal load cell produced by Strainsert, West Conshohocken, Pennsylvania, USA. The SHS was clamped to the machine as shown Figure 5.1. The load cell was positioned in a fixed position above the SHS and load was produced by moving the specimen upwards.

A pin was manufactured from mild steel (Figure 5.2), this was inserted into the barrel of the SHS allowing it to be loaded without causing damage. The SHS was positioned so that the load cell would make contact with the flat surface of the test pin as the SHS was moved upwards.

Load was applied using displacement control at a rate of 0.2 mm/min with the force being recorded. It has been estimated that the vertical load on the hip can reach up to 3.9 times body weight during normal walking (Paul, 1966), this would equate to around 3000 N for a 75 kg person. However when implanted in the body the device is supported by the femur and much of the load is transmitted through the bone, it was therefore decided that a lower load could be used, this would also to ensure the specimen did not slip from the clamp. Therefore the test was stopped once the force reached 1000 N.

Figure 5.1: Setup for mechanical testing of the Synthes SHS.

Figure 5.2: Test pin used to apply load to the SHS.

5.2.1.2 FEA

A model of the Synthes SHS implant was created in Autodesk inventor, the lower half of the straight plate section was removed, leaving only the section of the plate which protruded above the clamp in the mechanical test. A model of the load pin was also created and inserted into the barrel of the SHS. The model was imported into Abaqus as a step file. A flat rigid body, which would be used to replicate the loader of the testing machine, was added in Abaqus. The model was seeded with the values shown in Table 7.2 and meshed with 57220 linear tetrahedral elements. The rigid body was meshed with linear quadrilateral elements. Contact was applied to all surfaces using general contact, with frictionless tangential behaviour and hard normal behaviour.

The model was fully fixed at the bottom surface and load was applied by displacing the rigid body downwards by 1mm over 100 evenly spaced increments. Although it would have been possible to load the model by applying a displacement directly to a node or a group of nodes on the loading pin it was decided that using the rigid body to apply the load was a more accurate way to model the loading in the mechanical test. As the implant deforms during the mechanical test, the point where the testing machine contacts the loading pin may change. If this was to happen, a model that applied the load through a displacement on a node would not accurately model the test. It was unlikely that the point of contact between the testing machine and loading pin would move a significant distance in this test, however it was possible that it may occur in subsequent models where the load is applied to the femoral head. It was therefore decided to use this loading method to maintain consistency between all tests.

Table 5.2: Mesh seeding for each part in implant models.

Part	Approximate Global Size
Loading Pin	1.25
Plate	1

5.2.2 Results

The graph in Figure 5.4 shows the results from both the mechanical test and the validation FEA carried out on the SHS. The least squares method for linear regression

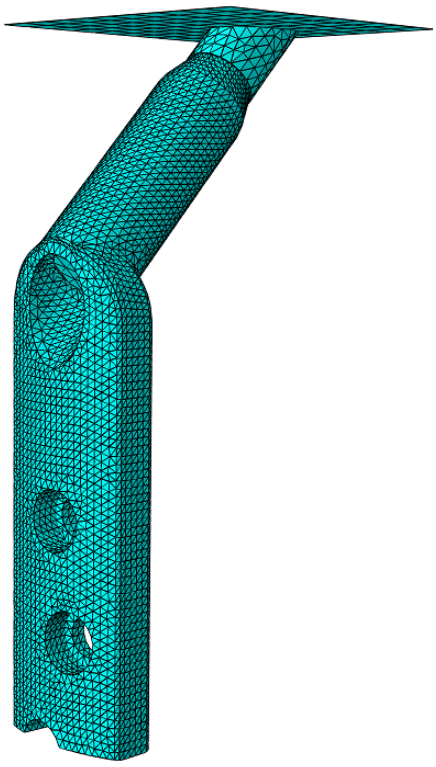

Figure 5.3: Synthes SHS bending test FE mesh.

was used to calculate the stiffness for the mechanical test and FEA results, giving 1419 N/mm and 1404 N/mm respectively. Therefore the error for the FEA was 1%.

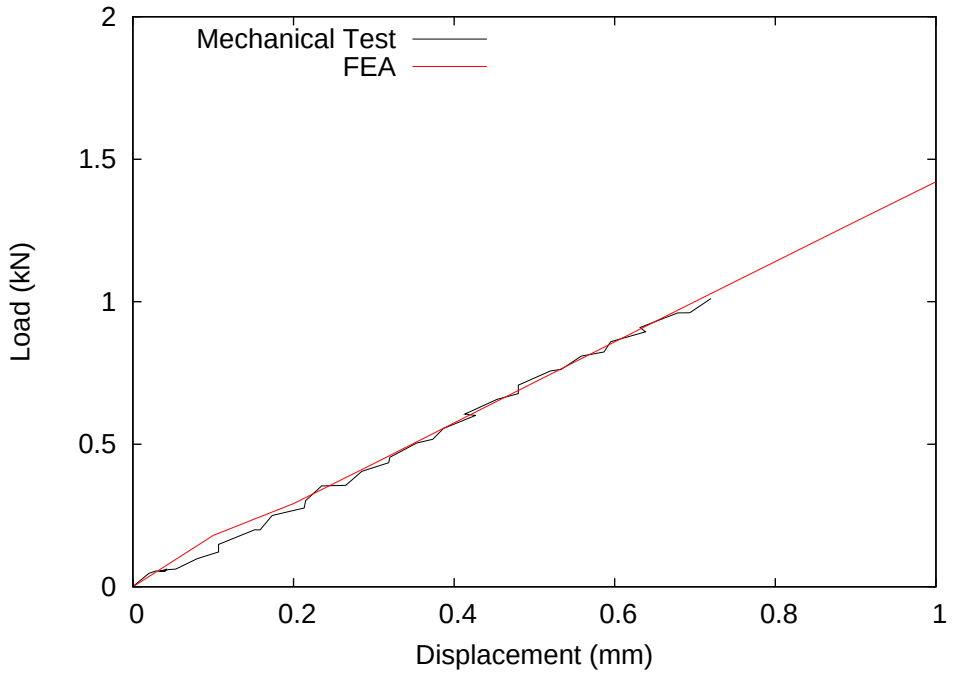

Figure 5.4: load-displacement curve for both the mechanical testing and FEA of an SHS in bending.

Figures 5.5 to 5.10 show contour plots of the stress in the model at 0.8 mm applied displacement at which point the load was close to the 1 kN load applied during the mechanical test. Figures 5.5 and 5.6 show the Von Mises stress in the straight section of the plate from the medial and lateral sides. Figures 5.7 and 5.8 show the stress concentrations which occur around holes in the straight plate. Figures 5.9 and 5.10 show the Von Mises stress in the barrel and the stress concentration which occurs at the transition between the barrel and the plate.

5.2.3 Discussion

The results for the validation study show the FE model having a stiffness the same as that of the mechanical test. This confirms that the FE model is an accurate representation of the SHS and gives confidence to the results gained during the concept comparison study (Chapter 7).

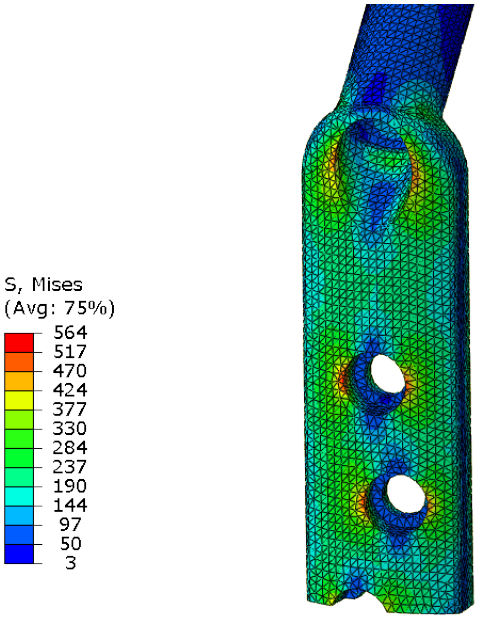

Figure 5.5: Von Mises Stress (MPa) - lateral side of plate

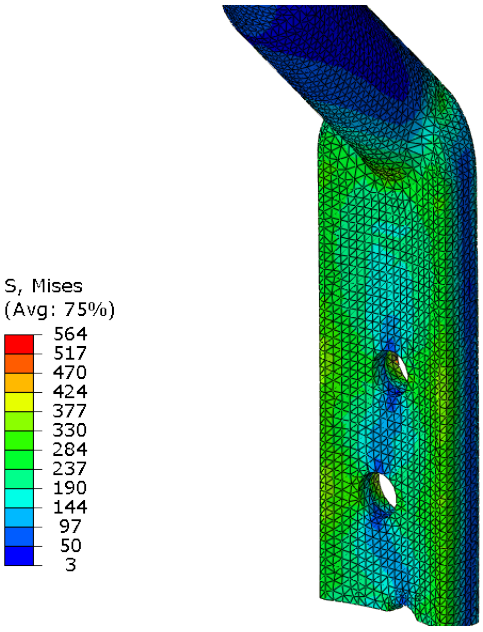

Figure 5.6: Von Mises Stress (MPa) - medial side of plate

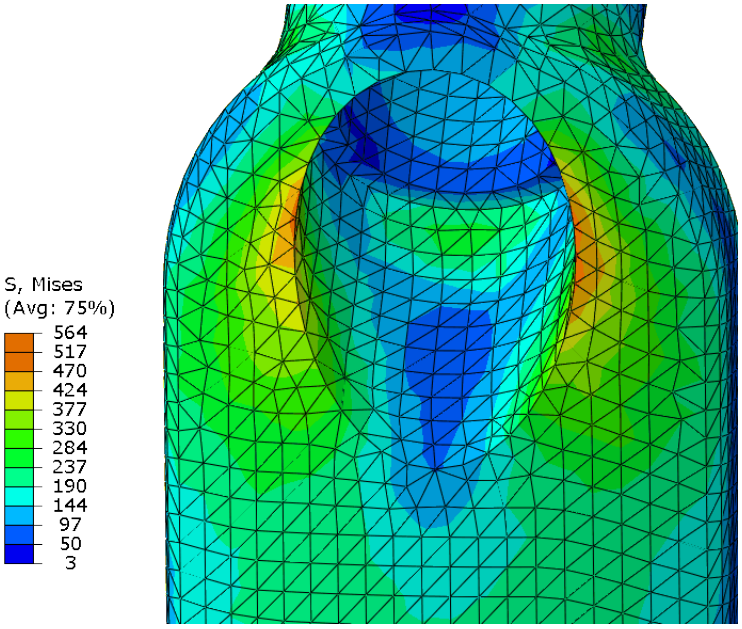

Figure 5.7: Von Mises Stress (MPa) - barrel hole

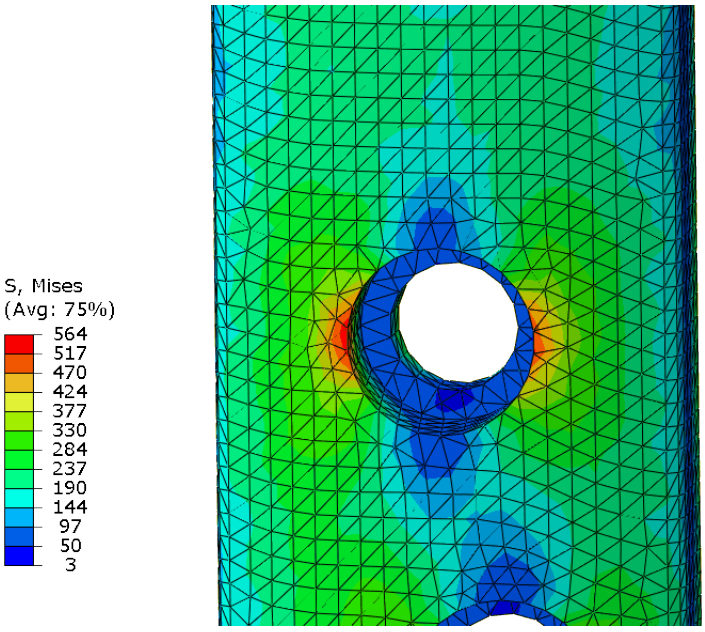

Figure 5.8: Von Mises Stress (MPa) - proximal screw hole

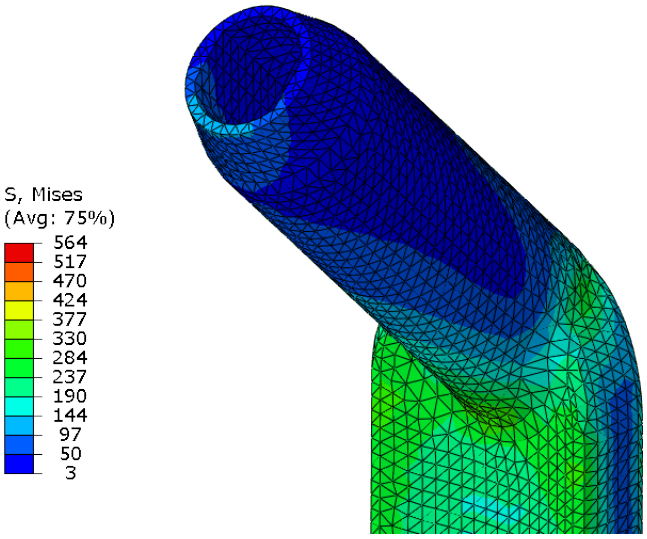

Figure 5.9: Von Mises Stress (MPa) - barrel

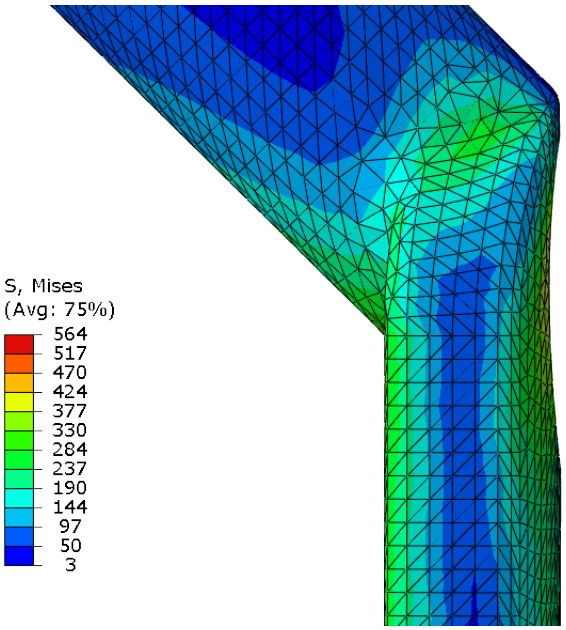

Figure 5.10: Von Mises Stress (MPa) - transition between plate and barrel

From the stress contour plots it can be seen that the straight plate section behaves as would be expected for a beam under bending, with higher stress at the medial and lateral sides of the plate and lower stress in the centre close to the neutral axis. Stress concentrations occur at the edges of holes in the plate. The barrel itself is subject to relatively small stresses, this is due to it's short length resulting in a low bending moment and relatively high second moment of area. Another stress concentration can be seen at transition between the barrel and the plate. The stresses in the plate are higher than the yield strength for 316 stainless steel (approx. 205 MPa) in many areas of the model, with the stress concentrations being more than double the yield stress. As no observable yielding occurred during the mechanical test it can be assumed that the magnitude of the stress in the model is not accurate, however the locations of high stress are in the areas where they would be expected.

5.3 Hip Screw in Femoral Shaft Test

Although it is useful to compare the stiffness of any new designs to the current device in isolation, this is not an accurate replication of how the device is loaded in its use. To gain a more accurate comparison between devices a model was created which assessed the stiffness of the device when implanted in bone.

As the intention of this study was to compare designs rather than model the behaviour of the device in the human body exactly it was decided that it was unnecessary to use cadaveric samples when validating the model. Therefore Sawbones® 4th generation composite femurs were used in place of cadaver samples.

The removal of the femoral head would allow the device to be loaded directly, removing any effect that the fracture site may have on the performance of the device. This would allow the interaction between the device and the femur to validated.

5.3.1 Method

5.3.1.1 Mechanical Testing

A Synthes SHS device was implanted, by an experienced orthopaedic surgeon, into a sawbones® 4th generation composite femur with the femoral head intact. Once implanted, the device was removed from the femur and the femoral head was removed using a hack saw. The SHS plate was then replaced and secured with screws inserted

into the same holes drilled during the original procedure. A pin manufactured from mild steel (Figure 5.11) was inserted into the barrel. It should be noted that the shape of this pin differs from that used in the previous model (Figure 5.2). Initially the pin used in this test had the same angled end (Figure 5.12) as used in the isolated hip screw test, however it was found that a slight difference between the positioning of the implant in the test and in the model, resulted in a significant change in the location of the contact point between the load pin and the testing machine. This change in position affected the stiffness results as it changed the length of the moment arm of the load. Using the alternative load pin with the square end reduced the possible variation in contact location.

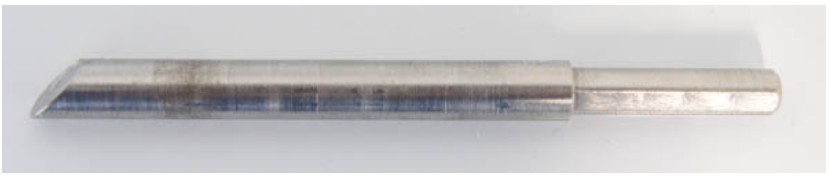

Figure 5.11: Original pin used to load SHS in femoral shaft test.

Figure 5.12: Modified pin used to load SHS in femoral shaft test.

The femur was secured was secured at the mid shaft using Isopon P38 polyester filler and a custom made clamp, as described in Section 4.1.2. The test was carried out using the Electroplus E10000 Linear-Torsion Floor Instrument, (Instron, Norwood, MA, USA). The test setup can be seen in Figure 5.13. The specimen was initially loaded by displacing the end of the pin downwards by 5 mm, however this resulted in plastic deformation of the pin (Figure 5.14). A new pin was manufactured and the applied displacement was reduced to 2 mm at a rate of 0.1 mm/s. The load was recorded using a 1 kN load cell. The test was run 5 times.

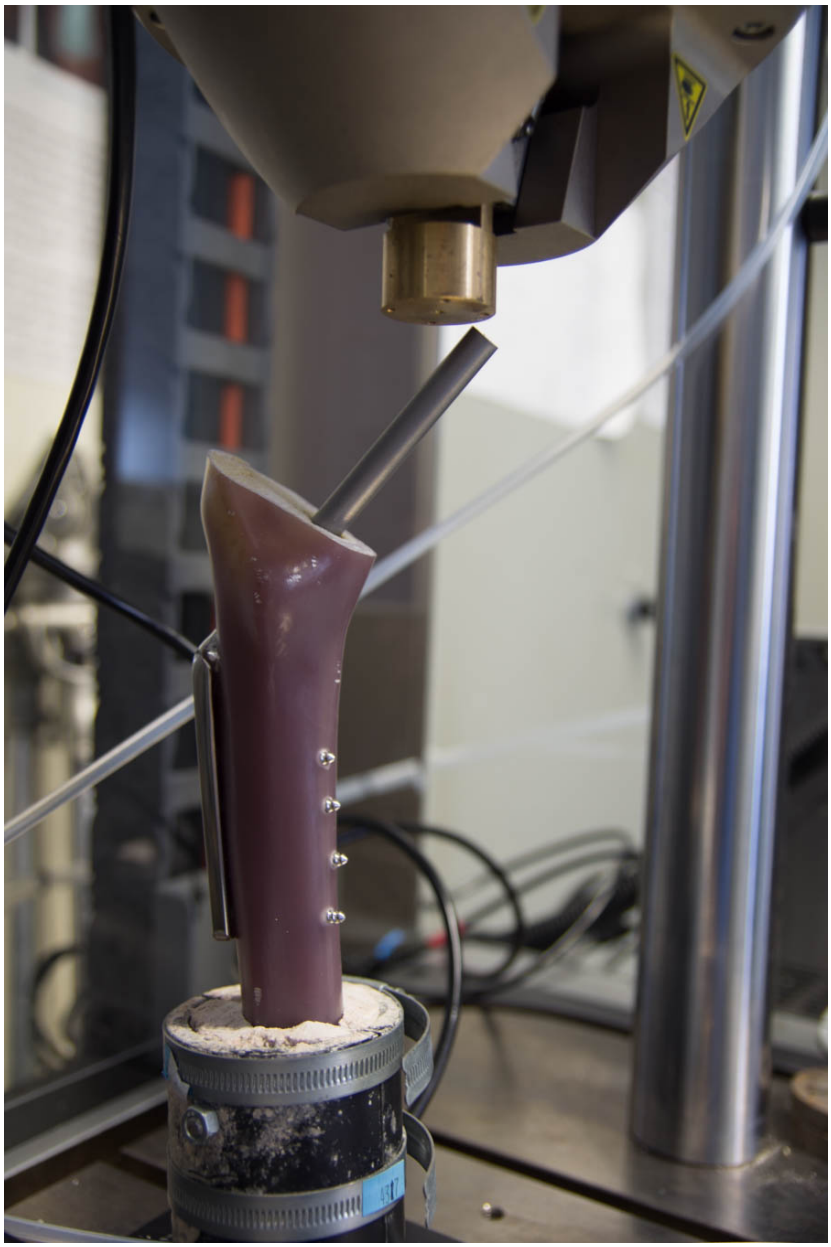

Figure 5.13: Mechanical test setup.

Figure 5.14: Deformed test pin after initial tests.

5.3.1.2 FEA

A model of each SHS design was implanted in a femur using Autodesk Inventor, the femur was cut at 45° to the femoral shaft. The head of the femur and neck screw of the implant were suppressed and a model of the loading pin was inserted. The distal end of the femur was removed and the model was then imported into Abaqus as a step file.

Each component of the model were seeded with the values shown in Table 5.3. These values were identical to those used in the previous validated models. The parts were meshed with linear tetrahedral elements. An extra, part, a flat rigid body, was added to replicate the loader of the testing machine. This loader was meshed with 4 node quadrilateral elements. The number of elements present in the model, excluding the loader, was 525597, the mesh can be seen in Figure 5.15.

Table 5.3: Mesh seeding for each part in femoral shaft models.

Part	Approximate Global Size
Cancellous Bone	1.8
Cortical Bone	2.4
Loading Pin	2
Plate	1

The material properties shown in Table 5.1 were applied with a linear elastic model for stainless steel being used. The screws were simplified to simple cylinders and were fixed to the femur using a tie constraint. The cortical and cancellous components of the femur were also fixed together using a tie constraint.

In order to accurately model the interaction between the implant and the femur it was essential to apply a pretension load to the shaft screws during the analysis of this model. A step was added to the analysis in which pretension of 100 N was applied to each screw, allowing the plate to be brought into contact with the femoral shaft. The magnitude of the pretension load was selected by running the model several times with gradually increasing loads until the load was sufficient to bring the plate into contact with the bone. The load is below the pull-out force for the 4.5 mm screws used when implanting the SHS, as measured in bone to be 600 N–6440 N by Strømsøe et al. (1993) and 5210 N–7470 N in third generation Sawbones® femurs by Zdero et al. (2006).

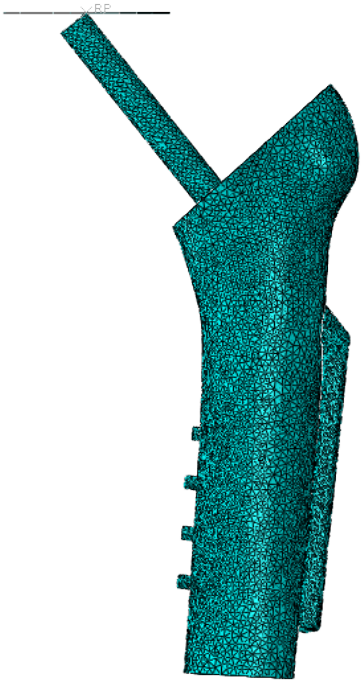

Figure 5.15: SHS implanted in proximal femur with head removed mesh.

A second step was the added in which the loader was displaced by 2 mm onto the pin. The model was solved over 500 automatic time steps with a maximum increment size of 1 and a minimum of 0.005.

During the pre-tensioning process it was possible for the model to become unstable due to unconstrained motion between components. It was therefore necessary to add weak springs between some components (Figures 5.16 and 5.17). Automatic stabilization was also used during the pretension step using the default settings (dissipated energy fraction 0.0002 and a maximum ration of stabilization to strain energy of 0.05).

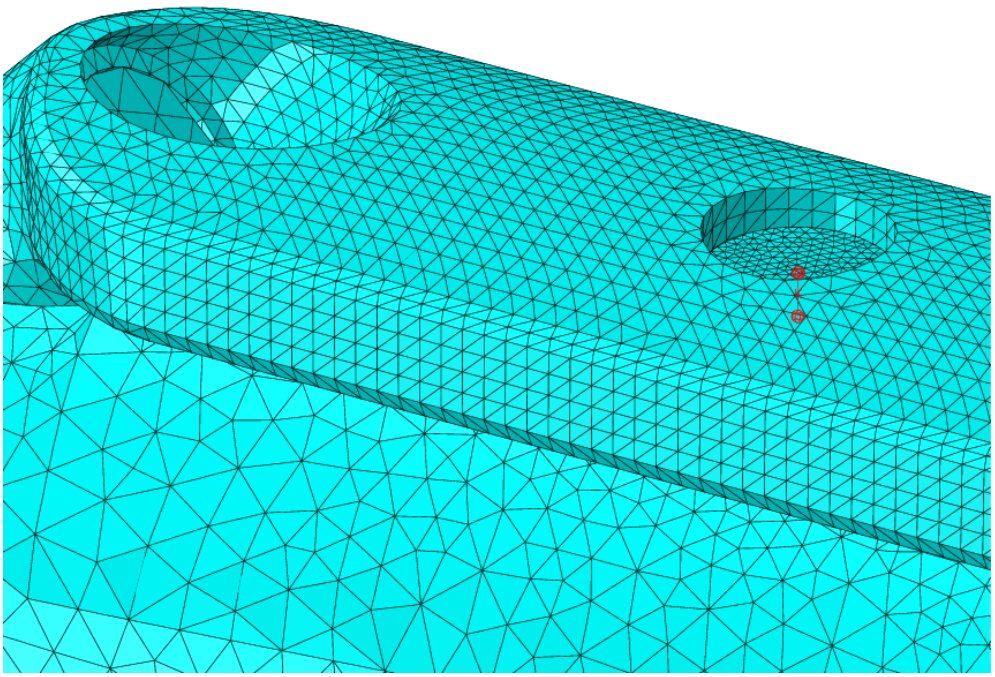

Figure 5.16: Spring added between proximal screw and SHS plate, shown in red.

5.3.2 Results

The results from the 5 mechanical test runs are shown in Figure 5.18 along with the results from the FEA of the Synthes device.

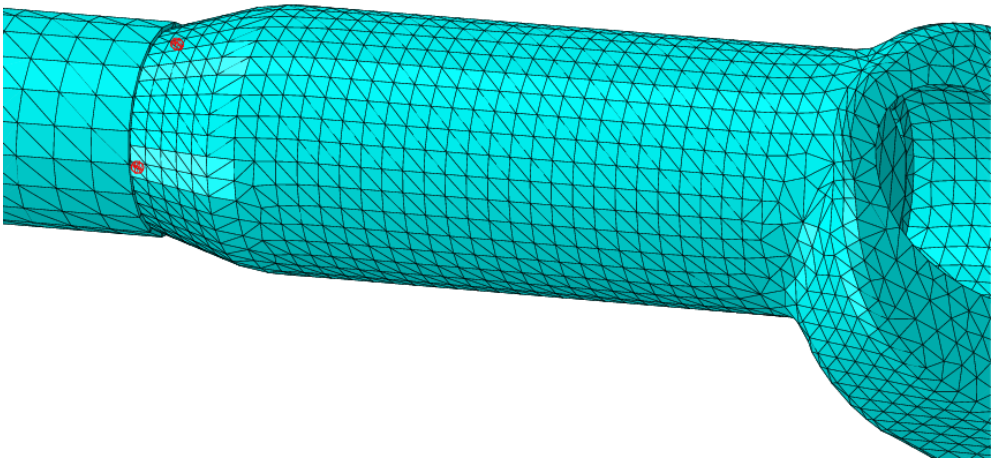

Figure 5.17: Springs added between pin and SHS plate, shown in red.

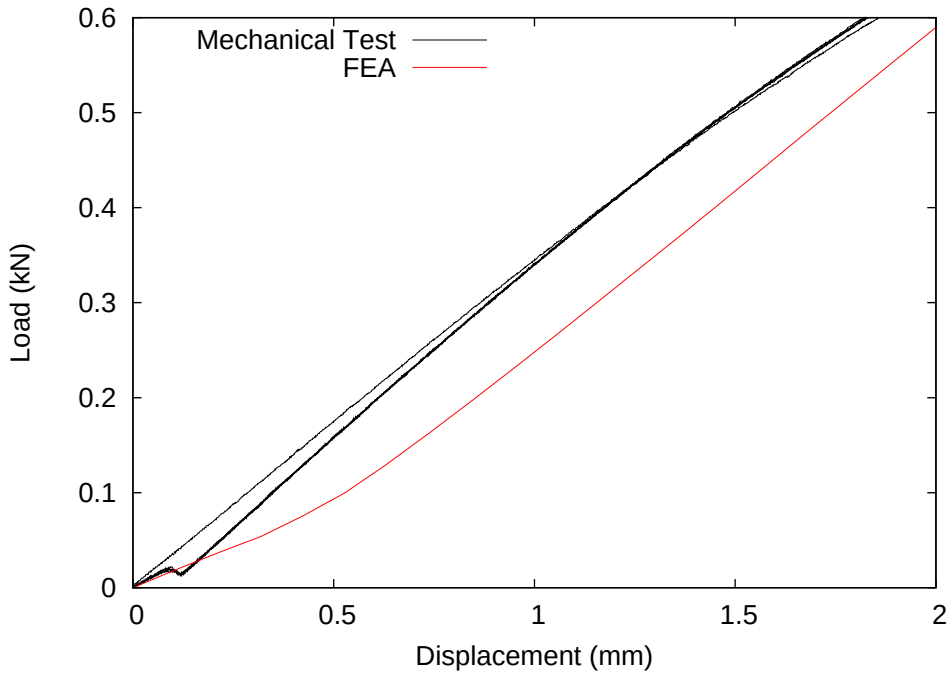

Figure 5.18: Load displacement curves for the mechanical tests and the final FE analysis

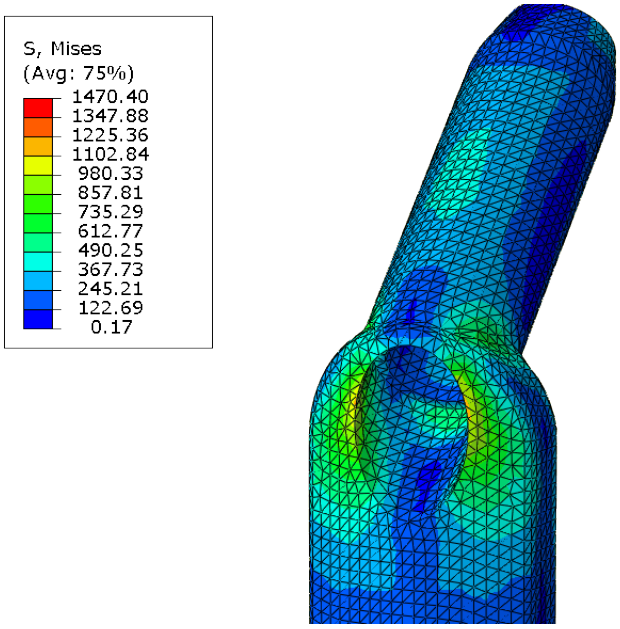

Figure 5.19: Von Mises Stress (MPa) - Plate-barrel joint, lateral side.

Results from the mechanical test show an approximately linear behaviour, 4 of the 5 tests exhibit a small dip in the load at around 0.1 mm of displacement. The average stiffness of the test runs was 0.332 kN/mm. The during the initial 0.5 mm displacement the FE model does not behave linearly, however after 0.5 mm the model exhibits linear behaviour with a stiffness of 0.338 kN/mm, which differs from the stiffness recorded in the mechanical test by less than 2%.

Figures 5.19 to 5.21 show contour plots of the stress within the plate. The maximum stress seen in the plate was 1470 MPa at the contact point between the loading pin and the proximal end of the barrel.

Figures 5.22 and 5.23 show the stress in the bone around the area which interacts with the barrel. The highest stress seen in this region was 56.9 MPa in the cortical bone at the lateral side of the hole into which the barrel is inserted.

5.3.3 Discussion

During the initial 0.5 mm of displacement the FE model does not behave in a similar manner to the mechanical test. This may be due to the design of the femoral shaft screws and the pretension that was applied. The screws and screw holes on the current

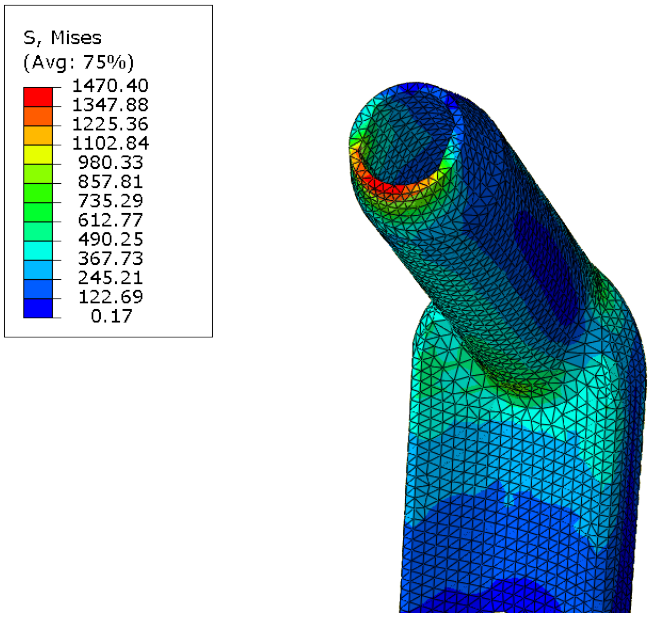

Figure 5.20: Von Mises Stress (MPa) - Plate-barrel joint, medial side.

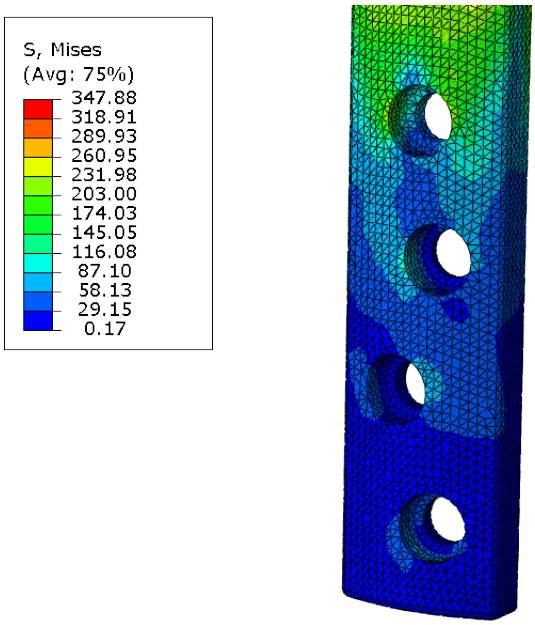

Figure 5.21: Von Mises Stress (MPa) - Lateral side of plate.

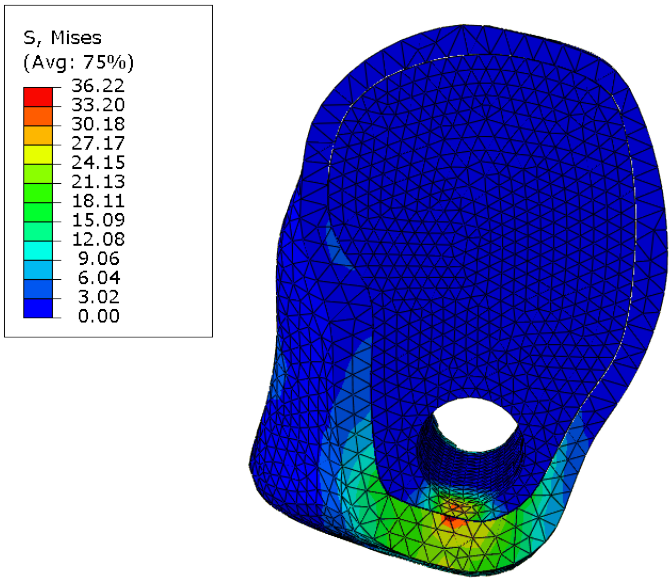

Figure 5.22: Von Mises Stress (MPa) - Medial side of fractured shaft.

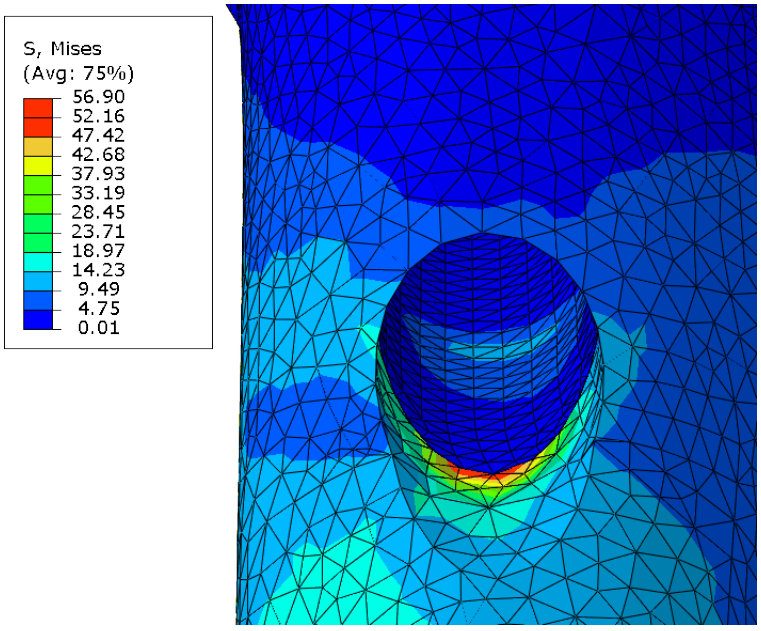

Figure 5.23: Von Mises Stress (MPa) - Lateral side of fractured shaft.

designs of SHS are complex geometries. Due to the complexity of contact simulation it was decided to simplify these screws and screw holes. This may have lead to the model behaving a different manner to the device during the initial stages of loading. This difference in initial behaviour may also be caused by the lack of friction in the model. However when displaced beyond 0.5 mm the model displays linear behaviour with a stiffness of 0.338 kN/mm, effectively the same stiffness recorded during the mechanical test. Past the initial loading the model can therefore be considered an accurate representation of the device implanted in an artificial femur.

The stress results from this model are not directly comparable with the results gained from the isolated hip screw test as the loading was not identical between the tests. However it is interesting to note the differences in stress patterns. Looking at the stress in Figures 5.19 to 5.21 it can be seen that the stress around the transition region between the barrel and the plate is much higher relative to the stress in the plate, than the stress seen in Figures 5.5 to 5.10. This indicates that the straight plate section of the SHS is supported by the shaft of the femur and that the majority of the deflection must therefore take place in the angled region.

Figure 5.22 shows an area of high stress around the hole, this stress was caused by contact between the loading pin and the bone. As the loading pin has a larger diameter than the screw used with the device, it cannot be said whether this stress would exist when the device is in clinical use as the screw may not come into contact with the bone. Figure 5.23 shows two interesting areas of stress, firstly a region of high stress occurs in the cortical bone at the edge of the hole. This stress is caused by the implant making contact with the bone. Further into the hole a region of lower stress can be seen, this has occurred due to contact between the tip of the barrel and the cancellous bone. These two regions of bone are the areas which appear to support the device, providing resistance to bending and therefore it will be interesting to see how the stresses in these regions vary when different implant designs are modelled.

5.4 Fractured Femur Test

This test aimed to replicate the behaviour of the implant within a fractured femur including the femoral head. Due to necessary simplifications, the model cannot be considered to replicate the behaviour of the device in vivo. However it is the most

realistic model created within this study and is useful for the comparison of different designs of device.

5.4.1 Method

5.4.1.1 Mechanical Testing

An SHS was implanted in a Sawbones® artificial femur which had been cut at 45° to the femoral shaft in the trochanteric region to simulate a extracapsular proximal femoral fracture. The distal end of the femur was removed and the femur was secured at the mid shaft using Isopon P38 polyester filler and a custom made clamp. The test was carried out using the Electroplus E10000 Linear-Torsion Floor Instrument, (Instron, Norwood, MA, USA). The specimen was loaded by displacing the end of the head downwards at a rate of 0.1 mm/s. The load was recorded using a 10 kN load cell, the experimental setup can be seen in Figure 5.24.

A displacement of 1 mm was applied to the specimen 5 times in order to bed the specimen in and reduce the chance of any slippage occurring during the testing. The specimen was then displaced by 5 mm 15 times, before being tested to failure in either the bone or the implant.

This loading condition represents mid-stance in a patients gait, with a single force acting vertically downwards. During normal walking the head of the femur will experience a force which varies throughout the gait and which has components acting in the lateral, and anterior/posterior directions along with the vertical force included in this test. The decision to simplify the loading conditions to mid stance was taken in order to allow a relatively simple test jig to be manufactured to hold the specimen in place. The force acting in the lateral direction during walking would act to compact the the fracture site, therefore increasing frictional between the fragments, it could therefore be considered that it's exclusion from the test creates a more challenging loading condition for the implant to overcome. The anterior/posterior force acts to create a torque on the implant, which may play a more important role than the lateral load. The fracture site in the test was a straight cut and could therefore be considered a conservative representation of a fracture site before any healing had occurred. It has been shown that patients after surgery load their injured leg to only 50% of the load which they support on their uninjured leg (Koval et al., 1998). It is also stated by Hoppenfeld and Murthy

(2000) that a patients step length is shortened after fracture and that they may have a "tentative, fearful gait". These shortened steps and reduced loads along with the possible use of walking aids such as crutches, may lead to the magnitude of the forces in the anterior/posterior directions being reduced. As the patient heals and becomes more confident these loads may begin to return back to their pre-fracture levels, however as they do so the fracture will be in a different condition to that modelled in this test. It was therefore decided that the use of mid-stance loading was acceptable for this test, however its exclusion should be taken into account when drawing conclusions from the results.

5.4.1.2 FEA

The model of the device was created in Autodesk Inventor and Implanted into a femur. The femur was cut at 45° to the femoral shaft in the trochanteric region to simulate a fracture. The position of this cut was identical to that made in the femoral shaft test(Section 5.3). The model was imported into Abaqus as a step file. A flat rigid body was added to the models to replicate the loader of the test machine.

The models were meshed with linear tetrahedral elements, the mesh contained 742422 elements, the seeding for each component is shown in Table 5.4. The rigid body was meshed with 4 node quadrilateral elements. The mesh can be seen in Figure 5.25.

The threads of all the screws were simplified to be cylinders and tie constraints were used to connect them to the holes in which they were placed. Contact was modelled using general contact, with frictionless tangential behaviour and hard normal behaviour.

As with the femoral shaft test (Section 5.3), a pre-tensioning step was added before the bending load was applied. This step involved applying pretension load of 100 N to the 4 shaft screws. As with the femoral shaft test, a weak spring was added between the proximal shaft screw and the plate, and automatic stabilisation was used, to prevent unconstrained motion during the pre-tensioning process.

The model was loaded by displacing the rigid body by 5 mm down onto the head of the femur. The model run over 500 time steps with a maximum increment of 1 and a minimum of 0.005.

Figure 5.24: Fractured femur test setup.

Table 5.4: Mesh seeding for each part in fractured femur models.

Part	Approximate Global Size
Cancellous Bone Shaft	1.8
Cortical Bone Shaft	2.4
Cancellous Bone Head	2
Cortical Bone Head	1.8
Plate	1
Neck Screw	2
Shaft Screws	0.5

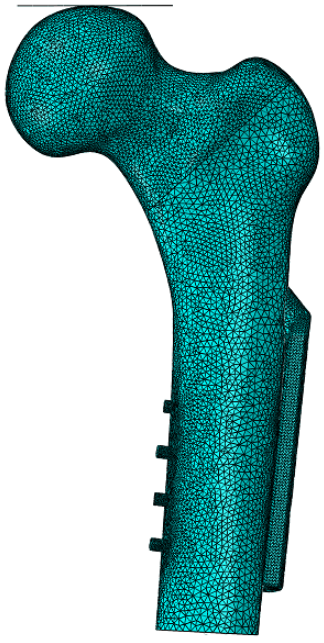

Figure 5.25: SHS implanted in proximal femur with fracture mesh.

5.4.2 Results

The mean and standard deviation of the 15 test results was calculate and plotted in Figure 5.26 along with the results from the FEA of the Synthes plate. It can be seen that the FEA results fall within the standard deviation of the mechanical test, however the stiffness curves do not have a similar shape.

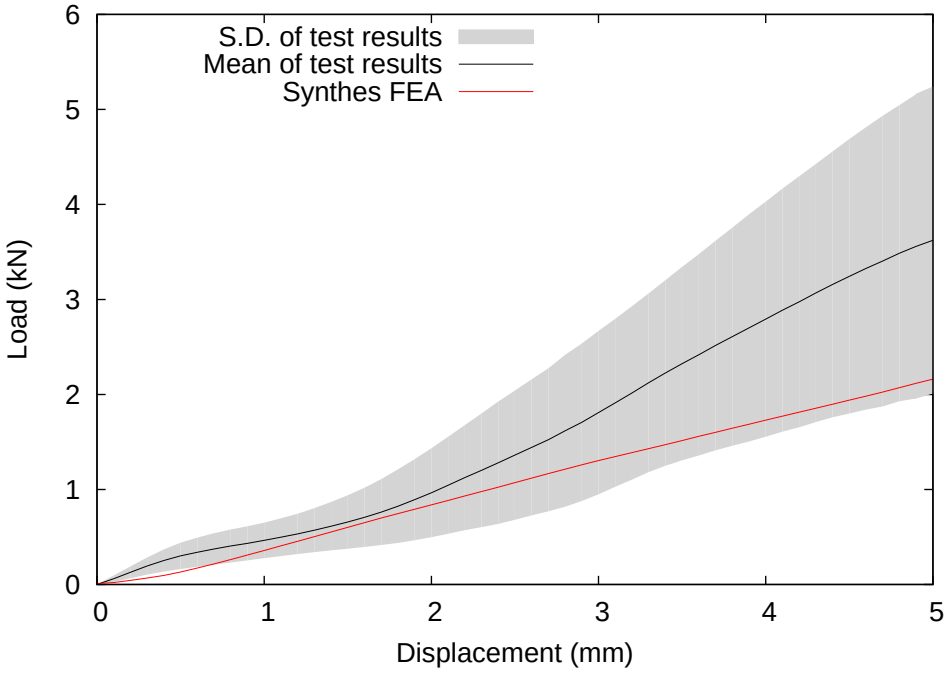

Figure 5.26: Mean load displacement curve for the mechanical test with standard deviation and Synthes FEA results.

During the 16th run of the test, fracture occurred on the femoral head of the femur. The fracture can be seen from two different views in Figure 5.27, the load displacement curve can be seen in figure 5.28. It can be seen that the failure occurred at a load of 6 kN.

Figures 5.29 and 5.30 show the maximum principle strain and the displacement contour plots from the model containing the Synthes device. Figures 5.31 and 5.32 show the maximum principle strain contour plots for the Synthes screw and plate respectively.

Figures 5.33 to 5.35, show the Von Mises stress within the cortical and cancellous components of the femoral shaft. Figures 5.36 to 5.38 show the Von Mises stress with

(a) Distal view. **(b)** Proximal view.

Figure 5.27: Fracture on femoral head fragment, which occurred during testing.

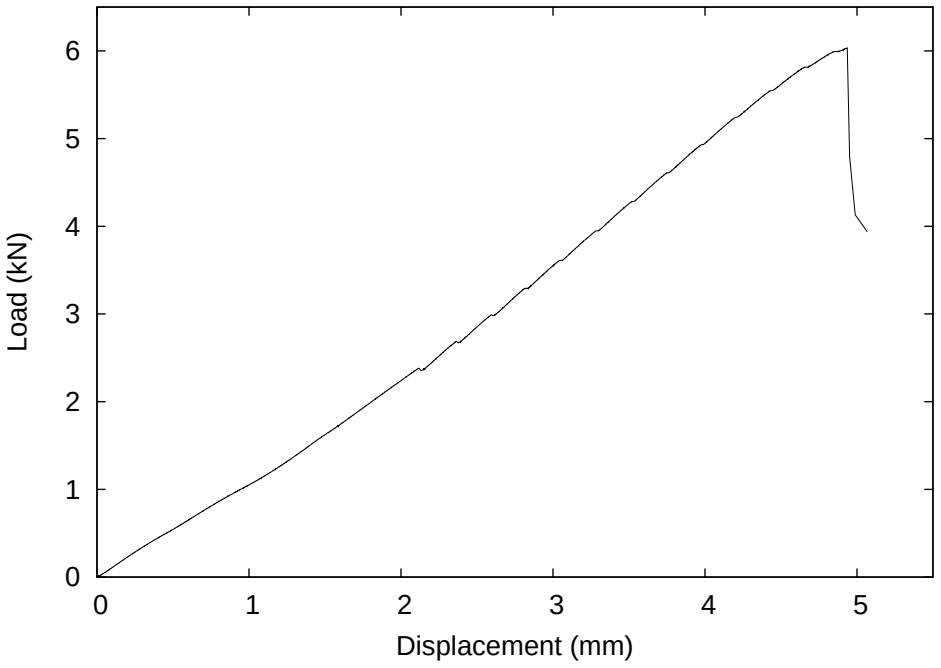

Figure 5.28: Load displacement curves 16th run of test during which fracture of the femoral head occurred.

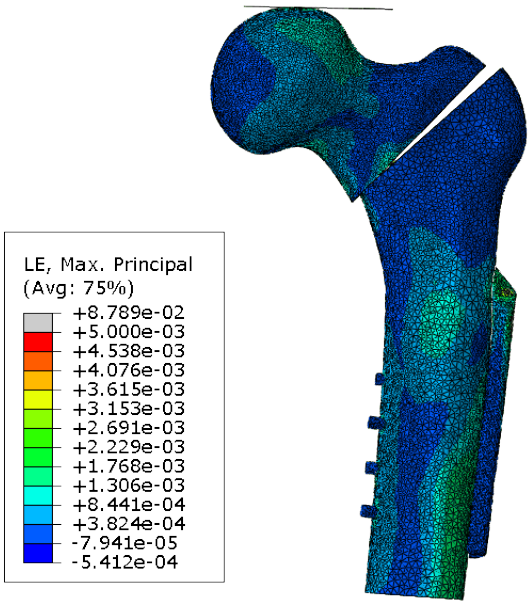

Figure 5.29: Strain contour plot for Synthes implant in fractured femur.

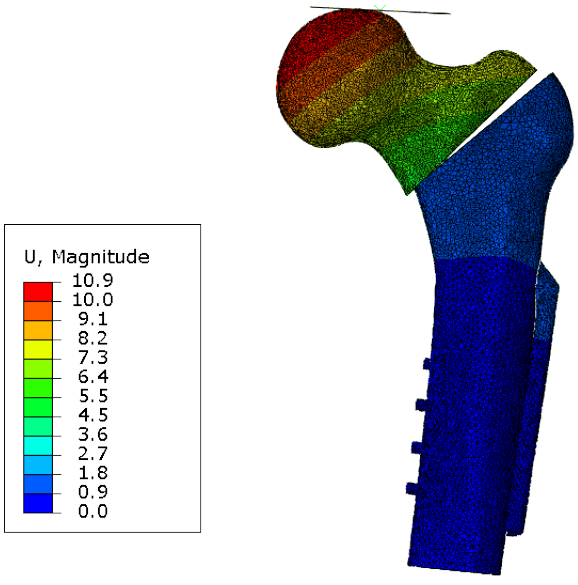

Figure 5.30: Displacement (mm) contour plot for Synthes implant in fractured femur.

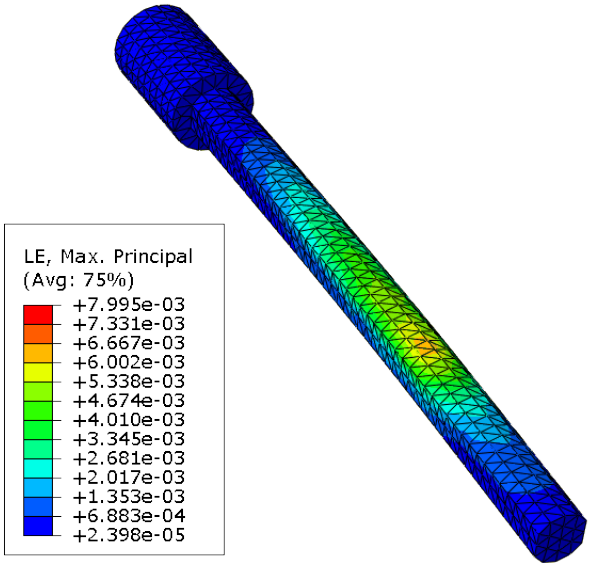

Figure 5.31: Strain contour plot of the neck screw for the Synthes implant in fractured femur.

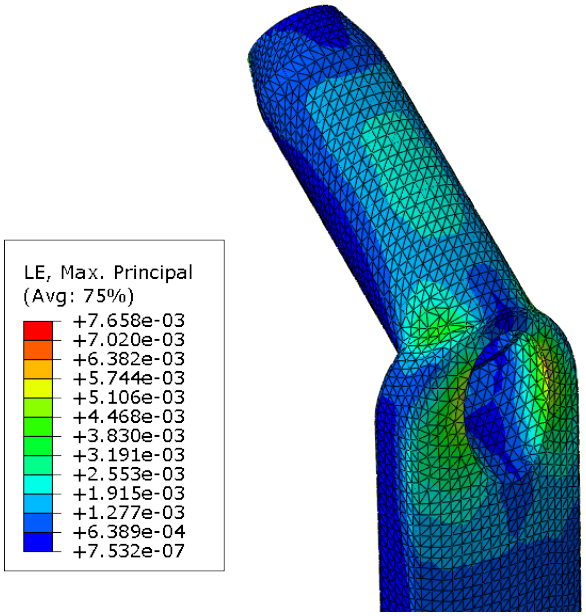

Figure 5.32: Strain contour plot of the plate for the Synthes implant in fractured femur.

in the cortical and cancellous components of the femoral head. Figures 5.39 to 5.41 show Von Mises stress in the SHS device.

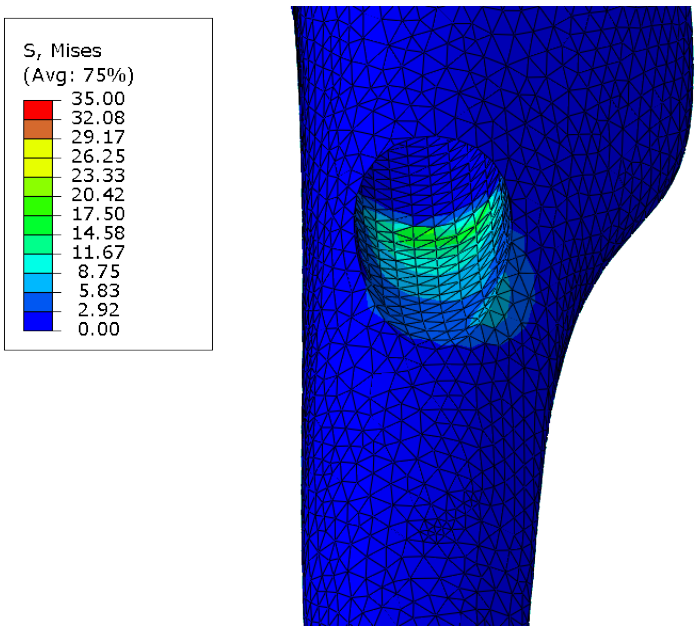

Figure 5.33: Von Mises Stress (MPa) - Lateral side of fractured shaft, cancellous bone.

5.4.3 Discussion

The results from the mechanical test show a reasonable amount of variation between test runs, this variability makes it difficult to produce a model which can be said to accurately model the mechanical test. The reason for this variation in mechanical test results, is likely due to the specimen not returning to its initial position after a test run. The materials used to manufacture the artificial bones are not linear elastic and exhibit some time dependant behaviour, therefore after loading and unloading the bone may not return exactly to its initial position. The the screw and barrel of the plate did not fit tightly together, therefore when unloaded the two fragments may return to different relative positions from where they started. The device may have moved within the bone, this could occur with either the neck screw or the plate. Finally the specimen could have moved within test rig or the test rig could have deformed. However as the specimen is held in place in a clamp with two screws passing through it, any permanent displacement of the specimen within the clamp would have to have resulted

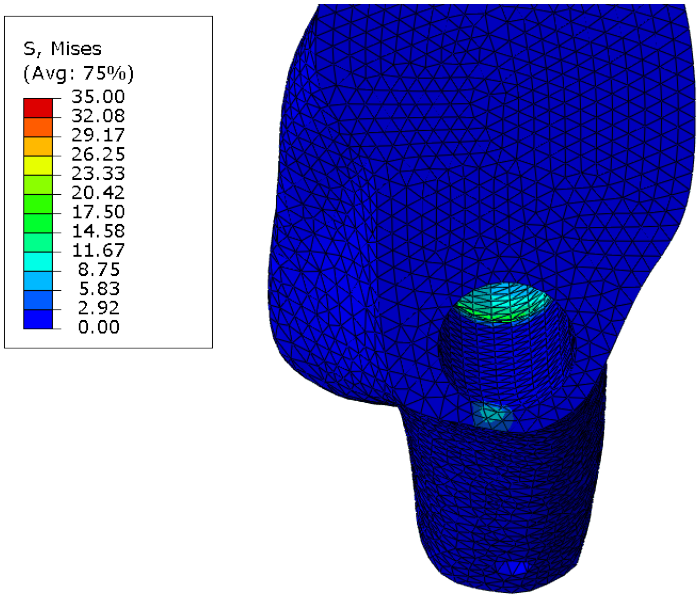

Figure 5.34: Von Mises Stress (MPa) - Medial side of fractured shaft, cancellous bone.

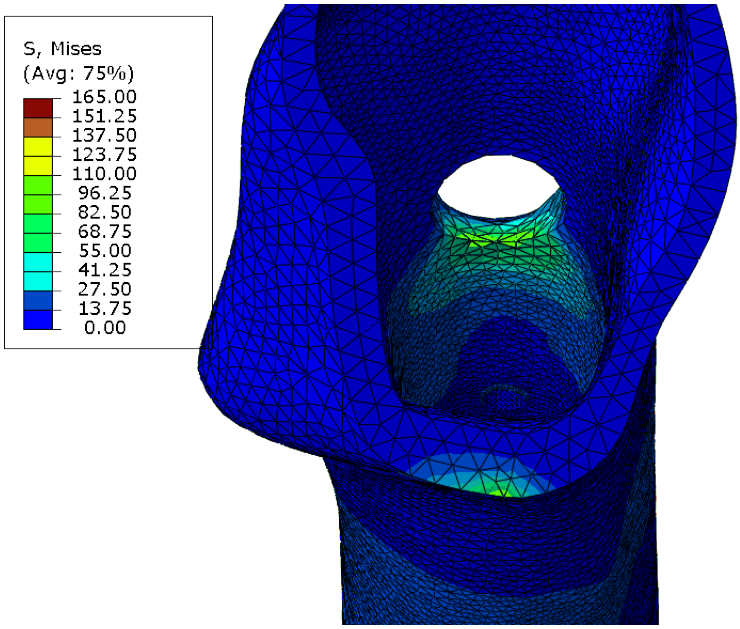

Figure 5.35: Von Mises Stress (MPa) - Medial side of fractured shaft, cancellous bone.

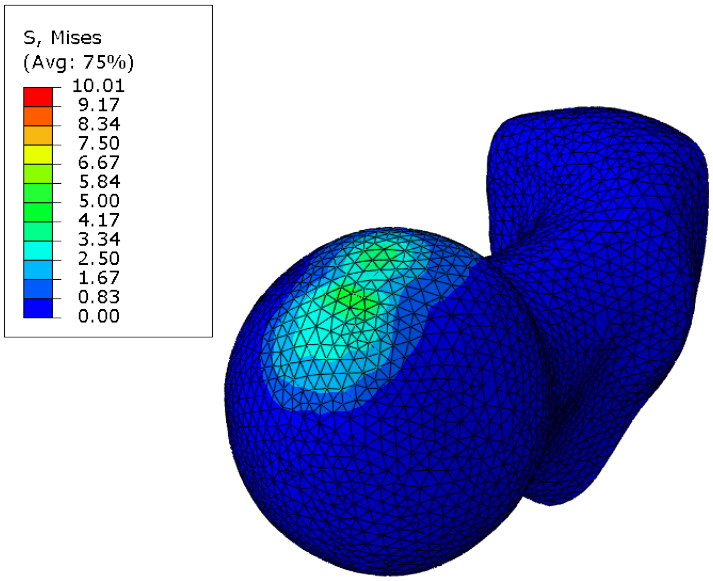

Figure 5.36: Von Mises Stress (MPa) - Femoral head, cancellous bone.

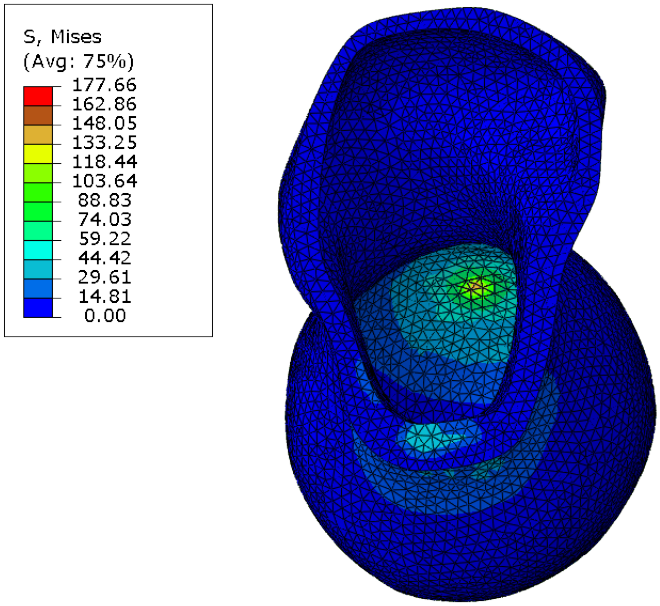

Figure 5.37: Von Mises Stress (MPa) - Femoral head, cortical bone internal view.

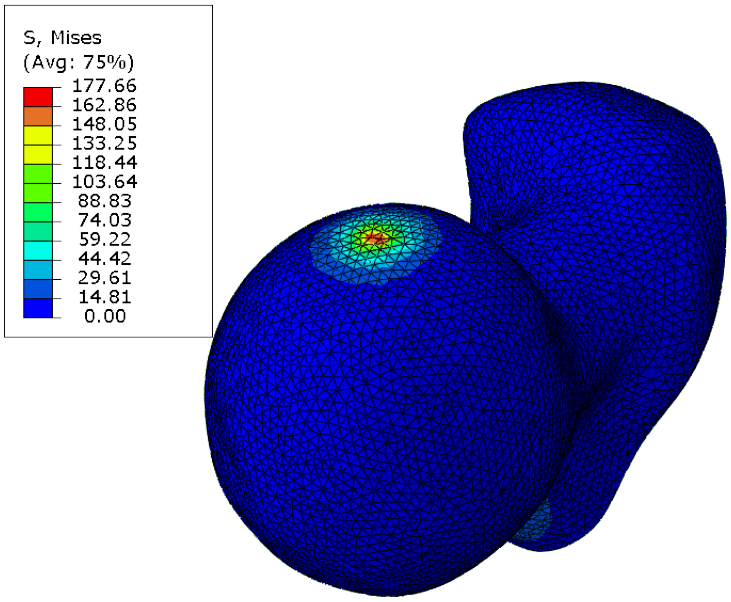

Figure 5.38: Von Mises Stress (MPa) - Femoral head, cortical bone external view.

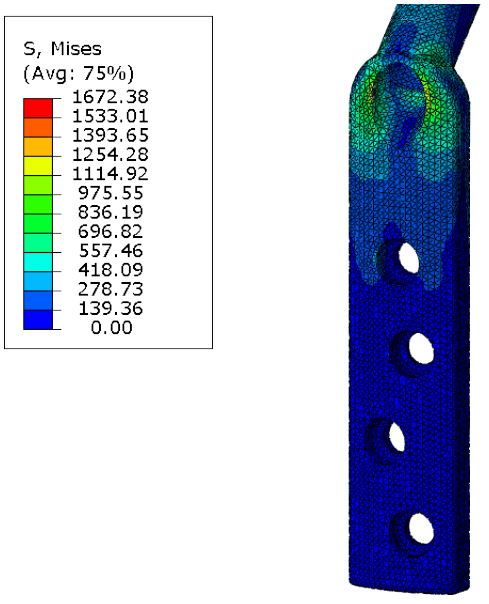

Figure 5.39: Von Mises Stress (MPa) - Plate.

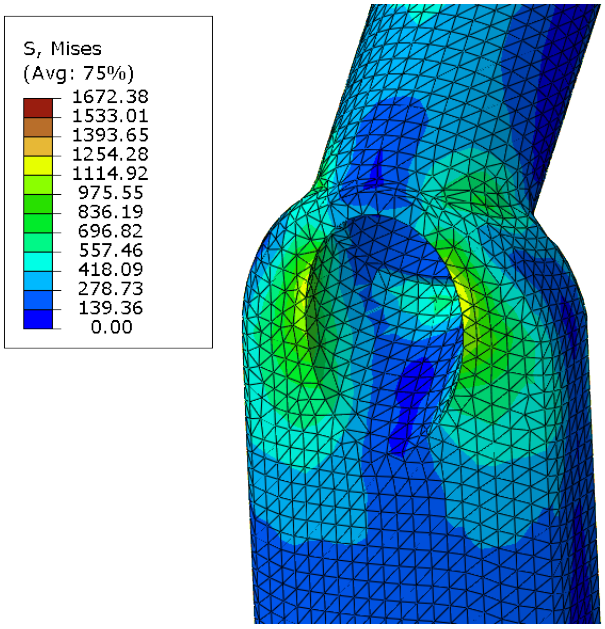

Figure 5.40: Von Mises Stress (MPa) - Plate to barrel transition region, lateral side.

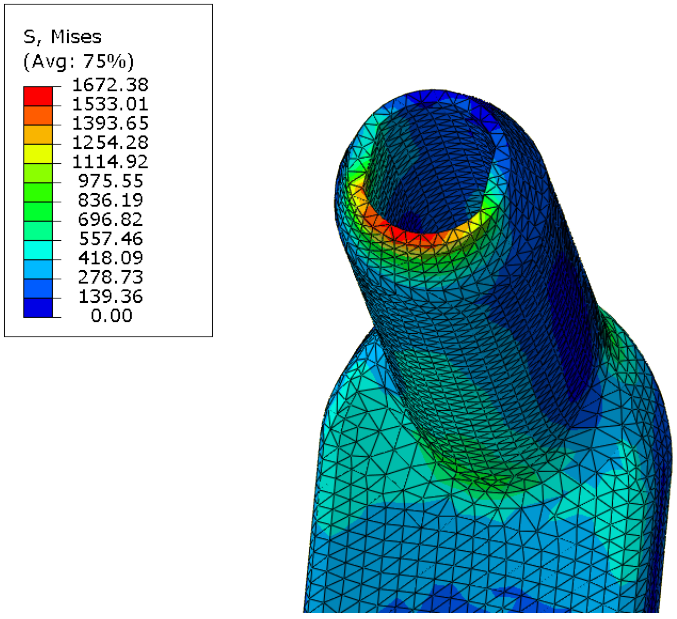

Figure 5.41: Von Mises Stress (MPa) - Plate to barrel transition region, medial side.

in plastic deformation of these screws. As no plastic deformation of these screws was observed the possibility that the specimen moved within the clamp can be excluded. It is also unlikely that there was any significant deformation of the clamp itself as it is considerably stiffer than the specimen. Of the remaining possibilities all could occur within the human body, when the device is under cyclic loading, it is therefore acceptable that these may occur during mechanical testing.

During the 16th run of the test fracture occurred in the femoral head of the test specimen at 6 kN of applied load. This correlates with the results of literature discussed in Section 2.7 which found that cut out of the screw was the was the most common failure mechanism of device (Chirodian et al., 2005; Matre et al., 2013). Figure 5.38 shows an area of high stress at the top of the femoral head. This stress is most likely to be caused by the contact area between the loader and the bone being relatively small. It is possible therefore that the mechanism which caused this fracture is slightly different from cut out seen in patients, which is primarily caused by stress concentrations at the tip of the screw. The model however cannot accurately predict the stress at the screw as the thread geometry was not modelled.

The results from the FEA model do fall mostly within the standard deviation of the mechanical test data and therefore may still be considered useful for comparing different concept designs. However the shapes of the stiffness curves for the mechanical test data cannot be seen in the results from the FEA. There are multiple issues which may have caused this difference in behaviour. The position of the implant in the femur is not identical for both the FE model and the mechanical test specimen. Although this is also true for the for the femoral shaft test (Section 5.3) which used the same femur and implant, and did not show a difference between the model and the mechanical test, it is possible that this misalignment may cause the difference seen in this test. The alignment of the implant in the mechanical test specimen results in separation at the fracture site when unloaded (Figure 5.42a), during loading the fracture sight comes into contact and then begins to separate again. However in the model there is no large separation at the fracture site when unloaded (Figure 5.42b). It is this difference at the fracture it that may cause the model to behave differently from the mechanical test. Alignment of the implant within the model is difficult as it is not possible to ensure the model is identical to the mechanical test.

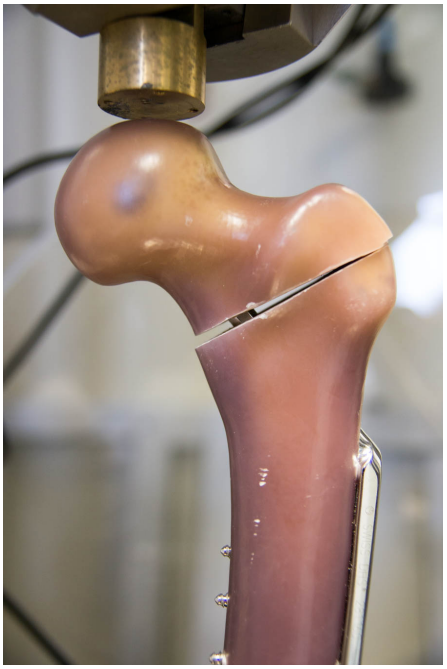

(a) Mechanical Test

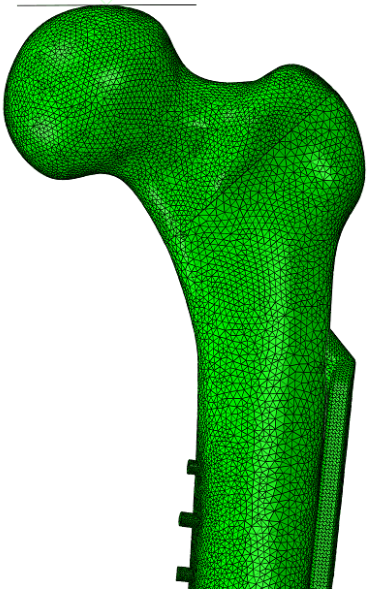

(b) FEA

Figure 5.42: Position of fracture site when unloaded.

Another possible reason for the difference in results may be due to the contact conditions at the fracture site. The fracture site was assumed to be frictionless in the model, in reality the contact conditions were not frictionless however the friction coefficient was unknown. The inclusion of friction within the model increases the computational requirements and can lead to problems solving the model. It was therefore decided that the use of frictionless contact was the best option and this may have lead to the difference in results.

From Figure 5.29 it can be seen that aside from the distal lateral area the femoral shaft is under relatively little strain as is the femoral head. When the displacement is viewed in Figure 5.30 it can be seen that the shaft undergoes very little displacement compared to the femoral head. This indicates this lack of strain within the cortical bone and significant displacement of the head indicates that the majority of the displacement is being accommodated by either bending of the screw or plate or displacement of the screw within the barrel.

Figures 5.31 and 5.32 show contour plots of the maximum principle strain in the neck

screw strain and plate. It can be seen that the maximum strains in both components are similar. This would indicate that bending of the screw and the plate both contribute to the displacement of the femoral head.

The area of stress shown in Figure 5.34 corresponds with the area of cancellous bone with which the end of the barrel comes into contact, while the area of high stress around the hole in Figure 5.35 is caused by the distal end of the barrel. As with the results from the femoral shaft tests, it may be interesting to observe the difference in these stress areas when different device designs are modelled. A small area of stress can be seen at the bottom of the hole in Figure 5.34, this indicates that the screw must have come into contact with the cancellous bone, although the stress is relatively low and therefore it is not likely to be providing any considerable support. It may be the case that more compliant devices result in a higher stress in this region which could increase the risk of fractures occurring.

The stress within the plate appears to show a similar pattern to that seen in the femoral shaft test. The magnitude of these stresses cannot be directly compared due to the difference in loading, however the similar pattern gives some confidence that the shaft test is a reasonable simulation of the the interaction between the plate and bone.

6

Concept Generation

The development of a product is a complicated process that involves balancing several different requirements to create a design which is suitable for the purpose intended. A robust design procedure can be a valuable tool to aid this process and help to ensure that the best design is produced, one such procedure is "Total Design", developed by Stuart Pugh (1991).

Pugh's method centres around a six stage process know as the design core:

- Market
- Product Design Specification
- Conceptual Design
- Detailed Design
- Manufacturing
- Sales

While it is important to progress through the design procedure in a logical manner, from beginning to end, product design is an iterative process and it is therefore often essential to return to previous steps in the procedure to take into account new information that was gained from subsequent steps.

The chapter describes application of the first three stages of the Pugh total design process to the development of a MISHS. The aim of this project was to produce a

prototype of the device, as such the detailed design, manufacture and sales stages were not carried out within this project.

6.1 Market

The market stage of the process is centred around research of the current devices on the market and the needs of the users. It begins with a design brief which states what is to be designed and aims to collect the information required to create the product design specification.

The design brief for this project was to create an SHS device which can be inserted using MI surgical techniques. As the project aim was the further development of a current device, the main focus of the research stage was in understanding the features of the current design along with identifying any existing patents for similar devices.

A literature search, into the history of proximal femoral fracture treatment, was carried out. The results of this search, detailed in Section 2.4, give a valuable insight into the development of the current design and what features would have to be maintained in any new design.

A patent search was carried out which identified two similar devices, Gotfried (1994) and Kyle (1984), the Gotfried device is discussed in Section 2.6.2 however the Kyle device could not be found in any scientific literature. The Kyle device appears to remove a key feature from the SHS design, current SHS devices use flats on the neck screw to prevent rotation of the screw within the barrel of the plate, there is no such feature on the Kyle device. The lack of a de-rotation feature could cause instability at the fracture site.

6.2 Product Design Specification

The results from the research phase of the design procedure were utilised to form a product design specification.

The design requirements of an SHS device:

- Maintain alignment of bone fragments
- Prevent rotation of the femoral Head

- Allow sliding between screw and plate
- Support full weight bearing
- Be manufactured from grade 316 stainless steel

It was important to incorporate all the design requirements of a standard SHS device into the design requirements for the new device, this would ensure that the new device would function in a similar manner to the old. In addition to the design requirements for the current device, several new requirements were added.

- Minimise the length of incision required for implantation
- Simple surgical procedure
- Have similar overall dimensions to current devices
- Device should be compatible with current screw designs
- Have a similar mechanical performance to current devices

The implantation procedure requires the barrel of the plate to be inserted along a guide wire at approximately 45° the shaft of the femur. The incision length required is therefore related to the height of the barrel (h_B) as shown in 6.1. As the current barrel and plate section of the current device are rigidly fixed the h_B is the length of the plate. In order to reduce the incision size it was necessary to reduce the height of the barrel section which is slid along the guide wire.

The implantation of an SHS is a relatively simple procedure which consists of the following steps:

1. Reduce Fracture
2. Insert Guide Wire
3. Confirm Guide Wire Placement
4. Determine Insertion Depth
5. Calculate Reaming Depth

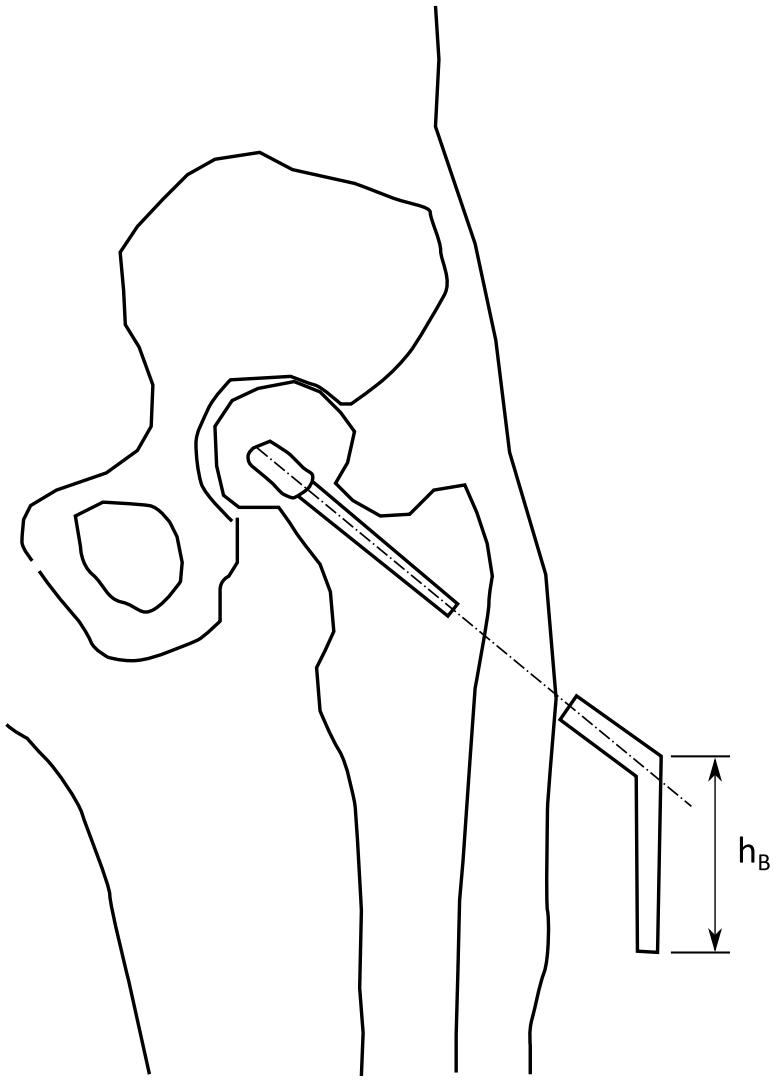

Figure 6.1: MI technique for inserting a standard SHS (Wong et al., 2009).

6. Ream Hole for Screw and Plate
7. Tap hole
8. Insert Lag Screw
9. Align Screw
10. Insert Plate
11. Seat Plate
12. Fix plate to femur

It was thought that significant changes to the surgical procedure may discourage adoption of the new device by surgeons, particularly any steps that added significant time or complication to what is currently a quick and routine surgery. It was therefore decided to maintain as much of the current procedure as possible. As the device would be designed to work with the current screws, steps 1-9 were to be identical for the new device. Step 10 would be replaced with a series of steps which would allow the newly designed plate to be inserted through a small incision, approximately 50 mm, before steps 11 and 12 were carried out. Step 12 would differ from the current surgery as the screws would have to be inserted percutaneously.

6.3 First Conceptual Design Stage

The process by which the first concepts were generated was unstructured, initial ideas were noted down and sketched over a period of a few weeks as background research into the device was carried out. During the design process these ideas were then refined and evaluated using Pugh's methodology.

The initial conceptual design stage generated three concepts (Figure 6.2): all three concepts followed a similar design, separating the one piece plate into a plate and a barrel that are fixed together using a a threaded connector. Concept 1 featured an external thread on the barrel which would be inserted though a hole in the plate and secured using a nut. Concepts 2 and 3 featured an internal thread on the barrel, a screw would be inserted through the plate and inserted into the barrel.

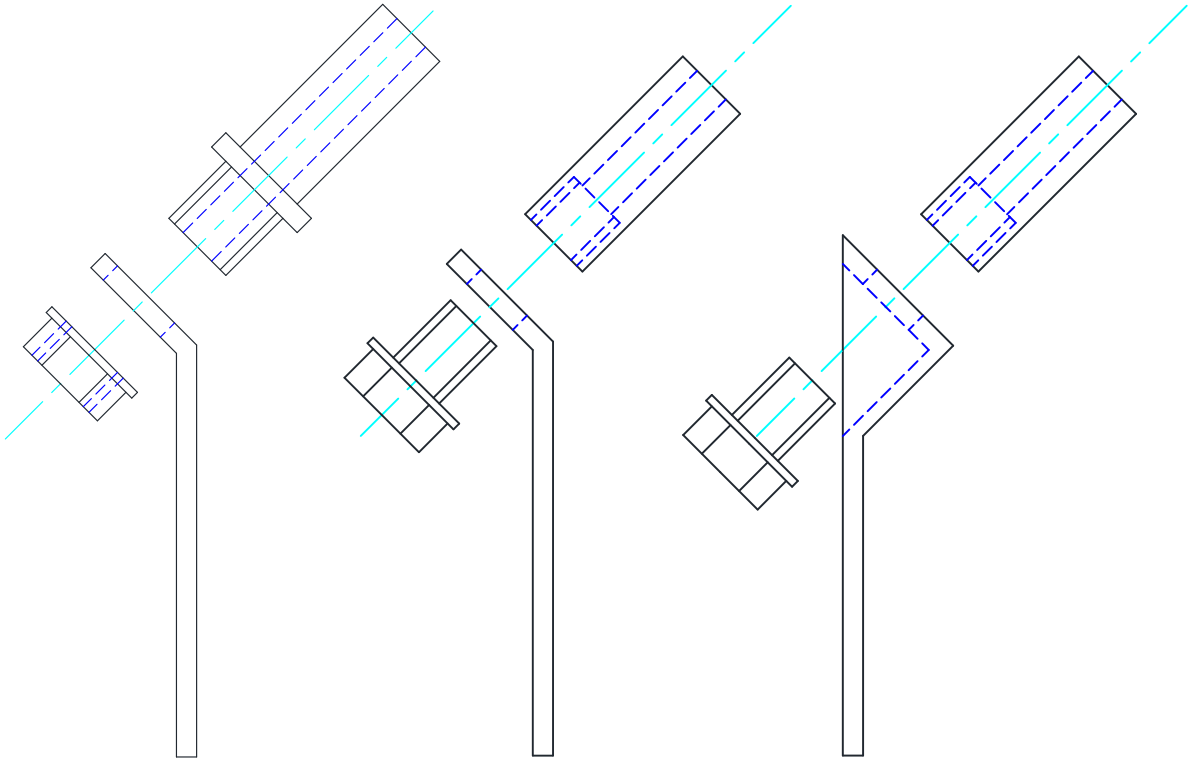

(a) Concept 1 **(b)** Concept 2 **(c)** Concept 3

Figure 6.2: Concepts generated in the first stage of conceptual design

Both concepts 1 and 2 have large protrusions on the lateral side, concept 3 was an attempt to remove this large intrusion by moving the connection medially. However when to scale sketches were drawn, it was realised that the proximal end of the plate would have to be very large to accommodate the joint and that a large section of bone would have to be removed to allow the plate to be implanted. It was also found that for concepts 2 and 3 the screw which connected the parts may block the screw from sliding completely through the device. It was therefore decided that concepts 2 and 3 should be removed from consideration completely.

Concept 1 was considered to be a viable design however it was felt that the design was significantly larger the current device and therefore it was decided that the conceptual design phase should be repeated.

6.4 Second Conceptual Design Stage

The second conceptual design stage generated a further three concepts (Figure 6.3). Concepts 4, 5 and 6 differ from the previous three concepts in that the connection between the plate and barrel is located below the barrel. This allows the overall dimensions of the device to remain similar to those of the current design, however the tab which projects down from the barrel increase the h_B measurement, shown in Figure 6.1, compared to concept 1, which may increase the required incision length.

Concepts 4 and 6 are similar designs in which the components are joined by two screws. In concept 4 the screws are inserted through holes in the tab into a threaded section of the plate where as in concept 6 the screws are inserted through holes in the plate into threaded sections of the barrel.

Concept 5 differs from 4 and 6 in that the tab of barrel has angled sides which slot into the plate. When the device is loaded in bending during normal use, the load will be transferred from the barrel to the plate through these angled sides rather than through the screws, as would be the case with concepts 4 and 6.

Due to the overall dimensions of the device, it would be necessary to use small screws to connect the barrel and plate together. It was decided that relying on these small screws to carry all the load would not be a sensible option. Concepts 4 and 6 were therefore removed from the list of possible designs.

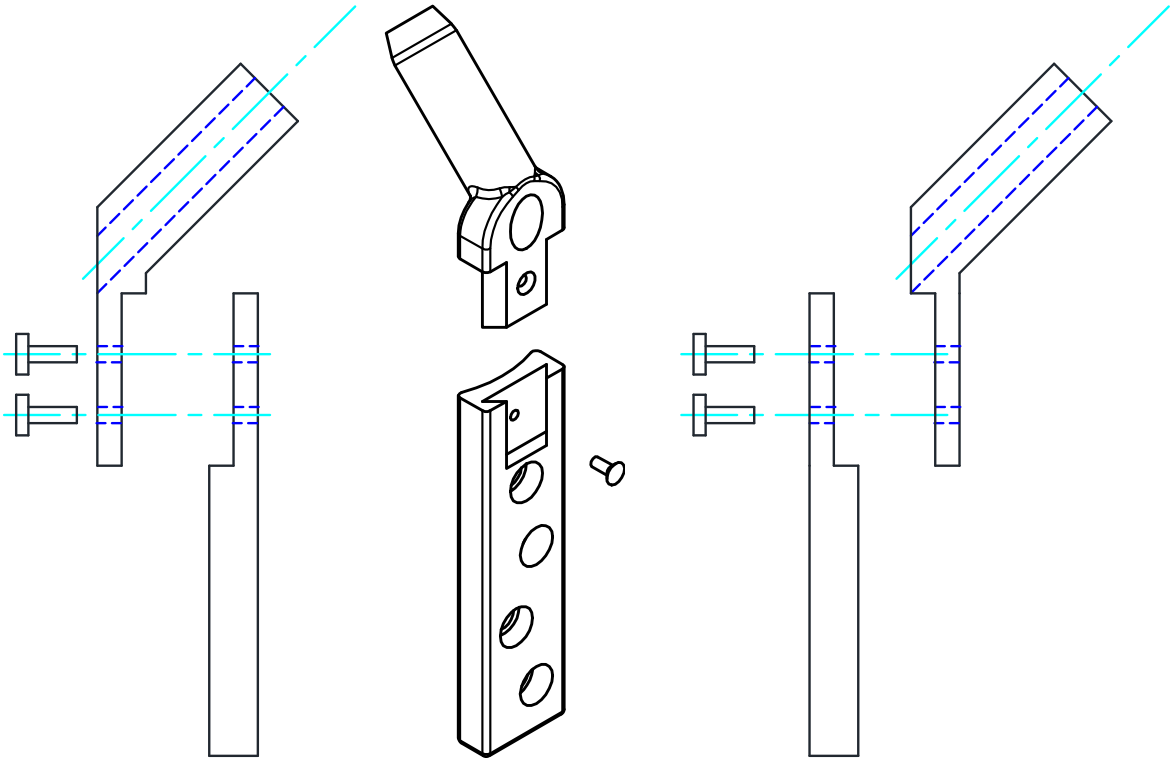

(a) Concept 4 **(b)** Concept 5 **(c)** Concept 6

Figure 6.3: Concepts generated in the second stage of conceptual design

Concept 1 was also removed from the running for two reasons, firstly it was significantly larger than the current design and secondly the design required all the load to be carried through the thread at the distal end of the barrel. The threaded end of the barrel would require both a hole through its centre to allow the neck screw to slide and external flats on the thread to prevent rotation of the barrel in the plate. These features would significantly reduce the strength of the connection between the components. It was therefore decided that concept one was not a viable design.

6.5 Third Conceptual Design Stage

The conceptual design stage was repeated for a third and final time, producing two designs, concepts 7 and 8, shown in Figure 6.4 along with concept 5. The connecting mechanism for concepts 7 and 8 uses a tongue and groove mechanism which runs up the sides of the barrel. The barrel of concept 7 contains a tab which protrudes downwards allowing the barrel to be secured to the plate with a screw. Concept 8 utilises a small locking plate which is inserted into a recess on the barrel and plate preventing them from separating, this locking plate is secured in place using a screw. It was decided that these three concepts were viable options and satisfied the design criteria qualitatively.

6.6 Matrix of Concepts

Pugh advocates using a matrix to select the best concept from a list of options, Table 6.1 shows a selection matrix for the MISHS designs. Concept 7 was chosen as the baseline by which the other concepts were measured against. For each criteria the concepts are marted as either worse than (-), better than (+) or the same as (s) the baseline option. The results are summed giving 1 for better than -1 for worse than and 0 for the same. The criteria it the matrix bellow were taken from the design specification, the incision length was estimated by looking at the height of the barrel (h_B) measurement discussed in Section 6.2. The implantation procedure was compared by looking at how the procedure for each device would deviate from the current procedure, it was found that all designs would have an almost identical implantation procedure. The mechanical performance was compared by carrying out FEA on each design, the methods and results of these analyses are discussed in Chapter 7.

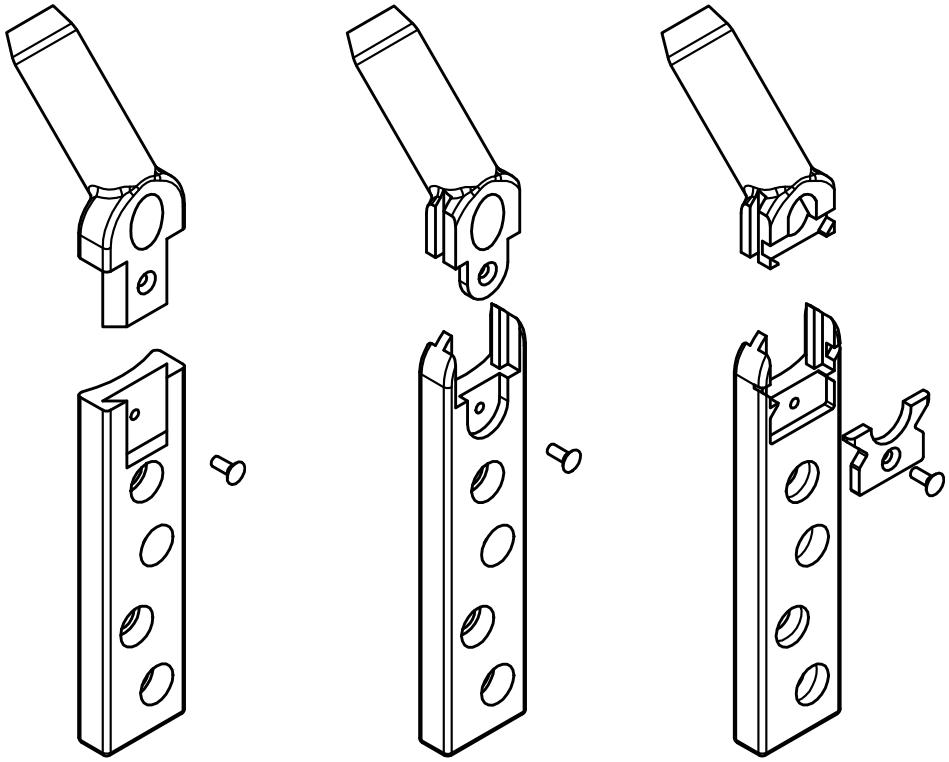

(a) Concept 5 **(b)** Concept 7 **(c)** Concept 8

Figure 6.4: Concepts selected for FEA

Table 6.1: Selection matrix, used to compare designs.

Concepts	5	7	8
Overall Size	s	s	s
Incision Length	-	s	+
Implantation Procedure	s	s	s
Mechanical Performance (Chapter 7)	?	?	?
Total	-1	0	1

7

Finite Element Analyses of Concepts

Due to the limited time and budget of this project it was not possible to manufacture prototypes of all three viable concepts. It was therefore necessary to model each design using FEA in order to compare the performance of each design and select the one most suitable to be taken to the prototyping stage.

This chapter discusses the results of the FEA of the MISHS concepts. The three models discussed in Chapter 5 were run with each of the MISHS concepts. The results from these models were compared against the those presented in Chapter 5 in order to evaluate whether the new concepts are capable of performing in a similar manner to the current device.

Each of the models were set up using identical methods to those discussed in Chapter 5.

7.1 Isolated MISHS Analysis

This test was designed in order to allow the stiffness of new devices to be compared against the current design. The model contained the proximal end of an SHS plate, the straight section of the plate was removed as it remained identical between all designs, the model setup is described in full in Section 5.2. It should be noted that the SHS model which was validated in Chapter 5 contained more of the straight section of the plate than was necessary for this comparison. It was therefore decided to create a

new shortened version of the SHS model so that the results could be compared directly against the shorter MISHS models. The meshes for each model are shown in Figure 7.1. The seeding of each component and number of elements in each model are shown in Tables 7.2 and 7.3. Each model was run twice with a linear elastic and a linear elastic perfectly plastic material model being used respectively, using the mechanical properties described in Table 7.1.

Table 7.1: Material Properties used in FE models.

Material	E(MPa)	ν	ρ(t/mm^3)	σ_{yield}(MPa)
Stainless Steel 316	200000	0.3	8.00E-09	241
Short-fibre-filled epoxy	10700	0.26	1.64E-09	
Rigid cellular foam	137	0.3	3.20E-10	

Table 7.2: Mesh seeding for each part in implant models.

Part	Approximate Global Size
Loading Pin	1.25
Plate	1
Barrel (Concepts)	0.75
Locking Screw (Concepts)	0.4
Locking Plate (Concept 8)	0.5

Table 7.3: Number of tetrahedral elements in each implant model.

Model	Number of Elements
Synthes (Validation)	57220
Synthes (Short)	35496
Concept 5	21010
Concept 7	33149
Concept 8	24950

7.1.1 Results

The results from the concept comparison models are shown in Figures 7.2 and 7.3

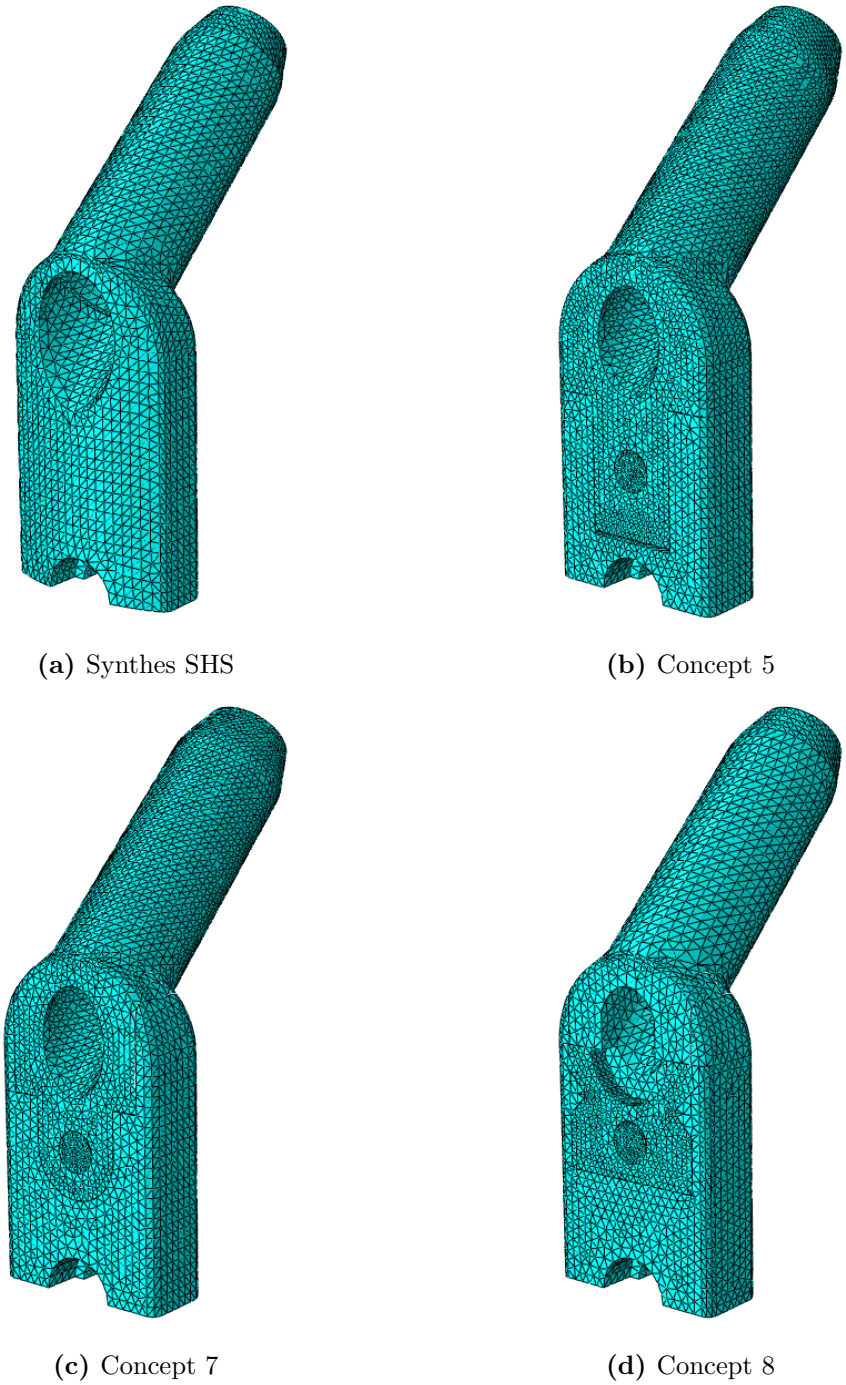

(a) Synthes SHS

(b) Concept 5

(c) Concept 7

(d) Concept 8

Figure 7.1: Isolated MISHS test meshes.

The results from the bending test with the linear elastic material model show that all designs behave linearly, the Synthes implant had a stiffness of 2.88 kN/mm. Concept 7 had a stiffness 6% lower than that of the Synthes implant (2.72 kN/mm), Concept 8 was 24% lower (2.18 kN/mm) and Concept 5 41% lower (1.7 kN/mm).

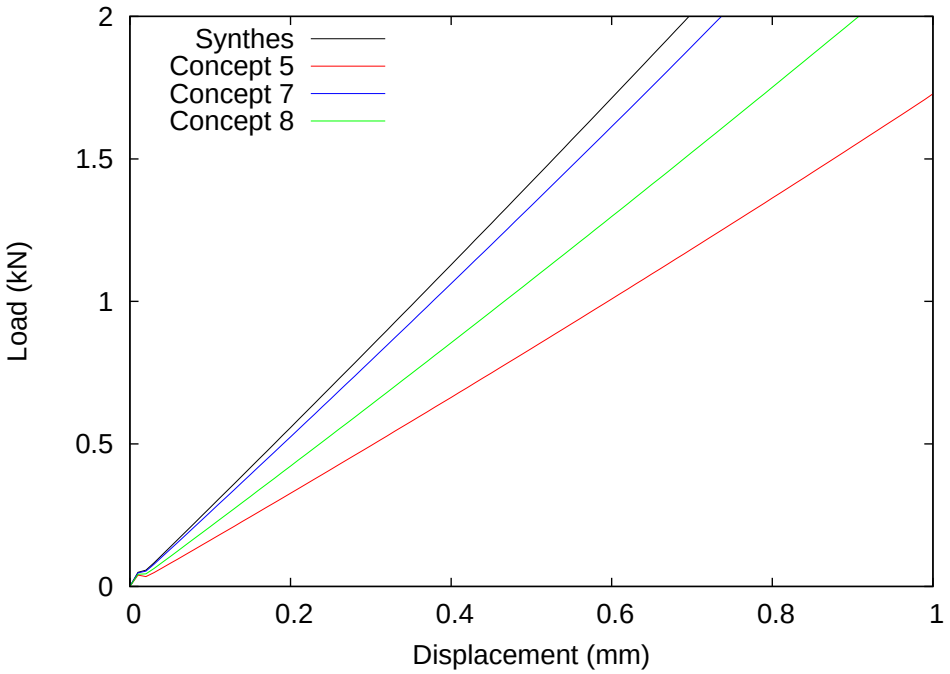

Figure 7.2: load-displacement curve for bending test of elastic model.

The results from the elasto-plastic model (Figure 7.3), show all concepts failing at lower loads than the Synthes implant, with concept 7 having the highest failure load followed by concept 8 then 5.

Figure 7.4 shows the Von Mises stress at the plate-barrel connection for all three concepts. For concepts 5 and 7 the maximum stresses, 2407 MPa and 2765 MPa respectively, occurred at the edge of the locking screw hole on the plate component. For concept 8 a maximum stress of 2034 MPa occurred in the barrel section at the internal corners of the grooves which the plate slides into.

Figure 7.5 shows the stress in the locking screw for each concept along with the locking plate from concept 8. For concepts 5 and 7 stresses in the screw are similar both exceeding 5000 MPa, however for concept 8 the maximum stress is 1660 MPa

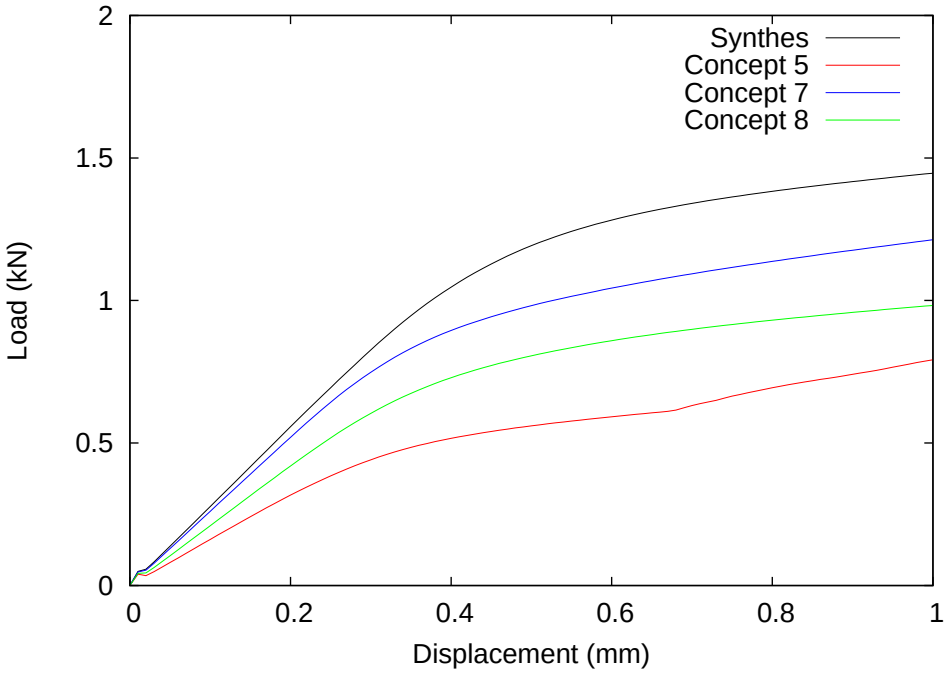

Figure 7.3: load-displacement curve for bending test of elasto-plastic model.

7.1.2 Discussion

The results from the concept comparison study show that when loaded in isolation the concept designs are not as stiff as the current design of the SHS. As the current design is a single piece of steel while the concepts are all multi component designs, this reduction in stiffness was expected. The deformation at the joint of each design can bee seen in Figure 7.6.

The components of concept 5 are connected via a flat tab on the barrel which is inserted into a slot on the plate, the tab and slot have angled edges which ensure that the components can only be separated by sliding them apart, this sliding motion is constrained by a small screw. When a vertical load is applied to the barrel a bending moment occurs at the joint which causes separation of the joint at the lateral side, this in turn causes the tab to bend and to be pulled upwards in the slot which applies a shear load to the screw.

The plate and barrel components of concept 7 are joined through a tongue and groove system which runs up the side of the barrel section. As with concept 5 there is a tab on the barrel which sits in a slot on the plate and is secured by a screw, however

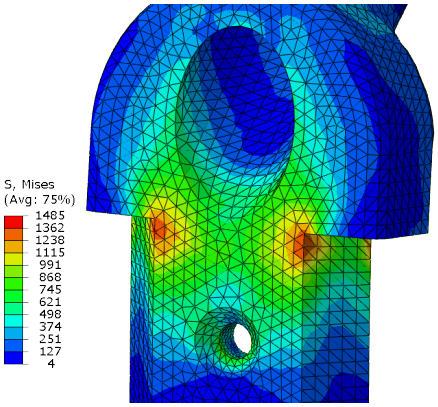

(a) Concept 5 - Barrel

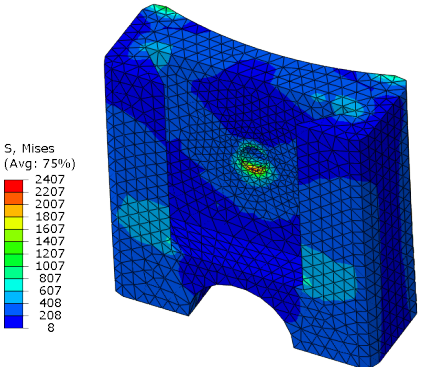

(b) Concept 5 - Plate

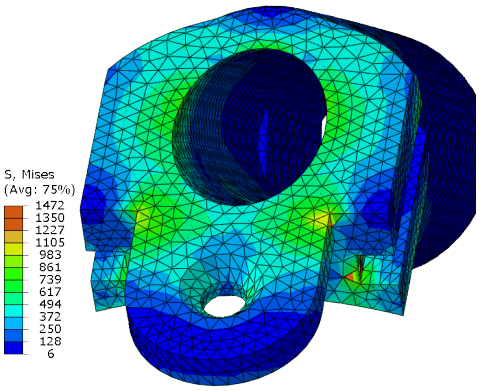

(c) Concept 7 - Barrel

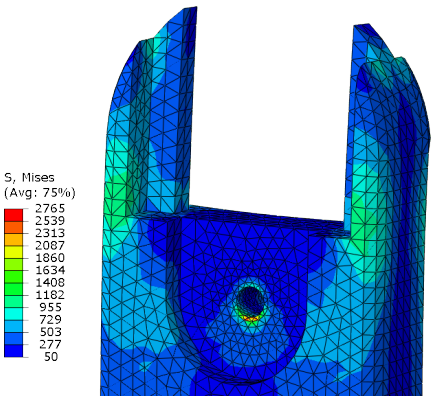

(d) Concept 7 - Plate

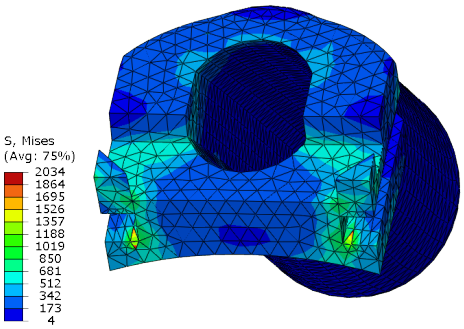

(e) Concept 8 - Barrel

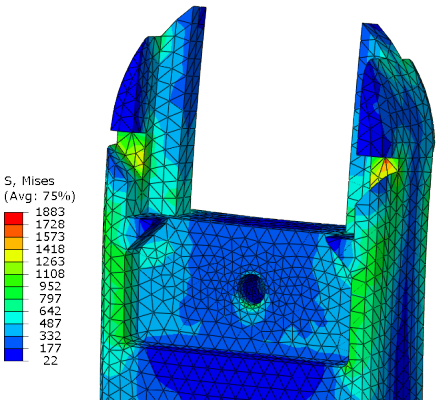

(f) Concept 8 - Plate

Figure 7.4: Von Mises Stress (MPa) - Plate-Barrel joints.

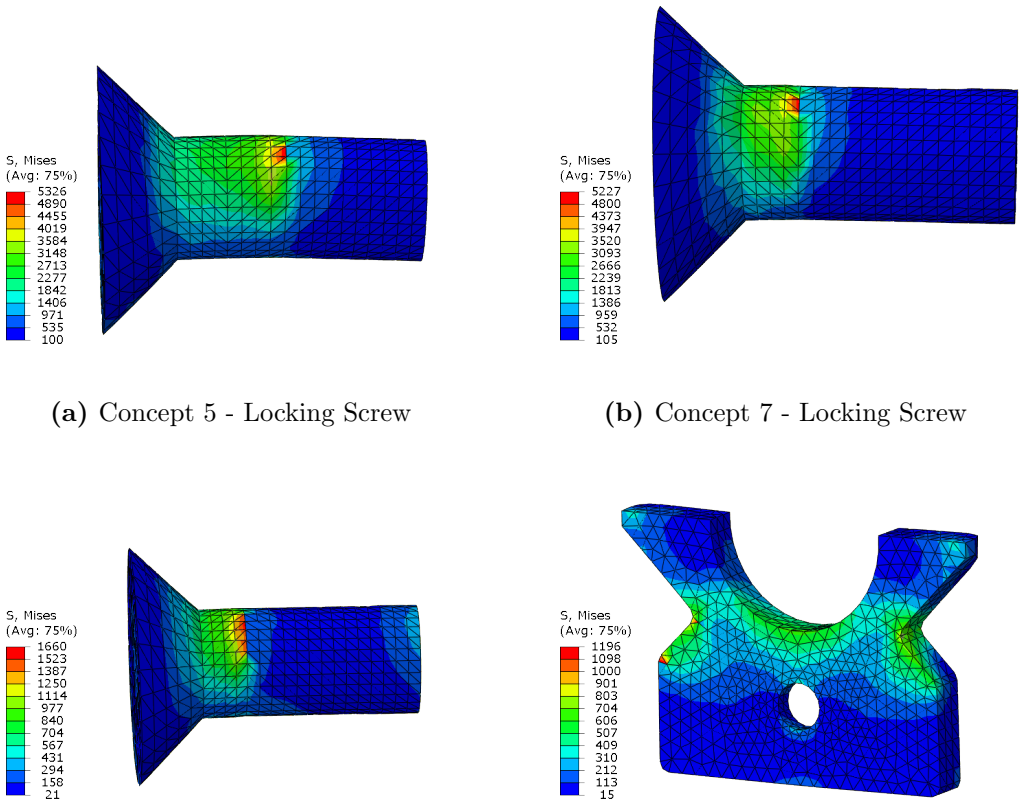

(a) Concept 5 - Locking Screw

(b) Concept 7 - Locking Screw

(c) Concept 8 - Locking Screw

(d) Concept 8 - Locking Plate

Figure 7.5: Von Mises Stress (MPa) - Locking screws and plate.

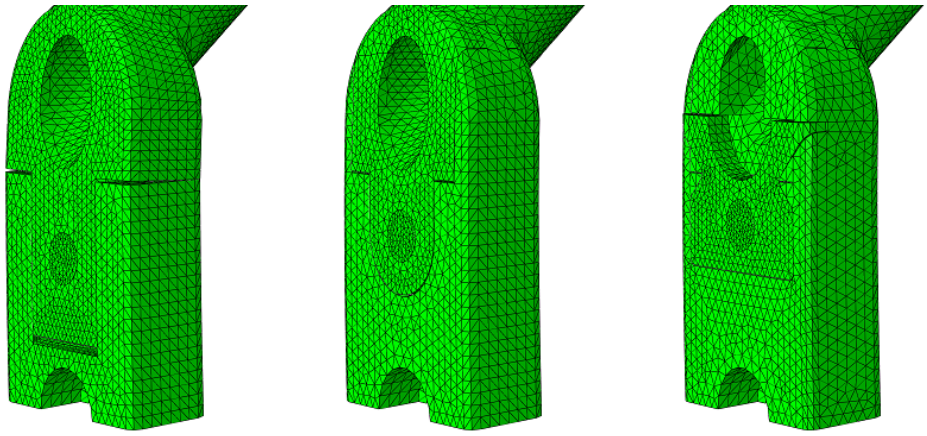

(a) Concept 5

(b) Concept 7

(c) Concept 8

Figure 7.6: Deformation at joint.

unlike concept 5 the sides of this tab are not angled therefore separation can occur between the tab and the plate. Load applied to the end of the barrel causes a bending moment which is transferred across the tongue and grove joint to the plate. A load is therefore applied to the sections of the plate which support the barrel, these sections are 3 times the thickness of the tab in concept 5 which allows them to be stiffer under bending. As with concept 5 separation occurs at the lateral side of the joint, however this separation is smaller , 0.084 mm compared to 0.149 mm. The separation causes the tab of the barrel to be pulled upwards and away from the slot on the plate, this applies both a tension and shear force to the screw.

The connection between the components of concept 8 is similar to the connection in concept 7. The same tongue and groove system is used which transfers the majority of the load across the joint however a different method is used to secure the joint. Rather than the tab and slot mechanism with securing screw that is used in concept 7, concept 8 is secured using a locking plate which is inserted into a cut out in the face of the plate and is secured by a screw. This locking plate prevents movement of the barrel section by obstructing the path of two protrusions on the barrel. As with concept 7 the design is relatively stiff due to the thickness of the sections of the plate which support the barrel. Separation at the joint section occurs on the lateral side as with the previous two designs, this separation causes the protrusions on the barrel to pull the locking plate upwards, the locking plate is supported against the edges of the cut-out in the plate in which it is placed and therefore no shearing is applied to the screw, however a shear load will be applied to the protrusions on the barrel. The separation also causes the locking plate to be pushed laterally away from the plate, this applies a tension and bending load to the screw.

From Figure 7.5 it can be seen that for concepts 5 and 7 the highest stresses occur in the locking screw, this indicates that the screw is responsible for transferring much of the load from the barrel to the plate and are likely to be the weakest area of the structure. In concept 8 the locking plate along with the tongue and groove system allows for a reduction in the load carried by the screw.

The results also show a lower failure load for the concepts, this again was expected due to the weakening effect of including a joining mechanism within the concept designs. For concepts 5 and 7 first yield occurred in the screw which secure the plate and barrel, for concept 8 yield first occurred in the barrel at the distal end of the the grove which

the plate slides into. Although the elasto-plastic analysis gives a valuable comparison between the failure loads of the devices, the absolute failure loads themselves cannot be considered accurate as local stress concentrations within the model may have caused yielding at unrealistically small loads.

7.2 MISHS in Femoral Shaft Analysis

The purpose of the femoral shaft test was to investigate the effect that the surrounding bone has on the stiffness of the device and to investigate whether it is possible for a device of lower stiffness to function in a similar way to a stiff device when implanted. The removal of the femoral head would allow the device to be loaded directly, removing any effect that the fracture site may have on the performance of the device.

A full description of the model setup can be found in Section 5.3. As each new concept had identical external dimension to the model current SHS design, including hole position, the implantation of these devices within the model was relatively simple. The screws used for each device would be identical and therefore the different plate designs were simply swapped in Autodesk Inventor with no need to reposition.

Meshes of each of the models can be seen in Figure 7.7. The seeding and number of elements for each model are shown in Tables 7.4 and 7.5. All materials were assumed to be linear elastic as described in Table 5.1.

Table 7.4: Mesh seeding for each part in femoral shaft models.

Part	Approximate Global Size
Cancellous Bone	1.8
Cortical Bone	2.4
Loading Pin	2
Plate	1
Shaft Screws	0.5
Barrel (Concepts)	0.75
Locking Screw (Concepts)	0.4
Locking Plate (Concept 8)	0.5

In addition to the applied displacement, two further displacement measurements were taken from each model and plotted against the reaction force at the fixed surface

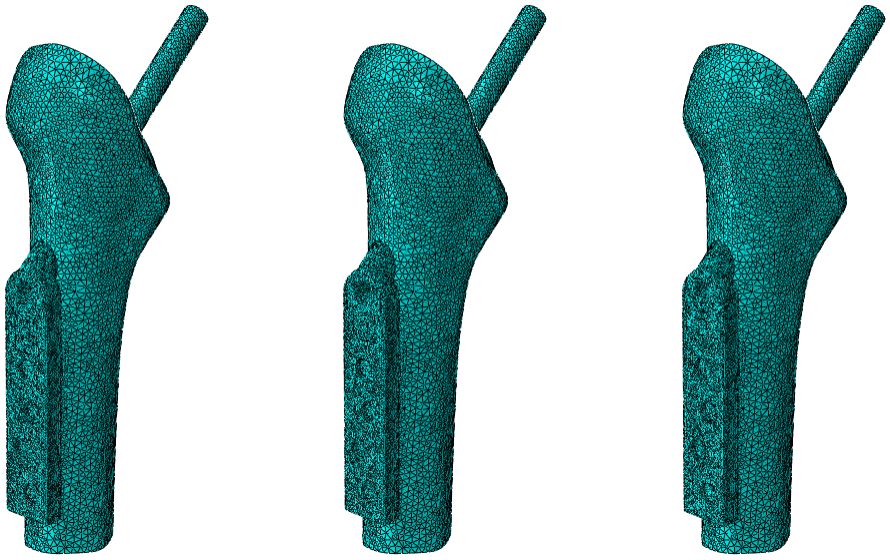

(a) Concept 5 **(b)** Concept 7 **(c)** Concept 8

Figure 7.7: Femoral shaft test meshes.

Table 7.5: Number of tetrahedral elements in each femoral shaft model.

Model	Number of Elements
Synthes	525597
Concept 5	649362
Concept 7	640216
Concept 8	671342

of the femur. Firstly the displacement of a node at the proximal end of the barrel was measure in order to remove the effects of the loading pin of the stiffness of the model, the location of the node can be seen in Figure 7.8. Secondly a new coordinate system was defined relative to the proximal screw hole in the cortical component of the femur (Figure 7.9). This coordinate system was fixed to the nodes on the cortical component an would therefore move with them as they were displaced. The displacement of the node shown in Figure 7.8 was measured relative to the x axis of this new coordinate system. By taking these measurements it was possible to remove the effect that sections of the model, which were identical for all designs, may have had on the overall stiffness. It was possible that these sections, being relatively compliant when compared to the rest of the model, may have lead to de-sensitivity within the model.

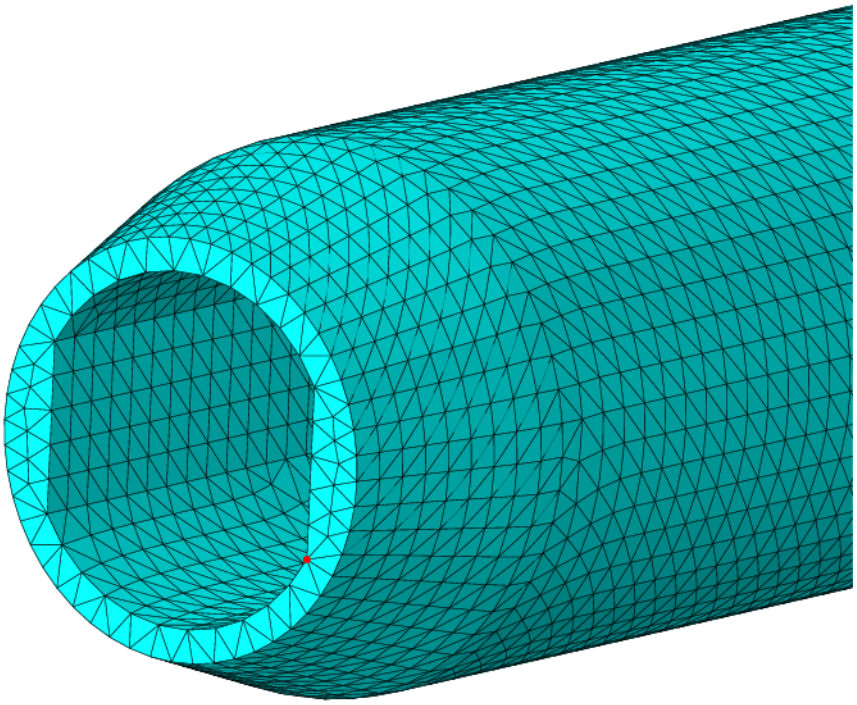

Figure 7.8: Node from which barrel displacement was measured.

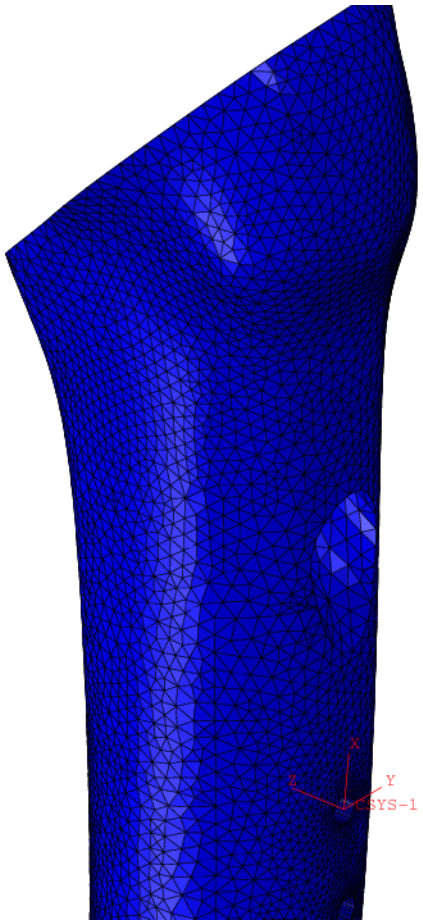

Figure 7.9: Coordinate system defined relative to the proximal screw hole in the cortical component of the femur.

7.2.1 Results

The results from the concept comparison study are shown in Figure 7.10. As with the results from the Synthes model each of the concepts exhibit linear behaviour above a displacement of 0.5 mm, with stiffness of 0.313 kN/mm, 0.318 kN/mm and 0.314 kN/mm for concepts 5, 7 and 8 respectively. The stiffness of the Synthes model was 0.338 kN/mm.

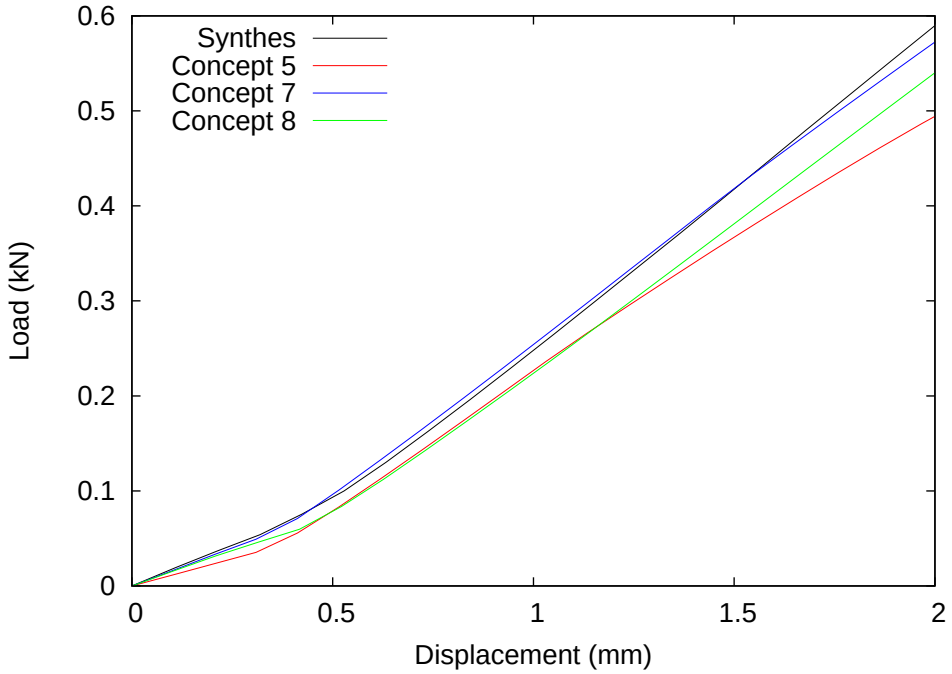

Figure 7.10: Load versus applied displacement for the femoral shaft FEA of concepts.

The displacement of the node at the proximal end of the barrel can be seen plotted against the reaction force at the fixed surface in Figure 7.11.

The displacement of the node at the proximal end of the barrel measured relative to the x axis of this new coordinate system is shown Figure 7.12 plotted against the reaction force.

Figures 7.13 and 7.14 show the Von Mises stress in the area around the barrel hole, from the lateral and medial sides respectively, for all 3 concepts and the Synthes implant.

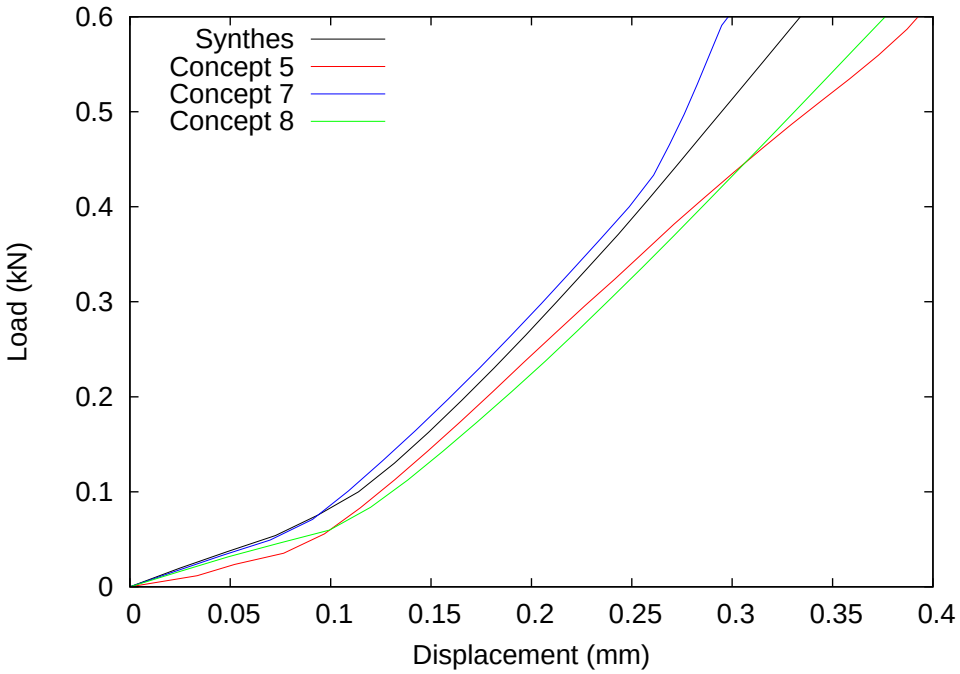

Figure 7.11: Load versus displacement of the barrel for the femoral shaft FEA of concepts.

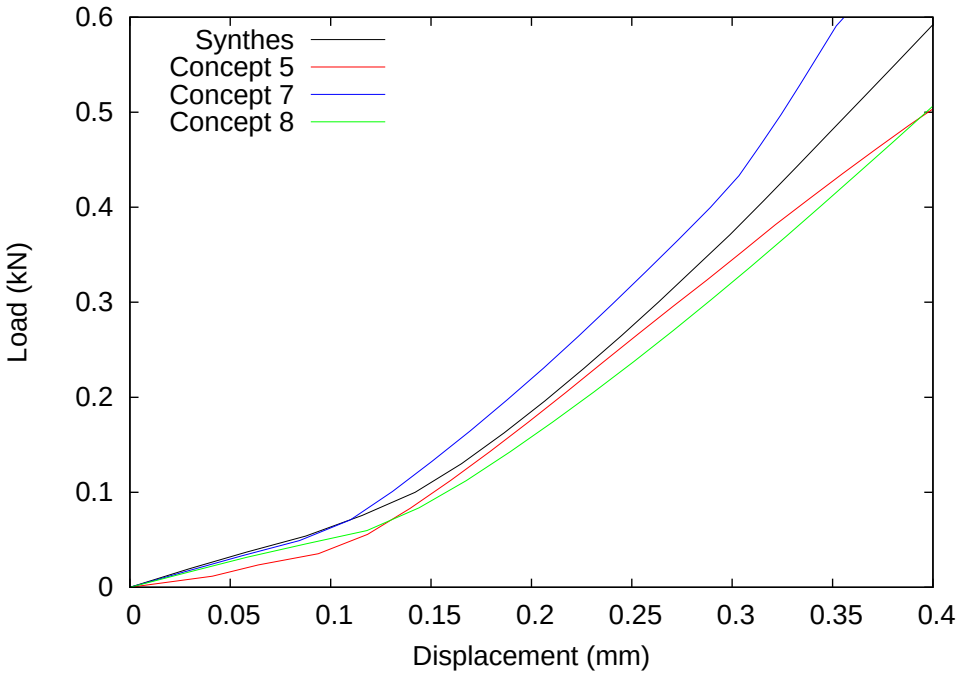

Figure 7.12: Load versus displacement of the barrel relative to the proximal screw hole of the femur for the femoral shaft FEA of concepts.

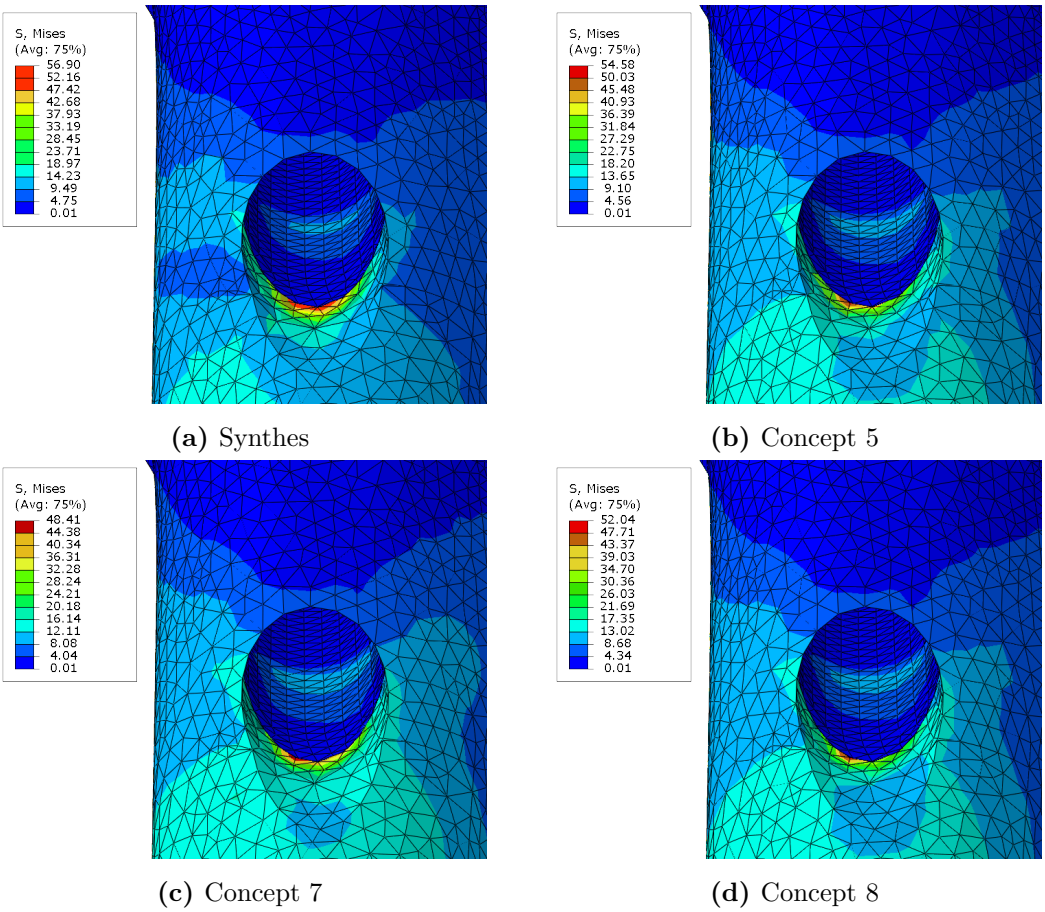

(a) Synthes **(b)** Concept 5

(c) Concept 7 **(d)** Concept 8

Figure 7.13: Von Mises Stress (MPa) - Lateral side of femoral shaft.

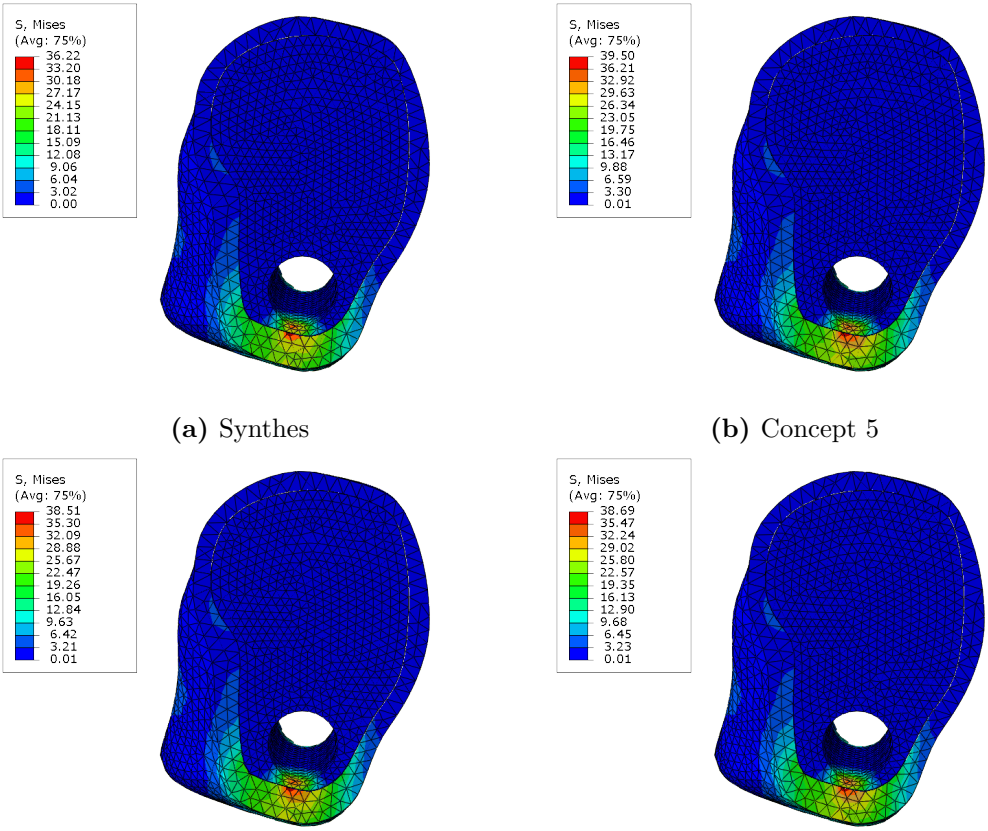

(a) Synthes **(b)** Concept 5

(c) Concept 7 **(d)** Concept 8

Figure 7.14: Von Mises Stress (MPa) - Fracture surface of femoral shaft.

7.2.2 Discussion

The results of the concept comparison study show that all three designs performed reasonably well compared to the Synthes model. Concept 7 performed best with a stiffness 6% lower than that of the Synthes model, this was closely followed by concept 8 at 7.4% lower.

By comparing the results in Figure 7.10 to those in Figure 7.2 the results of the femoral shaft test show less variation than the implant bending test, this may be due to two possibilities. Either the bone around the implant is supporting much of the load, meaning that the more compliant designs are made stiffer by the presence of the bone or that all implant designs are significantly stiffer than other parts of the test specimen, either the bone or the test pin, and that it is the stiffness of these more compliant components that defining the stiffness of the overall assembly.

By measuring the displacement of the barrel and plotting it against reaction force in Figure 7.11, the load pin has effectively been removed from the model, and therefore any effect it had on the stiffness results has also been removed. The results in Figure 7.11 show that all designs have a similar stiffness up until around 0.4 kN when the behaviour of concept 7 becomes more stiff.

By measuring the displacement of the barrel relative to the proximal shaft screw hole and plotting it against reaction force in Figure 7.12, any effect of the bone at the distal end of the specimen is removed. The results show that the stiffness of the different models remain similar.

It can therefore be said that the results from the different models in this test are not similar because other areas of the specimen are less stiff than the implant. As such it can be assumed that the the implants are being supported by the surrounding bone and that this leads to the increase in stiffness of the more compliant designs which leads to all models behaving in a similar manner.

As the the bone appears to support the device, increasing the overall stiffness of the model, it could be assumed that the use of more compliant devices would result in increased stresses within the bone. However when looking at Figures 7.13 and 7.14 it can be seen that the stress around the hole, into which the barrel is inserted, varies little between devices. This would suggest that more compliant designs would not cause

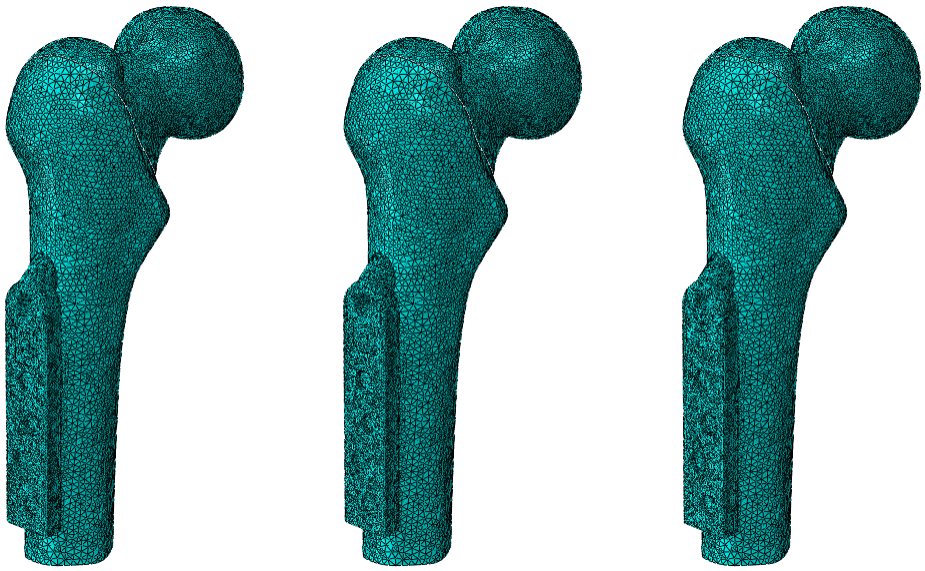

(a) Concept 5 **(b)** Concept 7 **(c)** Concept 8

Figure 7.15: Fractured femur test meshes.

increased stress in the bone and would therefore not increase risk of post operative fracture in this area.

7.3 MISHS in Fractured Femur Test

The fractured femur test was the most complex model developed during this study. It's purpose was to attempt to incorporate the effects of the fracture site into the model, allowing a more accurate simulation of in vivo behaviour than the previous models. However due to the complexity of the bone healing process, it was not possible to either accurately model the fracture site or simulate it within the lab. It was therefore necessary to simplify the fracture site. The full setup for the model is described in Section 5.4

As with the previous model the identical dimensions of the different designs allowed the models to be easily swapped and placed in position. The meshes for all the concept models can be seen in Figure 7.15, the seeding and number of elements in each mesh are shown in Tables 7.6 and 7.7. All components were modelled as linear elastic, as described in Table 5.1.

Table 7.6: Mesh seeding for each part in fractured femur models.

Part	Approximate Global Size
Cancellous Bone Shaft	1.8
Cortical Bone Shaft	2.4
Cancellous Bone Head	2
Cortical Bone Head	1.8
Plate	1
Neck Screw	2
Shaft Screws	0.5
Barrel (Concepts)	0.75
Locking Screw (Concepts)	0.4
Locking Plate (Concept 8)	0.5

Table 7.7: Number of tetrahedral elements in each fractured femur test.

Model	Number of Elements
Synthes	742422
Concept 5	789108
Concept 7	779962
Concept 8	803784

7.3.1 Results

The results for the FE models of each concepts and the Synthes device implanted in the fractured femur are shown in Figure 7.16. Both the Synthes implant and concept 8 have a stiffness curve that is close to linear with gradients of 0.452 kN/mm and 0.426 kN/mm respectively. Both concepts 5 and 7 exhibited more non linear behaviour.

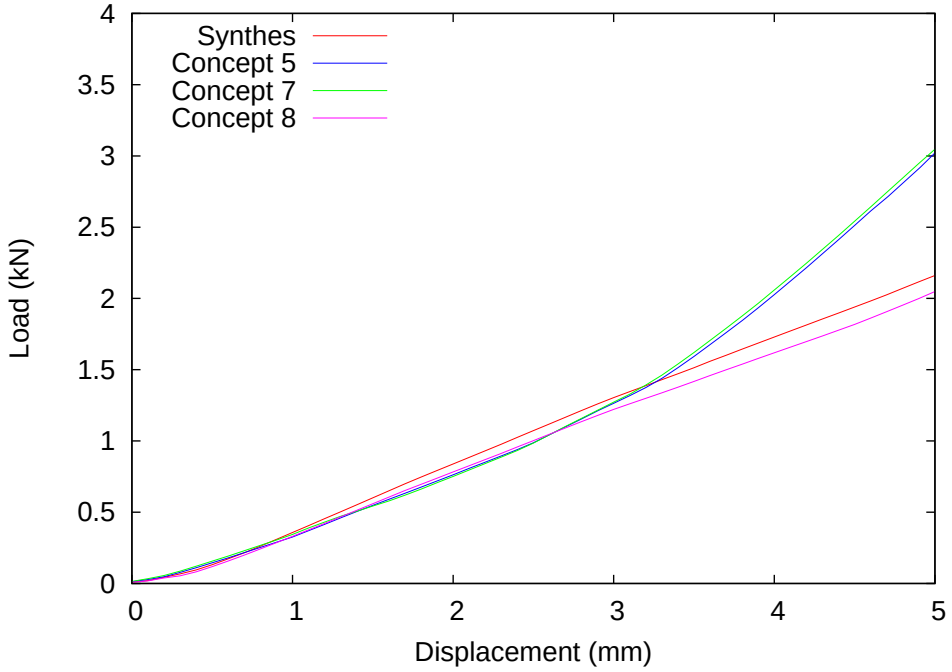

Figure 7.16: Load displacement curves for each of the FE models of the fractured femur.

Figures 7.17 and 7.18 show the Von Mises stress in the area around the barrel hole, from the lateral and medial sides respectively, for all 3 concepts and the Synthes implant.

7.3.2 Discussion

The stiffness results from the model indicate that Concept 8 is the closet match to the Synthes implant. All devices have a similar stiffness up until around 3 mm applied displacement, at which point concepts 5 and 7 appear to become more stiff, it is not clear why these designs increase in stiffness.

When looking at the stress around the barrel hole on the lateral side of the femur

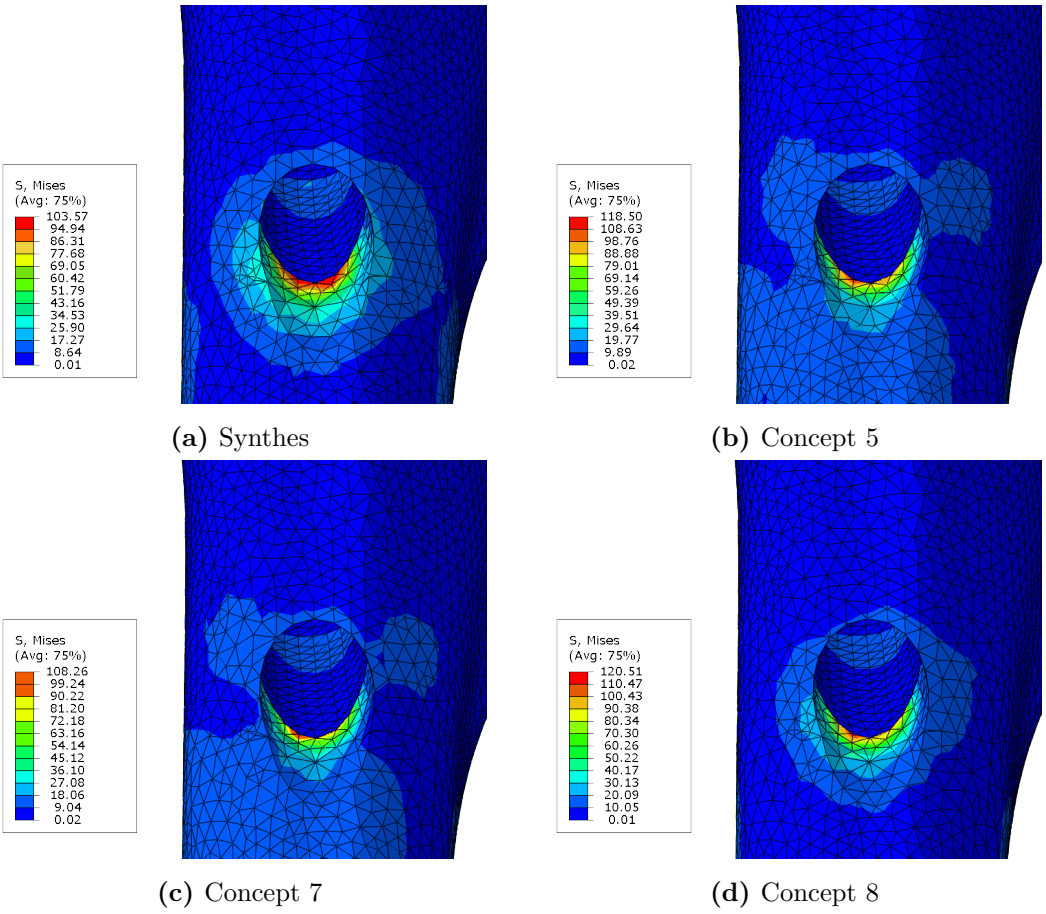

(a) Synthes **(b)** Concept 5

(c) Concept 7 **(d)** Concept 8

Figure 7.17: Von Mises Stress (MPa) - Lateral side of femoral shaft.

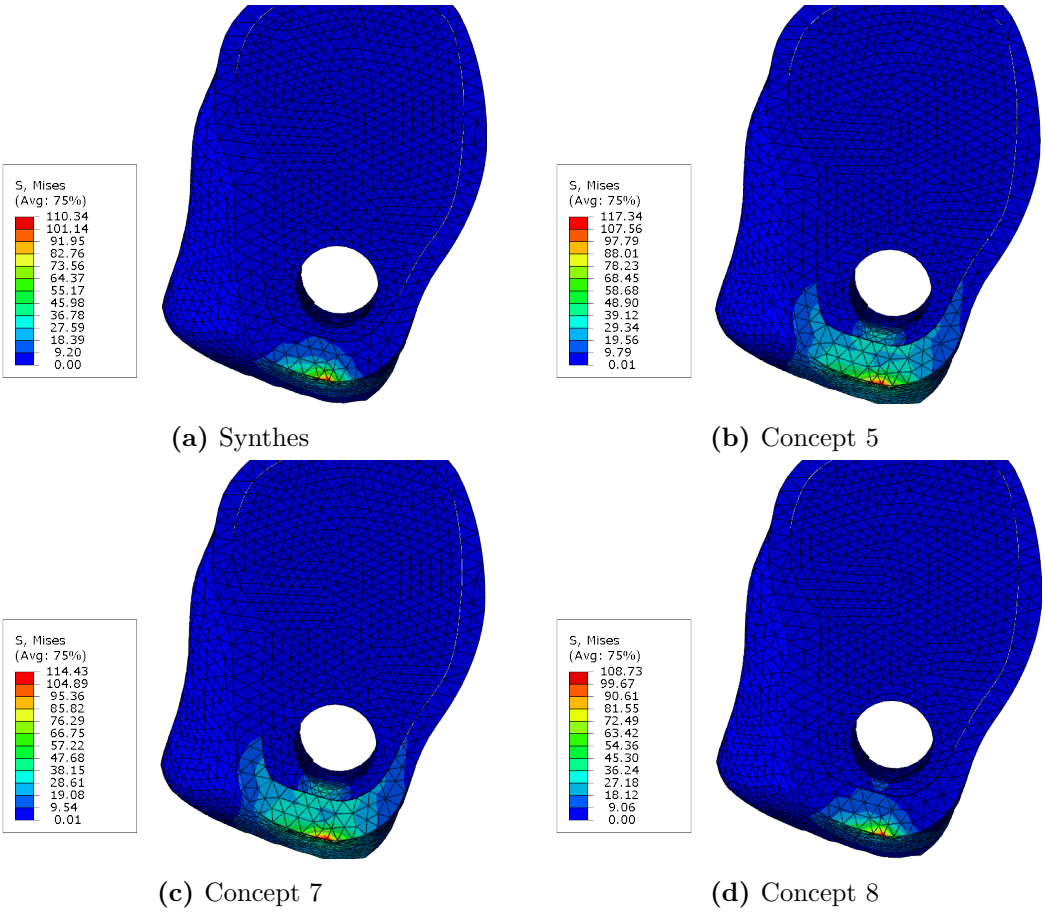

(a) Synthes **(b)** Concept 5

(c) Concept 7 **(d)** Concept 8

Figure 7.18: Von Mises Stress (MPa) - Fracture surface of femoral shaft.

(Figure 7.17), it can be seen that unlike in the shaft test there is a difference in stress between devices. The maximum stress in the cortical bone at the edge of the hole is highest in the concept 8 model (121 MPa) and lowest in the Synthes model (104 MPa). When the cancellous bone inside the hole is observed it can be seen that the stress, at the area where the end of the barrel contacts the bone, varies little between devices. From the results in Figure 7.18 it can be seen that the stress at the fracture follows two different patterns, with concept 8 and the Synthes implant displaying lower stresses than concept 5 and 7. It is likely that the higher stresses seen in concept 5 and 7, in particular the stress in the cancellous bone, may indicate that the neck screw is coming into contact with the cortical bone on the medial side of the distal fragment. This may go some way to explaining the increase in stiffness of these devices, discussed earlier. However if the increased stiffness is caused by the screw contacting the bone it would be expected that this would occur in all devices if displaced enough. As all devices showed a similar stiffness up until this point, it would also be assumed that in all devices the screw would come into contact with the bone at a similar load.

7.4 Summary

The results from these models revealed several important pieces of information. The models of the isolated devices showed, that the new designs were both more compliant and less strong than the current device. This was expected as it was known that the joining mechanism would have a weakening effect on the device. However the models showed the magnitude of that weakening effect, with one design being almost half the stiffness of the SHS. The isolated models also showed the areas of high stress in each design. It was noted that in concepts 5 and 7 the highest loads appeared in the locking screws, which were subject to stress more than three times higher than those seen in concept 8.

The models of the devices implanted in the femoral shaft showed that when implanted in bone, all devices had a similar stiffness. This gave some weight to the hypothesis that the new device would not have to be as stiff as the SHS in order to function as required. The model also showed that the stress in the bone around the implant varied little between devices. This was surprising as it was thought that a more compliant device would result in higher stresses within the bone.

The results from the fractured femur test show all the devices behaving similarly over the initial 3 mm of applied displacement after which concepts 5 and 7 become stiffer. This increase in stiffness appears to occur due to the neck screw coming into contact with the cortical bone. What is not clear is why for the same displacement, the neck screws in the concept 5 and 7 models come into contact with the bone while those in the concept 8 and the SHS models do not.

The results these models demonstrate that, while each of the new concepts are less stiff than the SHS in isolation, when implanted in bone the stiffness of the device has very little effect on the overall stiffness. The concept comparison study found that concept 8 more closely matches the performance of the Synthes implant than either concept 5 or 7, it also found that concepts 5 and 7 showed areas of stress around the locking screws which were higher than any seen in concept 8. It was therefore concluded that concept 8 had a more suitable mechanical performance than either concept 5 or 7.

The conclusion from this FEA was used to complete the design selection process discussed in 6. Table 7.8 shows the completed matrix of concepts, it can be seen that concept 8 was determined to be the most suitable design and was therefore taken forward to manufacture.

Table 7.8: Selection matrix, used to compare designs.

Concepts	5	7	8
Overall Size	s	s	s
Incision Length	-	s	+
Implantation Procedure	s	s	s
Mechanical Performance	-	s	+
Total	-2	0	2

8

Manufacture of the MISHS Prototype

The current SHS design contains complex features which add difficulty to the manufacturing process, the majority of these features would also be included within the final MISHS design. The resources available for manufacturing a prototype can be very different from those available to manufacture a large number of finalised devices for sale and as such many of the features desired in the final design may have to be excluded from the prototype. This chapter will discuss the manufacturing of the MISHS prototype, it will give details of the current device design features and those included in the prototype as well as material selection and manufacturing processes used.

8.1 Material Selection

Current SHS devices are manufactured from stainless steel. It was decided that, as the MISHS device was to remain as similar as possible to the current device, the material selection would remain identical.

The materials from which surgical implants may be manufactured are defined in BS ISO 5832, with the standards for stainless steel implants being defined in part 1 of the standard (British Standards Institute, 2007). The standard states that stainless steel surgical implants must be manufactured from stainless steel 316LVM (UNS S31673/WNR 1.4441). This alloy is a low carbon vacuum melt version of 316 stainless steel, this process removes impurities and increases the corrosion resistance of the

material.

Due to the high cost of this material and the fact that it would not be used in patients the prototypes were not manufactured from 316LVM but rather grade 316 which has similar material properties while having less corrosion resistance.

8.2 Features of the current device

The current SHS design contains several features which add complexity to the manufacturing process. Some of these features are critical to the functioning of the device while others have been perceived to be less critical and may consequently be excluded from the prototype to simplify the manufacturing process.

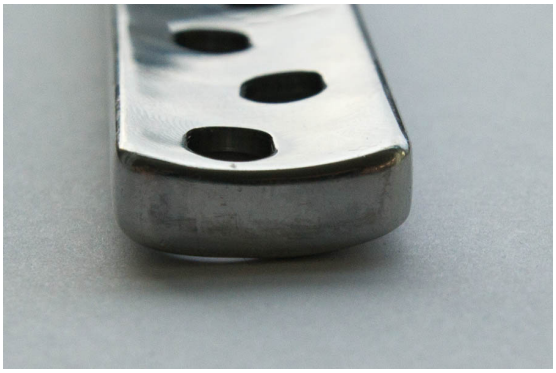

Figure 8.1: Curve in plate of the SHS.

Both the medial and lateral sides of the plate are curved to a diameter of 62 mm (Figure 8.1). The curve on the medial side is designed to allow the device to fit against the curve of the bone, while the external curve is intended to reduce the overall size of the device and prevent discomfort caused by the implant protruding into the soft tissue.

The straight plate section of the SHS contains screw holes for securing it to the femoral shaft(Figure 8.2). These holes are not round but rather an elongated circle. The holes are countersunk in a complex shape which causes the plate to slide distally as the screws are tightened, this ensures that the barrel is pulled tight against the bone which provides support when loaded.

The hole of the barrel, shown in Figure 8.3, is a circular hole with flats (Figure 8.3a). The flats on the hole are intended to prevent the neck screw from rotating within the

Figure 8.2: Shaft screw holes in plate of the SHS.

(a) Proximal

(b) Distal

Figure 8.3: SHS barrel hole.

(a) Medial **(b)** Lateral

Figure 8.4: Join between the barrel and plate sections of the SHS.

hole providing stability to the bone fragments. The distal end of the hole has a larger diameter with no flats (Figure 8.3b), this allows a compression screw to be added to the device. The flats on the barrel hole are essential to the functioning of the device and must be included in any prototype manufactured. The larger diameter at the distal end is not essential and may be excluded from the prototype to simplify manufacturing.

The section where the barrel and plate join, shown in 8.4, is a complex shape which transitions from the cylinder of the barrel to the curved plate. This shape is important in preventing an stress concentration which may occur due to sharp corners around which the device may fail. However the shape here is extremely complex and difficult to manufacture, it may therefore be necessary to exclude this from the prototype.

8.3 Manufacturing Process

It is most likely that the current devices are manufactured by either casting or machining using complex multi-axis computer numerical control (CNC) machines. However when manufacturing the prototype of the MISHS the resources available did not allow these techniques to be used and as such a simplified design had to be manufactured using a combination of conventional and CNC machining.

8.3.1 Plate

The plate was machined from a 25 mm square bar of 316 stainless steel. The bar was first machined down to a cross section of 20×8 mm using a conventional milling machine.

The steel was then machined further using an XYZ SMX 3500 3 axis CNC milling machine (Southwestern Industries Inc., Rancho Dominguez, CA, USA) controlled by a ProtoTRAK SMX controller. 3D cad models were exported to Edgecam CNC programming software (Vero UK Ltd, Cheltenham, UK) which produced a gcode script which was input to the CNC controller.

The finished plate can be seen in Figures 8.5 and 8.6, it can be seen that several details of the current SHS design have been removed from this prototype. While the curve on the medial side of the plate remains the curve on the lateral side was not included. It was decided that this feature added significant complexity to the manufacturing process and that its removal would have a small effect on the mechanical tests. The shaft screw holes have also been simplified, although these may have some effect on the functioning of the device, it was not possible to manufacture holes similar to those seen on the SHS using the resources available. The corners of the plate were also not rounded to as large a radius as those on current devices, these rounds were deemed necessary for the prototype and removed to reduce the work required to produce the prototype.

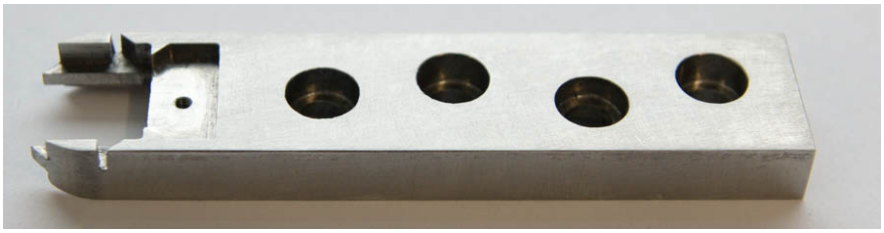

Figure 8.5: Lateral side of MISHS plate.

One feature which added significant complexity to the manufacturing process was the curve on the medial side of the plate, shown in Figure 8.6. It was machined by clamping the steel vertically then moving the milling tool in an arc of the required radius, the tool was the lowered and the process repeated until the curve ran the full length of the plate.

Figure 8.6: Medial side of MISHS plate.

8.4 Locking Plate

The finished locking plate can be seen in Figure 8.7, the locking plate was machined from 5 mm thick stainless steel plate in a conventional milling machine. When machining this it was found that the 1 mm diameter milling pieces required to machine the small rounds were breaking, the plate was therefore machined with larger a 3 mm milling piece before being filed down to size.

Figure 8.7: MISHS locking plate.

8.5 Barrel

The barrel section of the MISHS was the most complex component to manufacture. It was initially intended that the barrel would be manufactured using a 5 axis CNC milling machine within another department of the university. However due to work being carried out for the department which owned the machine, it was not possible to secure enough time to manufacture the MISHS on it. This delayed the manufacturing on the barrel section by several months, eventually it was decided that an alternative method for manufacturing the barrel, using conventional machining and 3 axis CNC machining, would have to be found.

The barrel was manufactured from a 19 mm across the flats hexagonal stainless steel bar. The steel clamped in a lathe with the centre of the hexagonal section of centre from the centre of the lathe. The steel was turned down to the diameter required for the barrel with material being left at one end to manufacture the joining mechanism. A jig was manufactured to hold the barrel section at 45° with the unturned end protruding, the steel was clamped in this jig and machined using a conventional milling machine to achieve the rough shape of the joining mechanism.

The remaining of the machining processes were carried out using the same XYZ SMX 35000 3 axis CNC milling machine, used to manufacture the plate. The curves between the cylindrical and rectangular sections of the barrel had to be estimated when machining, which resulted in very rough finishes as well as some large gouges in the implant.

The hole within the barrel was manufactured using electrical discharge machining (EDM), a process whereby material is removed through the use of electrical discharges. This process allows complex geometry to be created that would otherwise be impossible or difficult to create through conventional machining methods. This work was carried out by The Spark Erosion Centre, Blantyre, UK.

The finished barrel can be seen in Figures 8.8 to 8.10. It can be seen in Figure 8.9, that the medial side of the barrel joining mechanism does not feature the same curve that runs along the inside of the plate section, this was removed due to the complexity involved in manufacturing it.

Figure 8.11 shows the joint between the round and rectangular sections of the three barrel prototypes that were manufactured. It can be seen that the first two have

Figure 8.8: MISHS barrel.

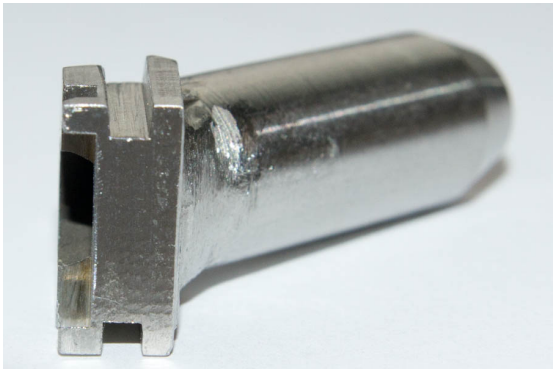

Figure 8.9: MISHS barrel distal view.

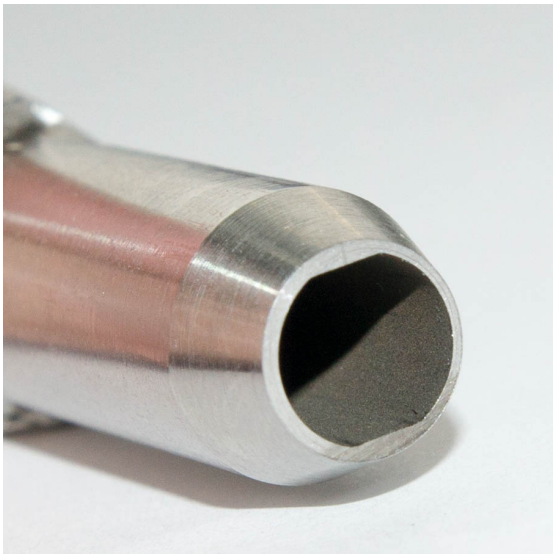

Figure 8.10: MISHS barrel hole.

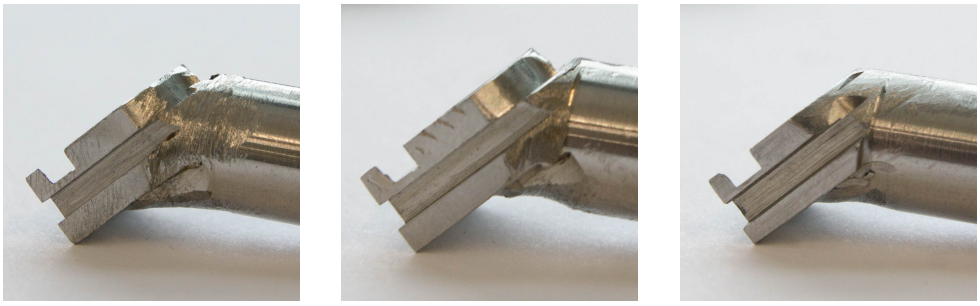

(a) (b) (c)

Figure 8.11: Variation in barrel prototypes.

large quantities of material removed at the distal end of the barrel, this is a result of the difficulty involved in machining this section. These large gouges could reduce the strength of the barrel and introduce stress concentrations around the sharp edges. However the devices were assumed to be appropriate for initial testing and further refinements were deemed to be outwith the scope and resources of the project.

9

Mechanical Testing of the MISHS Prototype

In order to ensure the MISHS design is capable of withstanding the loads required during normal use, mechanical testing was carried out on the prototype. It was important to investigate both how the device will perform in use and how it will fail. As such, several tests were performed.

The stiffness of the device, when implanted in a fractured femur, is vital to its function. If the device is not sufficiently stiff it will not be capable of maintaining the alignment of the bone fragments which may lead to mal-union or non-union of the fracture. The design aims stated that the MISHS device should have a similar mechanical performance to that of the SHS device and as such the stiffness of the MISHS prototype was tested in the same manner as the SHS and the results compared.

The MISHS device must be capable of withstanding the loads applied to it during weight bearing. As with the SHS the MISHS was tested until failure of either the device or the bone. It was important that failure of the device would not occur at loads lower than those expected for an average patient when walking.

As walking produces a cyclic load, the device is also at risk of fatigue failure. Fatigue failure can occur in structures which under go cyclic loading, the load required to cause fatigue failure can be significant lower than that which would be required to cause failure under static loading. The repeated loading can lead to small cracks forming within the structure, with each loading cycle the crack grows, until it can no longer support the load at which point a fast fracture occurs. The device was therefore tested

under cyclic loading conditions intended to simulate the loads that would occur while walking.

9.1 Aims

The aim of these experiments was to demonstrate that the MISHS device is capable of withstanding the loading which would be applied to it when implanted in the fractured femur of a patient and to investigate the conditions which would cause it to fail.

Three tests were to be carried out on two specimens implanted in artificial femurs. Static loading tests were to be carried out with the femoral head removed and included, in order to determine the stiffness of the specimen in situ. The specimen would then be loaded to failure under static conditions with the head attached, to determine the strength of the specimen. Finally cyclic loading would be applied to the second specimen in order to determine whether fatigue would occur in the device during normal walking.

9.2 Methods

Two MISHS prototypes were implanted in a Sawbones® artificial femur which had been cut at 45° to the femoral shaft in the trochanteric region to simulate a extracapsular proximal femoral fracture. The distal end of the femur was removed and the femur was secured was secured at the mid shaft using Isopon P38 polyester filler and a custom made clamp, as described in Section 4.1.2. The test was carried out using the Electroplus E10000 Linear-Torsion Floor Instrument, (Instron, Norwood, MA, USA) fitted with a 10 kN load cell.

The first specimen was tested in two different configurations, firstly the femoral head was removed and a steel pin was inserted into the barrel of the plate in order to replicate the tests carried out on the SHS in Section 5.3, the setup can be seen in Figure 9.1. The specimen was loaded by displacing the end of the pin downwards by 2 mm at a rate of 0.1 mm/s, the test was carried out 5 times.

The same specimen was the tested again with the femoral head secured to the shaft using the neck screw, as shown in Figure 9.2. It was intended that the specimen be loaded by displacing the head downwards by 5 mm at a rate of 0.1 mm/s. Before the

Figure 9.1: MISHS test setup for first specimen with head removed.

Figure 9.2: MISHS test setup for fractured femur.

test was run at the full displacement, preliminary tests were run with displacements of 2 mm, 3 mm and 4 mm, the test would then be run at the full displacement 5 times. However during the first 5 mm displacement test, fracture occurred on the medial side femoral shaft (Figure 9.3). It was decided that the test be run 5 times after the fractured occurred, to investigate how the behaviour of the specimen had changed post-failure.

The second specimen was loaded in a cyclic manner in order to simulate walking. Although in reality the angle of the load changes during walking, it was decided that the loading should be simplified and was therefore applied at a constant angle throughout the experiment. Koval et al. (1998) found that after three weeks of healing patients, who have been treated with SHS devices, bear around 60-80% of their body weight on their injured leg, which resulted in a hip load of around 2-3.5 times body weight. It was also found that the average duration of a gait cycle was 3.8 seconds. The hip force was calculated at 3.5 times body weight, for an 80 kg person, to be 2.75 kN. In order to reduce the running time of the experiment the load cycle time was reduced to 2 s split evenly between loading and unloading, the load was applied 100000 times. It was found during preliminary testing, that if the load was cycled between from 0 kN to 2.75 kN the actuator would often overshoot during the unloading step. It was therefore decided to cycle from 0.05 kN to 2.75 kN to prevent this from occurring. For both the static and cyclic tests, the specimen was subject to loading conditions which simulated mid-stance as discussed in Section 5.4.1.1.

When implanting the device in the second specimen the threads for the neck screw in the head of the femur were stripped. In order to secure the head to the femur it was necessary to fill the head with an expanding foam, Pedilen Rigid Foam 450 (Ottobock, Duderstadt, Germany). Although the foam is a similar material to that used to manufacture the artificial cancellous bone in the femur, it may have changed the behaviour of the screw within the head, most likely reducing the chance of cut out. However it will have had minimal effect on the loading which the MISHS plate is subject to, as the load will still be transferred from the femoral head through the thread in the neck screw and therefore the load conditions between the neck screw and the barrel should stay the same. The only difference that may have occurred would be that if the new foam prevented cut out, the failure test on the specimen may go to a higher load and failure may occur at a different location.

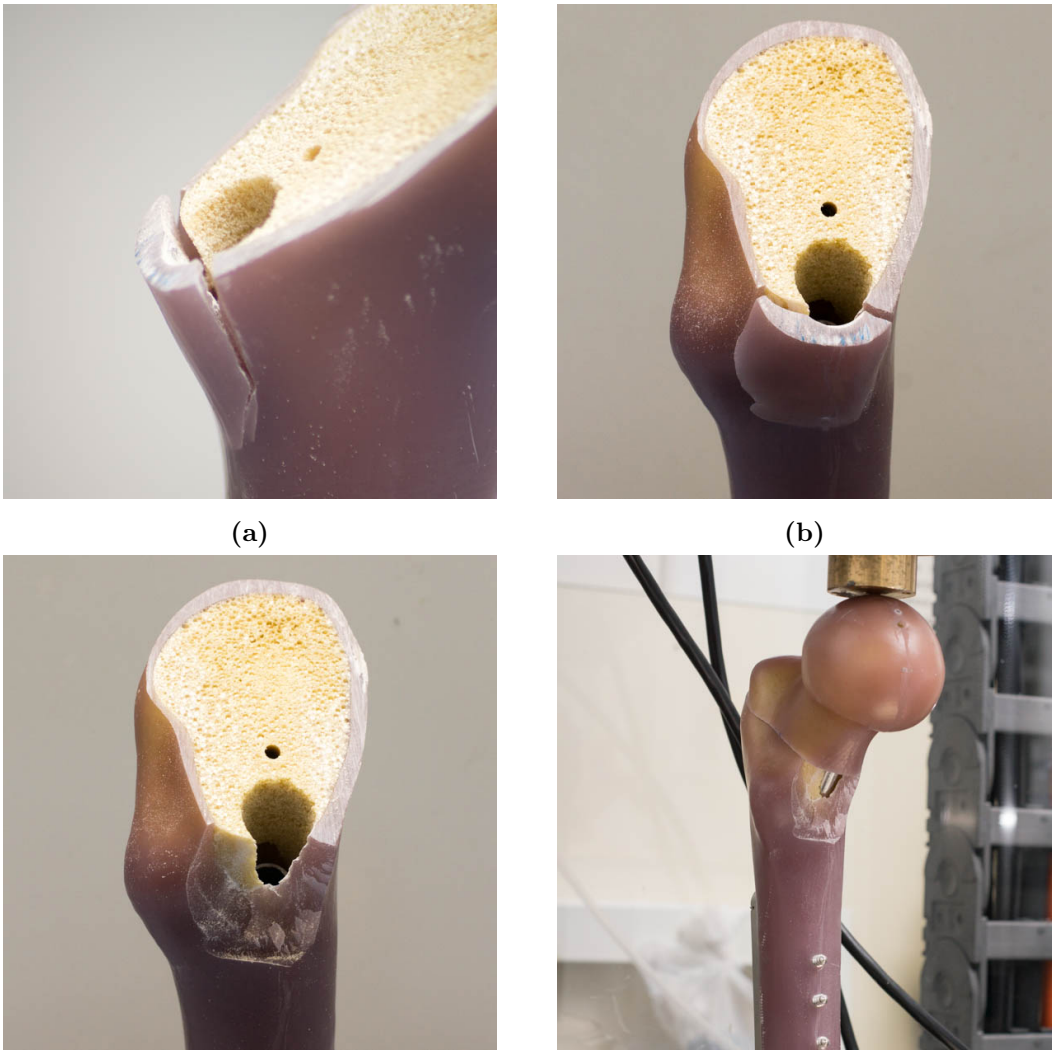

(a) **(b)**

(c) **(d)**

Figure 9.3: Fracture on femoral shaft, which occurred during testing.

9.3 Results

The load displacement results for the test with the femoral head removed are shown in Figure 9.4 alongside the results from FEA of the MISHS design and the mean of the SHS tests discussed in Section 5.3. The results show that the specimen in this test is twice as stiff as the specimen from the SHS tests and the FEA which were both of a similar stiffness.

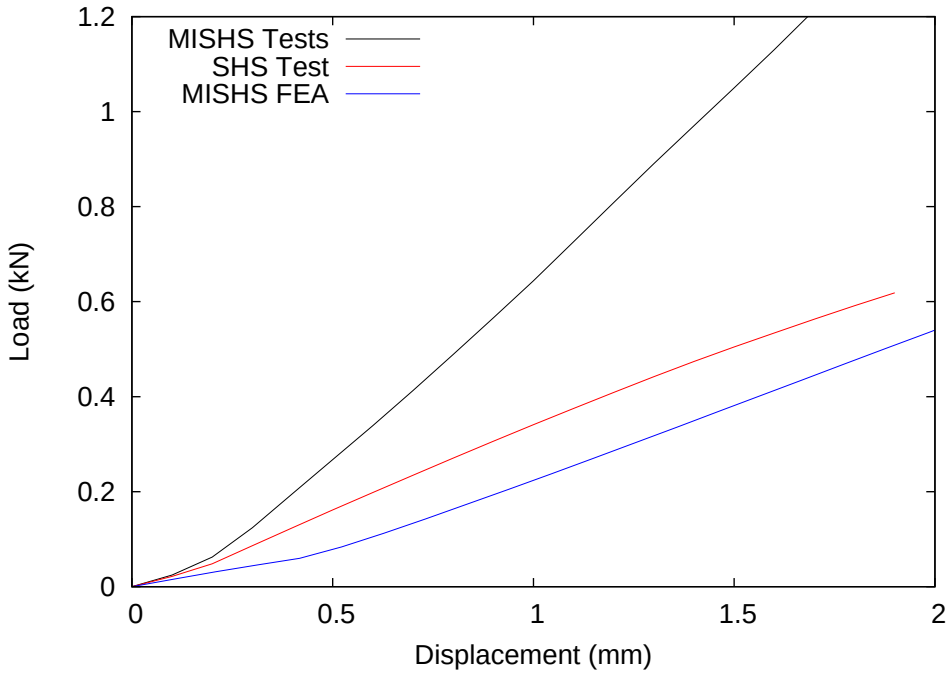

Figure 9.4: load-displacement curve for MISHS test in femoral shaft without head.

The load displacement curves from the first specimen test before fracture of the femur occurred can be seen in Figure 9.5. Test 1-3 are three preliminary tests in order of increasing applied displacement, while test 4 is the first full test run during which fracture occurred. The mean results from a similar test of the current SHS design discussed in Section 5.4 are also shown. It can be seen that the MISHS specimen has a similar stiffness to the SHS specimen. Fracture occurred at 3.18 kN on the medial side of the femur (Figure 9.3).

The results of the additional test runs which were carried out post-failure of the femoral shaft are shown in Figure 9.6. It can be seen that the stiffness is considerably

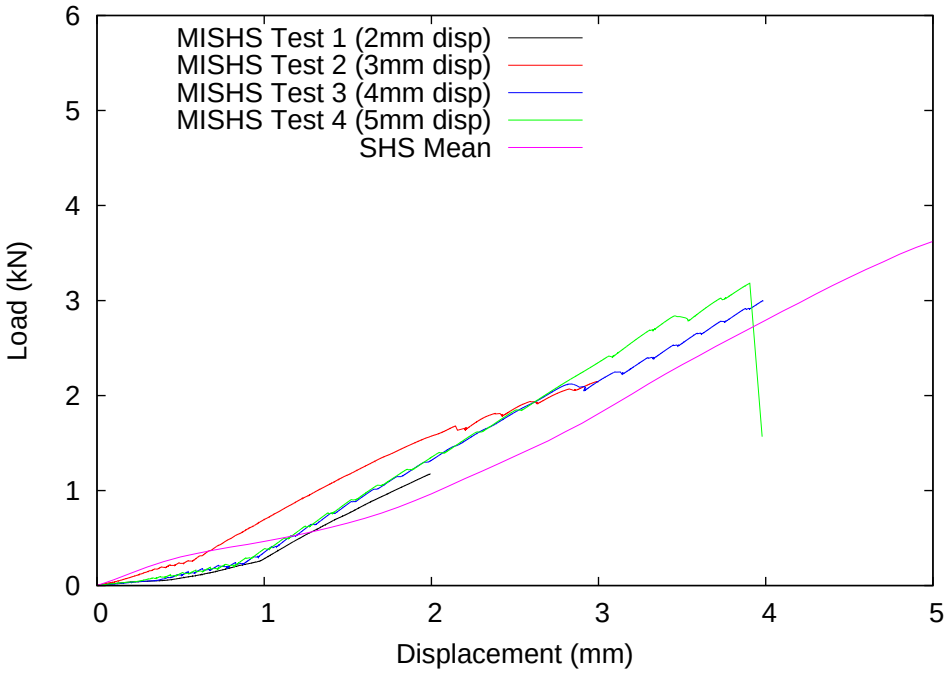

Figure 9.5: load-displacement curve for MISHS fractured femur tests with femoral head attached, before fracture occurred in the femoral shaft.

reduced compared to the pre-failure tests.

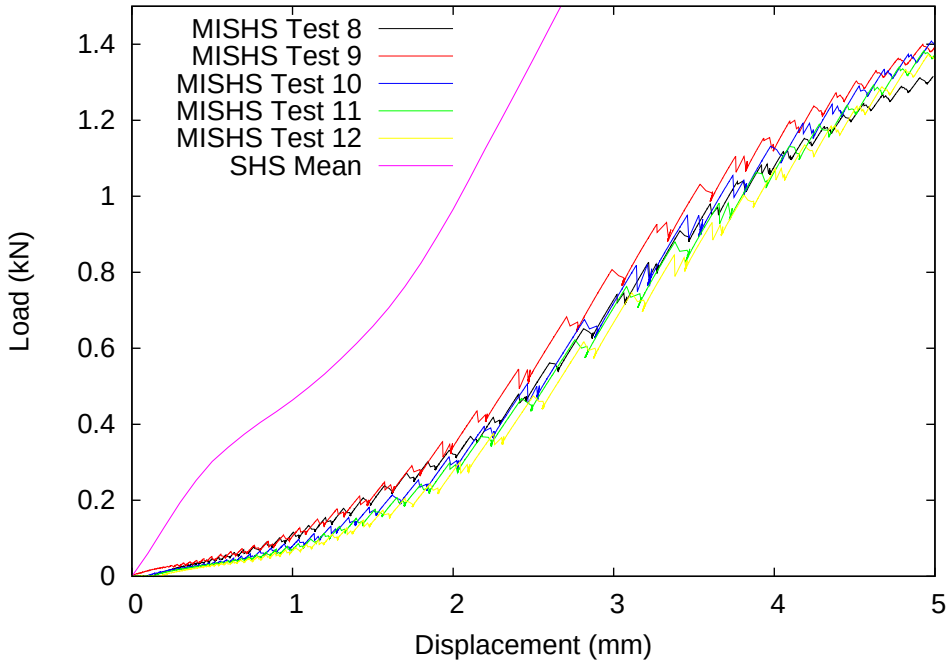

Figure 9.6: load-displacement curve for MISHS fractured femur tests, before fracture occurred in the femoral shaft.

The fatigue test ended on cycle 58229 when a soft displacement limit of 10mm was tripped. As with the previous bending tests fracture occurred on the medial side of the femur as shown in Figure 9.7, plastic deformation also occurred in the neck screw, shown in Figure 9.8.

Figure 9.9 shows the maximum and minimum position of the loader during each cycle of the test, while Figure 9.10 shows the displacement of the loader during each cycle. It can be seen that the displacement is approximately constant over the first 55000 cycles while the positions do show a small gradual increase. At around cycle 55750 a large increase in displacement can be seen along with a large increase in maximum position and a smaller increase in minimum position. For around 2500 further cycles a small increase in displacement can be seen along with increases in both minimum and maximum displacement. At cycle 58229 a sudden large increase in maximum displacement caused the displacement limit to be tripped.

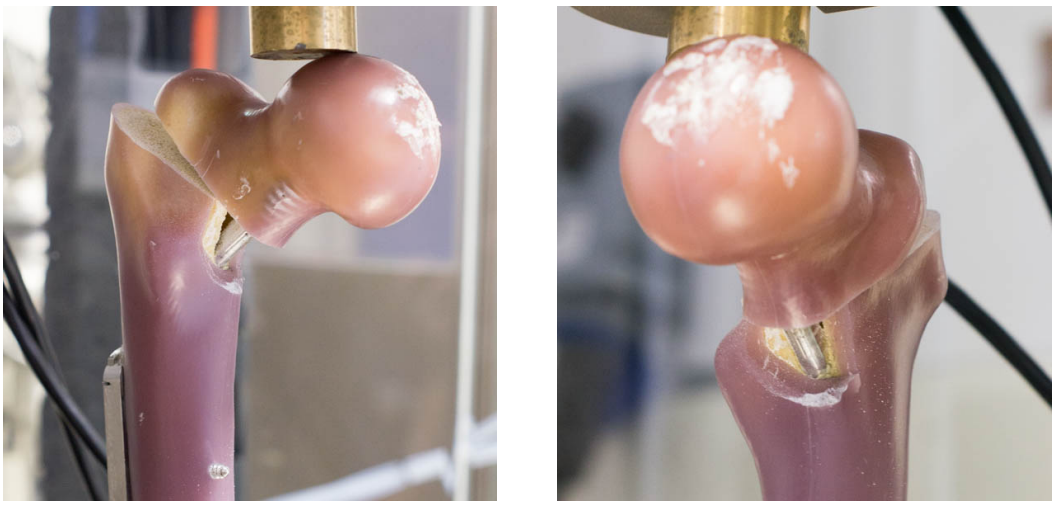

(a) (b)

Figure 9.7: Fracture of femur during fatigue test.

Figure 9.8: Plastic deformation of neck screw during fatigue test.

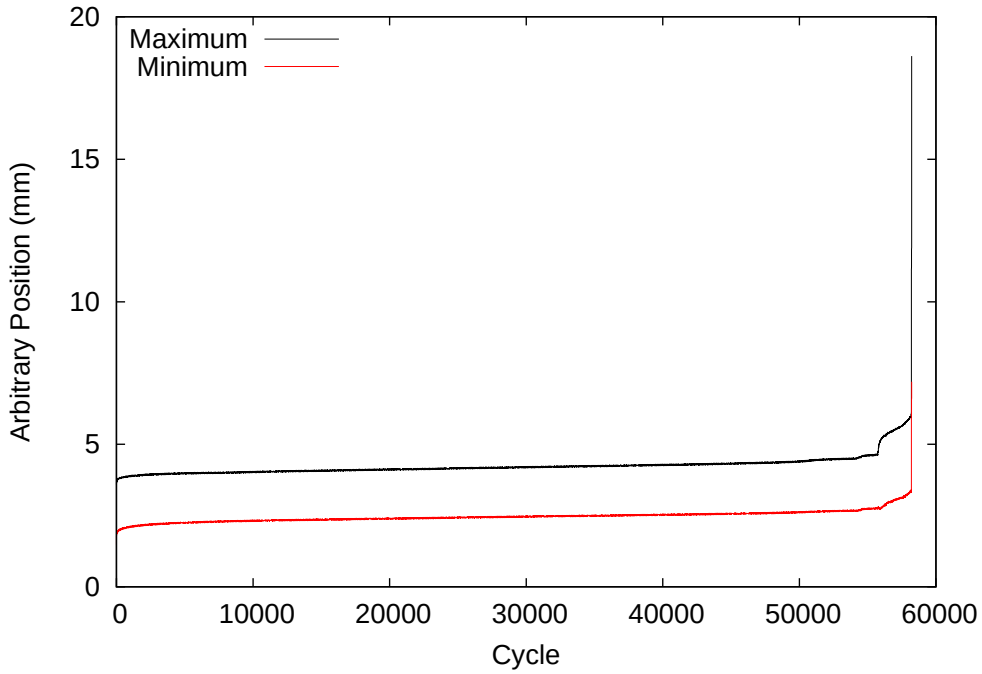

Figure 9.9: Maximum and minimum positions of actuator for each cycle during fatigue test.

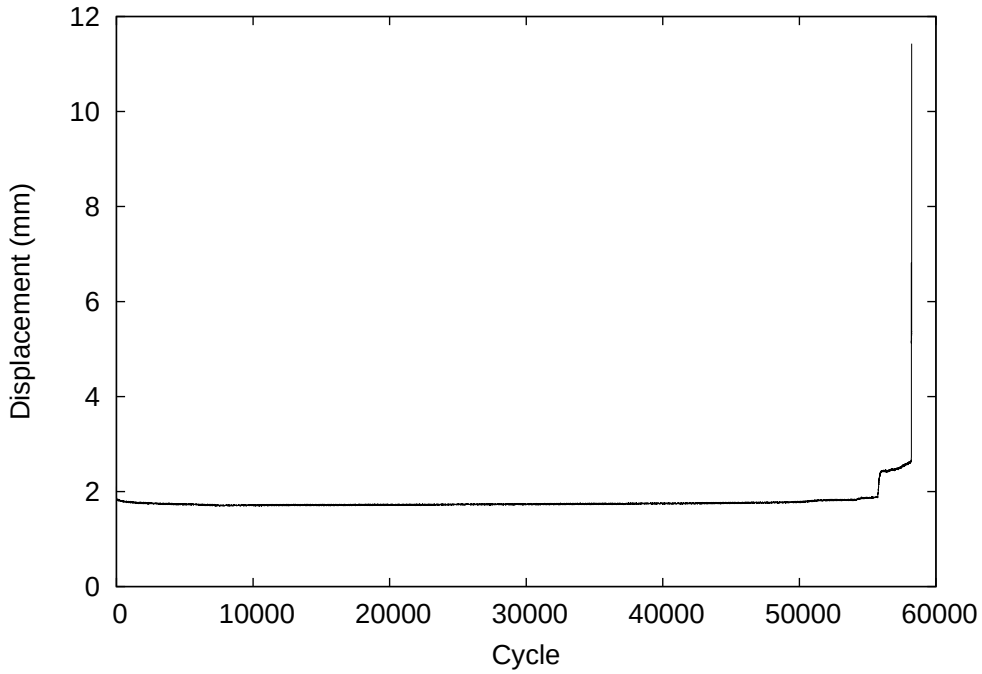

Figure 9.10: Applied displacement for each cycle in fatigue test.

9.4 Discussion

The results from the from the first specimen show some interesting behaviour when compared to the the similar tests carried out on the SHS. The results from the test without the femoral head show a stiffness of double that of the SHS in the same test and also of that predicted by the FEA. This considerable increase in stiffness can most likely be attributed to the position of the implant. Figure 9.11 shows the position of the hole in the neck of the femur for both the MISHS and SHS implants, it can be seen that the MISHS was implanted lower in the neck and therefore closer to the cortical bone than the SHS. Dark marks can be seen on the shaft of the femur where the tap has removed cortical bone material, similar white marks can be seen on the outside if the femoral head Figure 9.12. The increased stiffness observed in the first test is likely to have been caused by the implant or loading pin coming into contact with the cortical component of the femur which provided more support than the cancellous component.

The results from the second test, with the femoral head included, behaved similar to the SHS tests carried out previously and do not show the increase in stiffness that was observed in the first test. This may be due to the fact that the screw used to attach the head in the second test has a smaller diameter than the loading pin which was used in the first. While the increased stiffness seen during the first test may have been caused by the loading pin coming into contact with the cortical bone, the smaller diameter of the screw could have prevented it from contacting the cortical bone and therefore avoided the stiffening effect. However the fracture which occurred on the medial side of the femur is most likely due to the load being applied to the bone by the screw, and therefore it must be assumed that the screw did contact the bone. This poses a question as to why when the pin came into contact with the bone the structure became more stiff, whereas when the screw came into contact fracture occurred. There are two possible explanations: firstly the smaller diameter of the screw may have caused load to be transferred over a smaller area creating higher stresses or repeated loading of this area of bone during previous tests has caused cracks within the bone to grow until failure occurred. It seems unlikely that a higher contact stress at the area where the screw contacted the bone will have caused the fracture, as the fractures did not occur at the contact point. However the removal of cortical bone material during the drilling and tapping process weakened this region of the femur and likely caused small

fractures or defects, it is possible that this fracture occurred due to a small crack which grew during the first test and reach a critical length during the second test at which point fast fracture occurred.

As the fatigue test was to run for several days it was not possible to observe it at all times and therefore the order in which the bone and screw failed was not observed. From the displacement data two distinct incidents can be seen. Firstly at around 55750 the stiffness of the specimen decreases, this is shown in Figure 9.10 as a sudden increase in applied displacement. From the results of the bending tests (Figures 9.5 and 9.6) during which a similar bone fracture occurred, it can be seen that the change in stiffness before and after the fracture occurred is much larger than indicated in the fatigue test. It may therefore be possible to say that the sudden decrease in stiffness at around cycle 55750 was not caused by the fracture of the bone. It could therefore be assumed that the change in stiffness was caused in some way by plastic deformation of the screw. However the plastic deformation of the screw alone cannot fully explain the behaviour seen, after the screw plastically deformed it would be expected that both the maximum and minimum positions would change by similar values and that the displacement would not change significantly. However Figure 9.9 shows that while the maximum displacement changes suddenly the minimum only a small change. It may be that a small plastic deformation in the screw has caused the angle at which the head sits relative to the femur to change. This change in angle has caused less of the load to be transferred across the fracture site due to friction, this would in turn cause a decrease in the stiffness of the specimen. The initial large change in displacement is followed by a more slow increase in displacement along with an increase in both maximum and minimum positions. This is likely cause by further small plastic deformations in the screw. What cannot be deduced from the results is what caused the initial plastic deformation of the screw to occur.

The test ended with a sudden increase in maximum position which exceeded the limit set on the test, this was likely caused by fast fracture of the bone which reduced the stiffness of the the specimen instantly. The fracture of the bone was potentially caused by the increase in contact force between the screw and the cortical bone due to the plastic deformation of the screw. As the screw deformed further with each load cycle the load on the cortical bone increased until it could no longer support it and fast fracture occurred.

(a) SHS Head

(b) MISHS Head

(c) SHS Shaft

(d) MISHS Shaft

Figure 9.11: Position of implants in the femur.

Figure 9.12: Thread marks on neck of femur.

No instances of post-operative medial calcar fragments, such as those seen in out tests, could be found reported in literature. As discussed in Section 2.6.2, cut out of the screw has been reported as the most common reason for mechanical failure of the device. With Chirodian et al. (2005) reporting over half of the device failures in their study being due to screw cut out, with incidence occurring in around 1.85% of patients. This was also found by Parker and Handoll (2009a) in there meta analysis which found a cut out rate of 1.7%. There are several reason why this fracture, which does not appear to be common in clinical scenarios, may have occurred in the mechanical test specimens. These include increased loading on screw due to the simplification of the fracture site, position of the implant, the material properties of the artificial bone and the stiffness of the new implant. It is no currently possible to determine the exact cause of these fractures however it is likely to be a combination of these factors.

It may also be suggested that these fractures were caused by the more compliant MISHS generating higher loads on the supporting bone than the stiffer SHS device. While it is true that the bone must provided more support to more compliant devices, the results from Chapter 7 do not show a significant increase in stress in the region of the bone which fractured. Although this does not definitively prove that the fracture was not cause by the more compliant device, it does give some weight to the argument against that as a possible cause.

It should also be noted that the mid-stance loading conditions will have had some effect on the tests results, in particular the exclusion of any anterior/posterior force component will have removed the torque load which would have been applied to the plate if included. However given the effect that the presence of bone had on the stiffness of the implants loaded in the mid-stance condition, as shown in the isolated implant and femoral shaft tests in Chapter 5. It is not unreasonable to assume that the bone would provided similar support to the implant when subject to a force in the anterior/posterior direction, in effect reducing the torque on the plate. There is however a risk that the presence of osteoporotic bone in this region may effect the ability of the bone to support this load.

9.5 Conclusions

The results of these test show two important points, firstly the MISHS design performs similarly to the SHS when implanted in a fractured femur. While the test does not fully represent the exact conditions which the implant will be subject to when implanted in the human body, it does present a worst case scenario. By representing the fracture site as a straight cut with no intermediate tissue, it is assumed that it will behave in a much less stiff manner than a a fracture within the human body.

The fatigue test showed that when loaded cyclically the standard neck screw failed before the MISHS plate. As this neck screw is the same screw as is used in the current SHS device it can be assumed that MISHS would not fail in fatigue at any more than the SHS does as the weak point in both designs is the screw.

It can therefore be said that the MISHS design is capable of withstanding the mechanical loads applied to it during the treatment of a extracapsular proximal femoral fracture, however further tests are needed to better understand the effect of the device on the surrounding bone, and how the presence of osteoporotic bone and more realistic loading conditions affect the performance of the device. These test should include a study into the effect of implant position on the surrounding bone, in particular whether the fractures seen in this study are affected by the proximal position of the implant. This study should be carried out using both SHS and MISHS implants to allow comparison between the implants for each position.

10

Discussion

10.1 Finite Element Model

The model created in this study was developed specifically to be a tool to allow comparison between implant designs. The decision to develop a model was taken due to a lack of published modelling methodologies which could be used to carry out this task and give reliable results which could be used to select a design. The development of the model was successful with it's behaviour corresponding closely to the mechanical test data. The model was however simplified in many ways to allow this validation to be carried out. There have been many attempts by other authors to develop more complex models and it may be of some value to compare the results from the model developed in this study to those models, to gain a fuller understanding of how these simplifications may have affected the results.

Hrubina et al. (2013) utilised a model which was similar to that developed in the current study. Unlike the model developed in the current study, Hrubina's model includes frictional contact, an anisotropic material model for cortical bone and an elasto-plastic model of stainless steel. Although the validity of Hrubina's model is questionable, due to its lack of validated coefficients of friction, as was discussed in Section 2.10.2, it is interesting to see how the results of the models compare.

Figure 10.1 shows the stresses in the model at 2.4 mm applied displacement, this displacement corresponds to a reaction force of 1025 N. This load is the closet available to the 1000 N applied in Hrubina's model and will therefore allow for the best comparison. Figure 10.1a shows a maximum stress in the femoral shaft of 130.6 MPa in

the 4th (distal most) screw hole, this compares to a stress of 192.94 MPa reported by Hrubina, this model however included only a three hole plate and as such this stress value was taken from the third screw hole. Figure 10.1b shows a maximum stress in the femoral head of 177.66 MPa at the point of contact between the loader and the bone, the maximum stress in the head reported by Hrubina was 170.63 MPa however no location was given. Although these results are similar they tell us little about the behaviour of the models as this stress is only a result of the method by which the specimen was loaded and is dependent only on the load applied, and the shape and material properties of the loader and bone. The maximum stress in the plate was 746.47 MPa at the end of the barrel where it contacts the bone Figure 10.1c shows stresses around the neck screw hole of approximately 550–700 MPa, the stress around the distal shaft screw hole is < 50 MPa. Hrubina states that the highest stress within the plate in their model was 436.53 MPa, however no location is specified. From contour plots published (Figure 10.2) it appears that the highest stress occurs at the distal screw hole, with little stress in barrel or at the transition from barrel to plate. This is significantly different from this study which should very small stress at the screw holes and high stresses around the barrel and transition region. Figure 10.1d shows the highest stress found in the neck screw was 706.15 MPa, this is higher than the value of 435.31 MPa found by Hrubina. From the comparison of the stresses in the plate and the screw it is clear that there is a difference in behaviour between these models. It is possible that the lower stress seen in the neck screw in Hrubina's model is due to the frictional conditions at the fracture site. This friction may allow greater transfer of load across the fracture site and reduce the loading on the screw. It is possible that differences in stress around the screw holes is due to different size plates being used with different number of screws in each. Nevertheless the comparison is reassuring in that, whilst differences exist, they are not so different as to cause concern and are explainable.

Rooppakhun et al. (2010) developed at a model of a 2 hole SHS plate in a fractured femur, the fracture site was modelled using an intermediate layer to simulate tissue, the material properties of which were varied between test runs to simulate different stages of healing. The fracture site in this model is curved rather than straight, this should give a more stable fracture than a straight cut. It should also be noted that the barrel of the plate appears to extend past the fracture site (Figure 10.3). This will

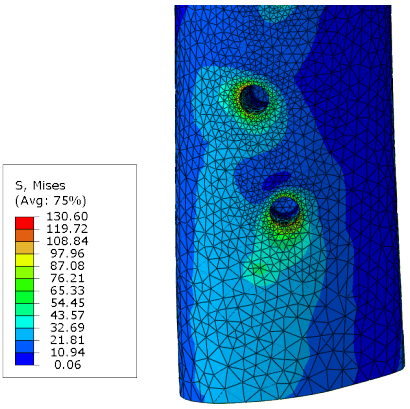

(a) Shaft

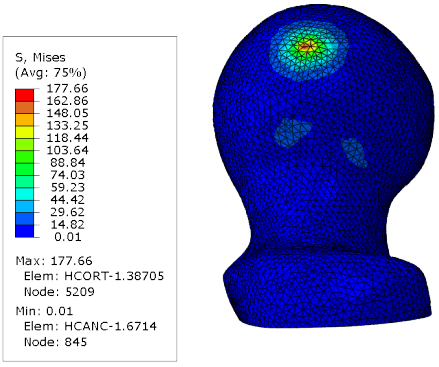

(b) Head fracture site

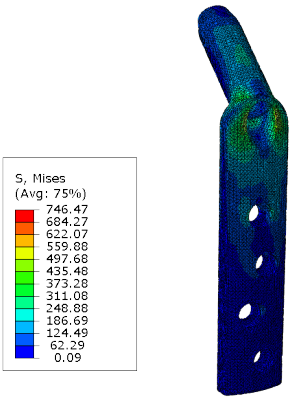

(c) Plate

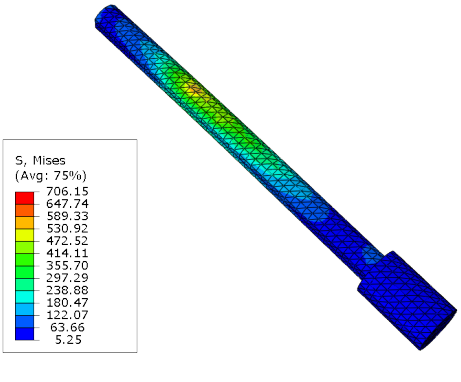

(d) Screw

Figure 10.1: Von Mises stress in model at 2.4 mm applied displacement

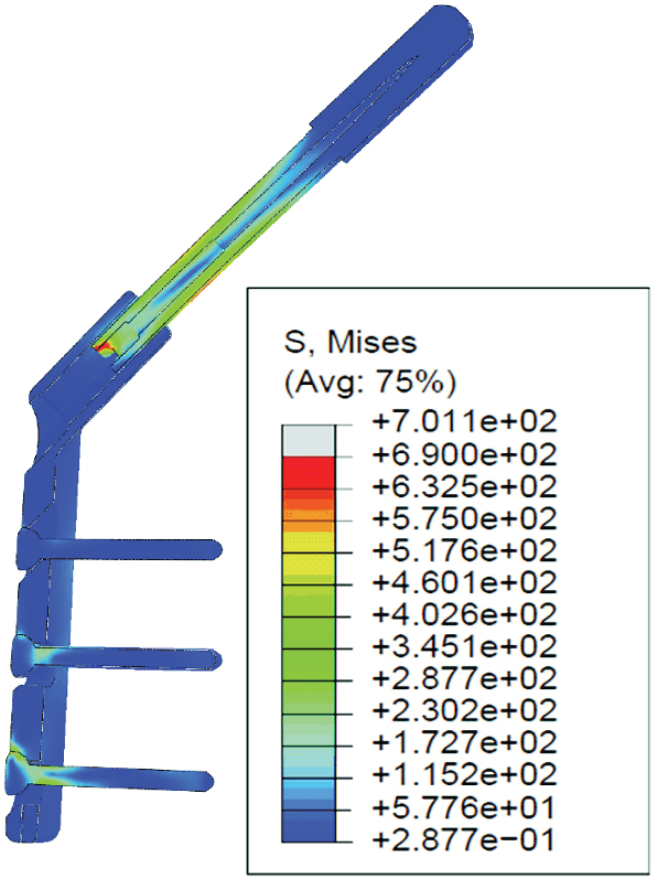

Reprinted from Journal of Applied Biomedicine, 11(3) , Hrubina et al., Computational modelling in the prediction of Dynamic Hip Screw failure in proximal femoral fractures, pp.143-151 , Copyright (2013), with permission from Elsevier.

Figure 10.2: Von Mises in plate and screw (Hrubina et al., 2013)

allow the head to be supported directly by the barrel, however in a clinical setting this may prevent the sliding mechanism from functioning properly.

Figure 10.4 shows the Von Mises stress in the plate and the screw at 4.6 mm applied displacement, this corresponds with an applied load of 1982 N, the load applied by Rooppakhun was 1987 N. It is difficult to compare results directly between these models as the stress in two of the key areas, in the neck screw and around the neck screw hole, exceeds the range of the contour plot (Figure 10.5). The stress in the plate is reported nowhere else in the paper. Some comparison can be made by looking at the areas surrounding the high stress areas, the stress in the plate around the neck screw hole is approximately half that seen in the model developed in this study, the neck screw also seems to be under considerably lower stress. It should be noted however that the load applied to this model was applied at a different angle and at the views do not give a clear indication of the stress values in the screw. The lower stresses in the Rooppakhun model are likely due to the different modelling of the fracture site, the shape of the fracture and material properties used to mode the tissue between the fragment has likely produced a much more stable fracture that needs less support for the device. It should also be noted that although the magnitude of the loading was matched fairly closely, the Rooppakhun model does not load the specimen directly downwards and therefore this may also have affected the comparison.

Goffin et al. (2014) presents the results from a range of finite element models developed to investigate how different material models will affect the stress modelled in the femoral head. The major difference between this model and the one developed in this study is that Goffin included the thread of the neck screw in the model and attempted to model the interaction between the screw and the bone using friction. Within the current study the interaction between the bone and the neck screw was not being investigated and therefore the thread was simplified and the components tied together. However comparison of the stresses within the head to those found by Goffin will give some insight into the effect of this simplification. Figure 10.6 shows the stress in the cancellous component of the femoral head, at 4.3 mm of applied displacement, which corresponds with a load of 1856 N. Figure 10.7 shows the results presented by Goffin, at an applied load of 1866 N. The stress patterns in the two results are very different, stress above 1.395 MPa, in the Goffin model were considered to have yielded, however it is not specified whether any yield behaviour was used in the model. It can be seen

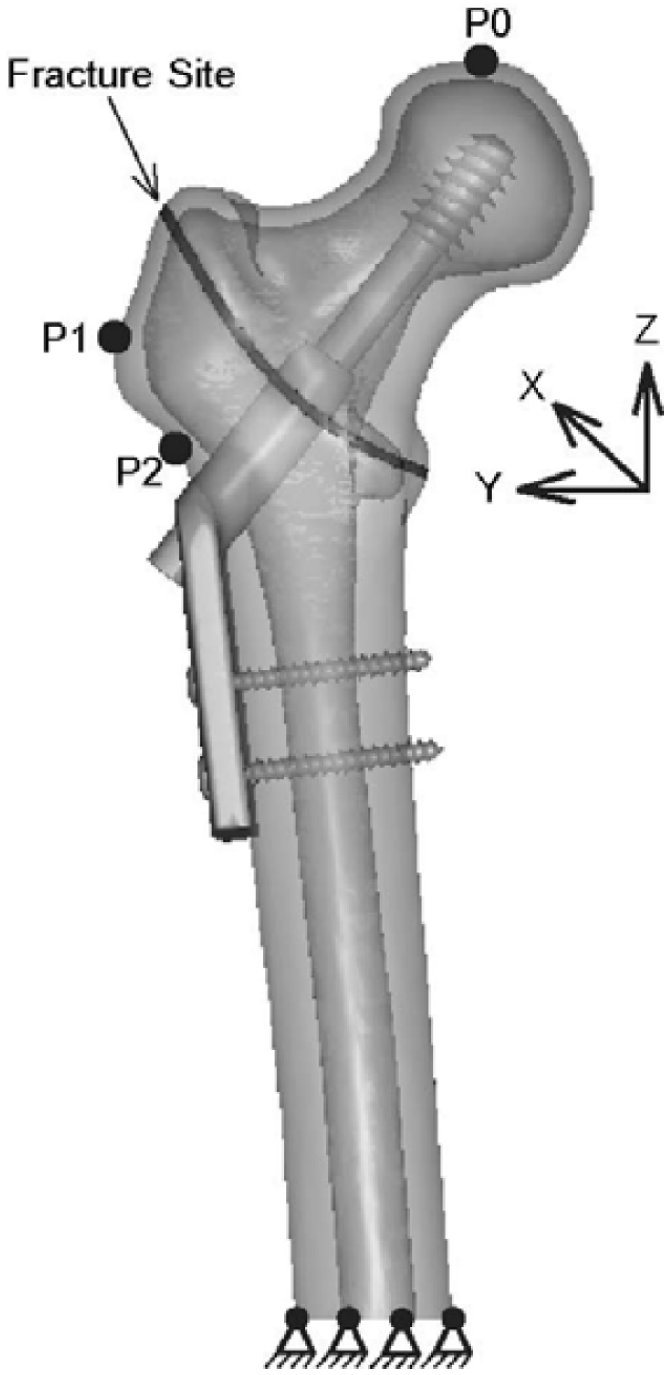

Figure 10.3: Model developed by Rooppakhun et al. (2010).

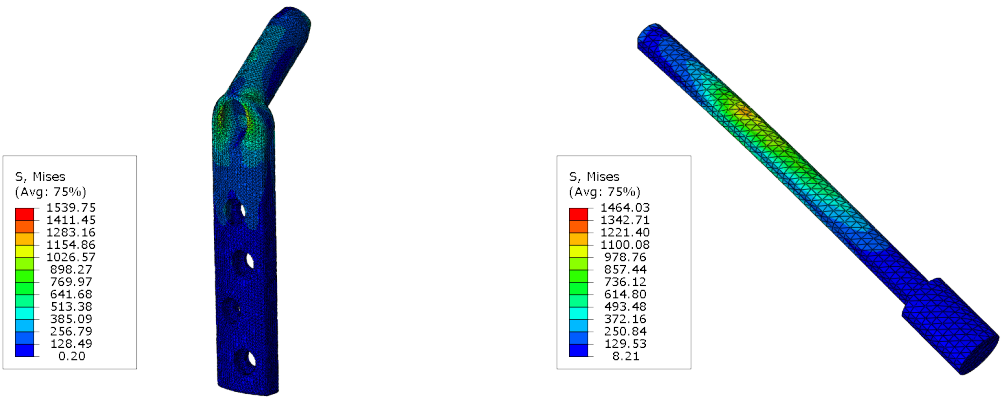

(a) Plate **(b)** Screw

Figure 10.4: Von Mises stress in model at 4.6 mm applied displacement

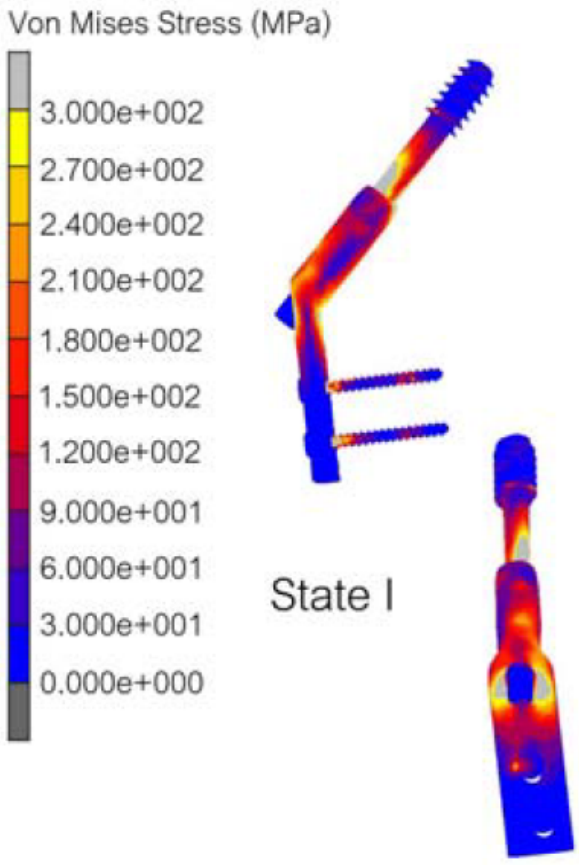

Figure 10.5: Von Mises in plate and screw (Rooppakhun et al., 2010).

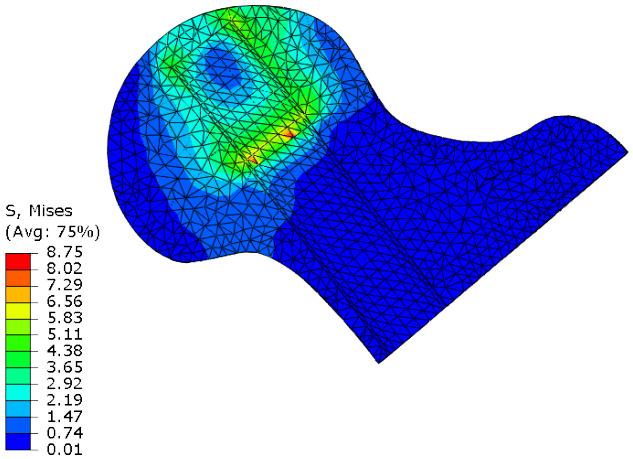

Figure 10.6: Von Mises in the cancellous bone of the femoral head at 4.3 mm applied displacement.

that there is an area of high stress above the screw in the Goffin results and very little stress below it. Where as the results from in Figure 10.6 show high stresses at both sides on the proximal end of the screw and much lower stresses distally. Goffin's result also shows an area of high stress at the distal end of the screw. This would signify that the neck screw is contacting the bone here, this contact has not been seen at all in this study. This may suggest that there is very little clearance between the screw and the bone in the Goffin model and that the author has not included the reamed hole that is created to allow the device to be implanted. This may cause high stresses in the bone surrounding the shank of the screw, which would usually have be removed. Although the stress patterns are different between the models the magnitude of the stress is similar.

When the reults from the FE model are compared to those from similar tests, it can be seen that there are several differences. This however is not unexpected as each model has been designed in order to answer different questions and as such simplifications or assumptions which are valid for one may not be valid for another. It should also be noted that the results published do not always allow a direct comparison to be carried out. The model was developed for this study as no suitable existing validated methodology could be found, it was therefore not expected that the results would match those of

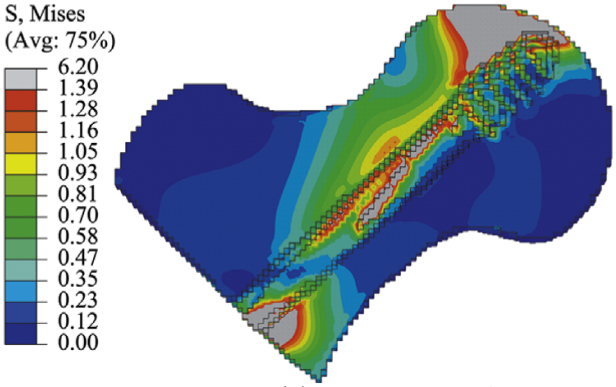

Reprinted from Journal of Biomechanics, 47(1) , Goffin et al., Are plasticity models required to predict relative risk of lag screw cut-out in finite element models of trochanteric fracture fixation?, pp.323-328 , Copyright (2016), with permission from Elsevier.

Figure 10.7: Von Mises in the cancellous bone of the femoral head (Goffin et al., 2014).

other models. The model developed in this study was validated against the stiffness of mechanical tests, and as such it should be seen as a suitable method for comparing SHS designs.

It may be possible to apply this methodology to similar applications such as alternative devices to the SHS similar devices. Although it was determined unnecessary to include friction within this model, there may be some value in developing the model further and including friction at the fracture site.

10.2 Effects of Osteoporotic Bone of the Performance of the MISHS

The testing and modelling carried out during this study has utilised artificially bones in place of cadaveric samples. These artificially bones have been shown to be good substitutes for healthy human bone and were chosen primary because they would provide a repeatability which would not be achievable with cadaveric samples. However many of the patients who are treated for hip fractures are elderly and suffer from osteoporosis and there strength of their bones will be significantly lower than that of healthy human bone.

As discussed in 2.7, a major cause of failure of treatment with an SHS is cut out of the screw from the femoral head. This failure can occur due to osteoporotic bone in

the femoral head insufficient strength to allow the neck screw to be secured. Another possible source of failure due to osetoporotic bone is pull out of the femoral shaft screws. As with the neck screw osteoporotic bone may be too weak to withstand the load which is applied to these screws by the plate.As the MISHS utilises the same screws as the current designs, it can be assumed that the quality of fixation will be identical and as such the MISHS should suffer for a similar rate of cut out of the neck screw and pull out of the shaft screws as the SHS.

The performance of the device could also be affected by by the presence of osteoporosis in the bone surrounding the barrel of the plate. As the MISHS implant is more compliant and weaker than the SHS device it may rely more on the surrounding bone to provide support. Therefore there is a risk that if the bone surrounding the barrel was osteoporotic the MISHS may fail when the SHS would not. Further investigation will be needed to compare the performance of the MISHS and SHS in osteoporotic bone.

10.3 Minimally Invasive Sliding Hip Screw

Although there is still some work to be done to prove that this device functions as intended the results from this study are promising and appear to show that the device is capable of with standing the loads required. If this device was to become the standard treatment for extracapsular proximal femoral fractures, it could reduce the recovery time of many patients and substantially reduce the cost to the health service.

When compared against similar devices, it can be seen that the MISHS has some advantages over them.

Gotfried (2000) developed the PCCP device, a minimally invasive alternative to the SHS, which utilises two neck screws. One area where this device may be superior to the MISHS is stiffness, the PCCP should be inherently stiffer than the MISHS device due to the double screw design, which effectively increases the second moment of area of the device increasing its stiffness in bending. The PCCP device being a stiffer design than the MISHS does not however mean that it is the superior device. Although the results from this study cannot conclusively say that the MISHS is stiff enough, the results do show a device which performs similarly to the SHS. If further tests show that the MISHS is sufficiently stiff, the additional stiffness of the PCCP will give it no advantage.

The PCCP may also provide some additional rotational stability when compared to the MISHS due to its double screw design. The MISHS does incorporate a feature which prevents rotation of the neck screw, however with a single screw there is always the possibility that the threaded will begin to loosen in the femoral head and the bone fragment will rotate.

Despite the two previous points which appear to show the double screw design of the PCCP being superior to the MISHS, the single screw design does have a distinct advantage. The double screw design of the PCCP device has been shown reduce sliding when compared to single screw designs Ropars et al. (2008). This design may lead to failure of the sliding mechanism, as any misalignment in the two screws may cause the assembly to jam, resulting in loss of contact between the bone fragments which would increase the risk of failure due to either bending of the screw or cut out. By utilising a single screw design the MISHS maintains one of the key features of the current device: to allow sliding between the screw and the plate.

The implantation procedure for the PCCP was found to be around to be significantly quicker than the that of the SHS by Brandt et al. (2002). However from the patent Gotfried (1994) it appears that the procedure may be a little more complicated and involve some fairly complex tooling. This may have lead the the lack of adoption of the PCCP amongst surgeons. The full implantation procedure and tooling have not yet been finalised for the MISHS and as such a direct comparison cannot be made. However the MISHS device was designed in such a way that the procedure would be as similar to the current procedure as possible.

The MISS device developed in France and tested by Ropars et al. (2008) is a device which appears to be very similar to the current device. No patent or detailed description of the device could be found, however as was discussed in Section 2.6.2, it appears that there is no feature incorporated into the design to prevent rotation of the neck screw. In order for the fracture site to be stable it would therefore be necessary to insert a secondary screw into the femoral head to prevent its rotation. The MISHS device is designed to prevent rotation of the neck screw and therefore provide a stable fracture.

As with the MISS, the device patented by Kyle (1984) lacks any feature to prevent rotation of the femoral head. The device utilises a two piece neck screw, with the self tapping thread at the top of the screw being separate from the shank. The two piece screw is assembled into the barrel before surgery, the screw and barrel are then inserted

at the same time. Therefore the screw must be able to rotate within the barrel to allow it to be inserted into the bone.

The MISHS incorporates key features of the SHS which previous designs have failed to include. The inclusion of the flats on the screw and barrel, will allow the MISHS to provide more rotational stability than either the MISS or the Kyle device. The use of a single neck screw will allow the sliding mechanism to perform with the same reliability as that found in the current device, without the risk of it jamming, that is associated with the double screw design of the PCCP. Therefore , in the opinion of the author, the design detailed in this thesis, if proven to be sufficiently stiff and once a suitable implantation procedure is developed, may be considered a superior device to the PCCP, MISS or Kyle device.

11

Further Work

Cadaveric Testing

The purpose of the testing carried out as part of this project was to establish proof of concept for the MISHS device and as such it was deemed acceptable to use artificial bones within these tests. However before these devices can be implanted into living humans it is advisable that a large scale cadaveric study should be carried out. Ideally mechanical testing should be carried out using cadaveric specimens of a variety of ages, sizes and health. In order to provide an accurate comparison the study should include testing of both the new MISHS device and the currently used SHS device preferably using the contralateral femur from each cadaver to test different implants. This cadaveric study will allow the performance of the MISHS device to be studied under and greater variety of conditions which may occur during its use in vivo.

Refinement of Design

The selected design of the MISHS contained many simplifications that were necessary to allow the prototype to be manufactured easily. It would therefore be desirable to carry out further refinement of this design to make it suitable for use in vivo, it may also be useful to add new features to the design.

The overall contours of the device were made square during the prototyping process. These should be altered to give more rounded edges to reduce the chance of tissue damage or pain caused by sharp edges. The transition between the barrel and the plate was also simplified and should again be rounded, this will reduce any stress concentrations that occur in this region.

The screw holes in the plate were simplified to round counterbored holes. However most fracture fixation devices contain holes which are contoured to apply tension to the plate as the screws are tightened. These features should be re incorporated into the device. It may also be useful to incorporate a self locking mechanism into the shaft screws preventing them for loosening.

It will be necessary to incorporate into the design a mechanism to ensure that the locking plate and screw, which maintain the connection between plate and the barrel, do not become loose. Potential mechanisms include: a self taping thread near the head of the screw which could cut into the locking plate, ridged surfaces where the screw head and plate make contact or a locking washer.

Manufacturing Process

In order to both incorporate new features into the device and produce enough devices for trials and clinical use, it is essential that a suitable manufacturing process be developed. There are several manufacturing methods which may be useful to consider:

Machining, it is possible to produce the device by machining from a block of material. However due to the complex shape of the device, a 5-axis computerized numerical control (CNC) milling machine will likely be required. There are also features on the device that, may not be possible to machine and will have to be produced using other techniques such as EDM. CNC machining of the device will be expensive and time consuming, and may not be a viable or cost effect method for large scale production.

Casting is another possible method which could be used for manufacturing. Casting is the process of pouring molten metal into a mould in order to create the required shape. Several different casting methods exist however most can be grouped into two categories: those that use an expendable mould and those that use a permanent mould. Both methods allow fairly complex shapes to be produced with very little machining required. However when using a permanent mould method care must be taken to ensure that the mould is designed in such a way that the piece can be removed after is solidifies, this places some limitations on what can be produced. Expendable mould methods have less limitations, as the moulds are not reused they can simply be broken apart to remove the finished piece. Permanent mould methods have a significantly higher initial cost than expendable mould, however set-up they components are relatively cheat and quick to produce. Expendable mould methods have a lower initial cost however the

need to produce a new mould for every time increase the cost and time per component. Cast components are typically less tough than components manufactured using other methods, there is also a reasonable risk of defects occurring during the casting process.

Forging offers another possible technique for manufacturing these devices. Forging is the process of compressing a piece of metal into shape, this can be done using various methods including drop forging, press forging or rolling and can be carried out with the material either hot or cold. A set of dies are produced and the metal is placed between them, the die are then forced together compressing the material into the required shape. Forging can produce components of relatively complex shapes however it cannot match those created by expendable mould casting. In order to produce a MISHS device in this way, machining would likely to be necessary afterwards in order to produce some of the features such as holes. In particular the hole within the barrel would need be produced using EDM. Forging produces materials that are tougher than those produced in casting, however the process leads to some anisotropy and heterogeneity within the material. As with permanent mould casting methods, forging has a high initial cost and is not suitable for small batch production.

Aside from selecting and designing a manufacture process that will satisfactorily produce the component to the required shape it is also essential that processes compliance to standards be considered. In particular the following process should be compliant with the following standards:

- BS ISO 5832 Implants for Surgery - Metallic Metals Part 1: Wrought Stainless Steel(British Standards Institute, 2007)
- BS ISO 15374 Implants for Surgery. Requirements for the production of forgings (British Standards Institute, 1998)
- BS 7254 Orthopaedic implants. Specification for general requirements for materials and finish (British Standards Institute, 1990b)

Design of Surgical Instruments

In order for the MISHS device to be implanted safely. it will be necessary to design bespoke instruments. While much of the implantation procedure remains similar to current device some additional steps are needed. As this device will be implanted

through a small incision it will be necessary to design a set of instruments that will allow each component to be inserted independently and assembled inside. This will have to involve a mechanism to align the barrel and plate allowing them to slide together, it will also require a mechanism to inset the locking plate and tighten the screw. Once the plate is assembled the shaft screws will have to be inserted percutaneously, this will require a guide to ensure the screws are inserted in the correct locations.

The design of the instruments may be a particularly difficult stage in the process, as poorly designed tooling may lead to lack of adoption of the device. It is therefore important to ensure that the instrument design is an iterative process carried out in conjunction with experienced surgeons. This will help insure that suitable instruments can be developed.

Cadaveric Surgical Trials

Throughout the process of tool development and after the final tools have been designed, it will be necessary to carry out cadaveric surgical trials. This will allow the tooling to be evaluated quantitatively by measuring metrics such as surgery duration, required incision length and accuracy of implant positioning. It will also allow qualitative evaluation through feedback from the surgeons.

Cadaveric surgical trials will be vital to ensuring that good quality practical tools can be produced.

Clinical Trails

Once the device as been proven to be safe enough for use in humans, it will be necessary to carry out a clinical trial to prove the efficacy of the device. Key metrics which would need to be measured during this trail include: procedure duration, incision length, duration of hospital stay, pain, rate and cause of failure, and healing time. The trail would have to compare the results from the use of the MISHS against those form the conventional SHS and show that there is a benefit to the use of the new device.

12

Conclusions

As the average age of the population increases the occurrences of extracapsular proximal femoral fractures is predicted to increase with it. The currently most common treatment for these fractures is the SHS, which although originally developed over 50 years ago is still more widely used than modern alternatives such as the the Gamma nail (Royal College of Physicians, 2013, 2014; Health service Bergen, 2010). The implantation procedure for the SHS involves a large incision being made down the lateral side of the patients thigh causing tissue damage and blood loss which leads to an extended recovery period. With the increasing rate of these fractures it is vital to improve the recovery time associated with these surgeries, reducing the risk of mortality and morbidity and thus reducing the cost to the healthcare system.

Minimally invasive surgical techniques has been shown to be an effective method for reducing the recovery time of patients in many different fields, including orthopaedics (DiGioia et al., 2003; Hata et al., 2001; Wong et al., 2009). Several attempts have been made to make minimally invasive SHS like devices, however none have been brought into common use. This may be due to several factors including poor design, or complex or lengthy implantation procedures. The development of a minimally invasive sliding hip screw (MISHS) which performs as well as the current device and utilises an implantation procedure which is a similar as possible could be a significant step in improving the treatment of extracapsular proximal femoral fractures.

The aim of this project was to develop a MISHS device which was capable of performing as well as the current device and could be implanted using a minimally invasive procedure which differed as little as possible from that used with the current

device. The difficulty in this project lay in determining whether a new design could perform as well as the current device. There are several criteria which SHS must be able to meet in order to function: it must be able to be secured to both the head and shaft of the femur without cutting out, it must be able to allow movement across the fracture site and maintain contact between the fragments, it must be stiff enough to maintain the alignment between the fragments, and it must be strong enough to support the load acting on it during walking in the days after surgery. The first two criteria could easily be achieved in the new device by simply using the same screws as the old device and designing the sliding mechanism to be identical, however determining how stiff and strong the device must be was not simple.

No publications or standards could be found which specified the strength or stiffness requirements of current SHS devices. It was not possible to simply specify that the new design should be as strong and stiff as the current design, as the inclusion of any joining mechanism would weaken the MISHS device which would then have to be made larger to achieve the same strength as the SHS. It was decided that in order to evaluate the performance of the new design it would have to be compared against the current device when implanted in bone. While the MISHS may be both more compliant and weaker than the SHS when tested in isolation, the presence of the bone could significantly affect the behaviour of each device.

Due to the complexity of the proposed MISHS designs it was not possible to manufacture and test many prototypes in the lab, it was therefore determined that only one design could be take to the prototyping stage. In order to evaluate which design would be most suitable to manufacture, the designs were modelled and their mechanical performance analysed using FEA.

It was first necessary to validate the material properties of the artificial femur. Three point bending tests of samples taken from the femur found that the stiffness of the cortical bone material was significantly lower than was stated by the manufacturer. When the Young's modulus, measured in the test, for cortical bone was applied to a FE model of the femur along with the manufacture supplied properties for the cancellous bone it was found that the model behaved similarly to artificial femur in laboratory tests. The material properties applied to this model were similar to those recorded in real bone, it was therefore concluded that the artificial bones were suitable to be used

as a replacement for cadaver samples and that they could be accurately modelled using FEA.

In order to investigate the performance of the SHS and to allow new designs to evaluated three FE models of the SHS were created and validate against mechanical tests:

Firstly, the SHS was modelled in isolation, this allowed validation of the mesh and material properties applied to the SHS model. As with the model of the femur it was found that the SHS model behaved similarly to the mechanical test. This validation test, along with that carried out on the femur, gave confidence that the two major components which would be used in more advanced models, were behaving in a realistic manner.

Secondly, a model of the SHS device implanted in a femoral shaft with the head removed was created. The purpose of this model was to validate the interaction of the plate with the femur and to allow the effect which the presence of the bone has on the stiffness of the device to be investigated. The results of the validation study found that although there was a difference in behaviour between the model and the mechanical tests over the initial 0.5 mm of applied displacement, past this point the results showed almost identical stiffnesses. It was therefore concluded that the model was sufficiently accurate to be used within the study.

Thirdly, a model was created which contained the SHS implanted in a fractured femur. It was intended to model as closely as possible the behaviour of the device when implanted within the human body while remaining simple enough that they could be validated within the lab. Several simplifications had to be made to the model to ensure that the model would solve and that validation was possible. The fracture site was simplified to a straight cut in the bone with no intermediate tissue between the fragments and modelled with frictionless contact. Initial it had been considered that the fracture site should be modelled in a more realistic manner containing a complex fracture geometry and intermediate tissue at different stages of healing. However accurate data about the material properties of the tissue at the fracture site could not be found and no practical way of validating the model could be thought of. It was therefore decided that it would not be possible to model the fracture in this manner.

The results from the mechanical test of the SHS implanted in the fractured femur showed a reasonable amount of variation and as such it was difficult to say that the FE

model created accurately modelled the mechanical test. The results from the FE did however fit mostly within one standard deviation of the mechanical test result mean. It could therefore be said that although the FE model is not an accurate representation of the implant in the human body, it does exhibit similar behaviour to the mechanical test and would therefore be useful in comparing the designs on the MISHS to the SHS.

Several MISHS design concepts were generated and evaluated using the The "Total Design" methodology developed by Stuart Pugh. This process allowed the designs to be objectively compared in order to select only those concepts which are viable designs. This process identified three designs which were suitable to take to the next stage of the design process.

Each of the three concepts chosen were modelled using the same methods which were validated for the SHS earlier. The results found that while the new concepts were significantly less stiff than the current device when tested in isolation, the presence of the bone effectively stiffened these devices bringing there performance much closer to that of the current device.

Although the FEA showed that the designs were capable of performing similarly to the SHS, it was essential that the designs be mechanically tested in the laboratory. Due to budgetary and time constraints it was only possible to manufacture prototypes of one design for mechanical testing. A single design was therefore taken forward to the prototype stage and three implants were manufactured for testing. Three mechanical tests were carried out on the new device:

Firstly, the device was implanted in a femoral shaft with the head removed and tested using the same method used to test the SHS previously. The results of this test found that the device was behaving roughly twice as stiff as both the model and the mechanical test of the SHS. On further investigation it was found that the positioning of the device during this test differed slightly from the previous test and the model. It is thought that the position of the MISHS device during this test may have caused it to come into contact with the cortical bone resulting in an increased stiffness. Unfortunately due to time constraints it was not possible to re-run this test, it may therefore be necessary to carry out further testing in the future in order to produce results which can be accurately compared to the previous tests.

Secondly, the device was tested in a fractured femur using the same methodology used to test the SHS. The results from this test found that the stiffness of the specimen

was similar to that seen during the equivalent test on the SHS. However the failure load was considerably lower and the failure mode was a calcar fracture rather than a fracture of the femoral head. The specimen used during this test was the same specimen used in the previous test and as such the difference in implant position may have played a role in the differing results. The results do however show a similar stiffness to the current device and it may therefore be concluded that the new design is suitably stiff to maintain alignment between the bone fragments. However further testing will be needed to determine whether the calcar fracture occurred due to the position of the implant or the increases compliance of the device itself.

Thirdly, a cyclic fatigue test of the device was carried out. The test setup was similar to the previous test with a cyclic load being applied to simulate walking. The test ran for 58229 cycles before failure. Two failures were found in the specimen, fracture of the calcar and deformation of the neck screw, however due to the duration of the trail it was not possible to observe the specimen at all times and therefore it is difficult to determine which failure occurred first. The implant position during this test was identical to that in the two previous tests and a such it cannot be determined whether the calcar fracture is due to this positioning. What can be said however is that it is unlikely that fatigue failure will occur within the MISHS plate. The risk of high cycle fatigue in the device is low, as the bone will have begun to heal before enough cycles are completed for failure to occur and it is likely that the high forces required to initiate low cycle fatigue would cause fractures in the bone or failure of other components first.

The results from the model and mechanical test have shown that the MISHS device is capable of providing the stiffness need to maintain alignment between the bone fragments and that the device is suitably strong to prevent low cycle fatigue. However further investigation will be needed to confirm whether the calcar fractures are caused by the reduced stiffness of the device.

The design presented in this thesis successfully incorporates the key features of the current SHS implant into a minimally invasive device. Once fully developed this device has the potential to significantly improve the treatment of extra capsular proximal femoral fractures. Allowing minimally invasive surgical techniques, which have become common for many other procedures, to be utilised to improve the treatment of patients and reduce demands on the health service.

References

AAOS, 2014. *Management of Hip Fractures in the Elderly Evidence-Based Clinical Practice Guideline.* 24, 33

ANZHFR, 2014. *Australia and New Zealand Guideline for Hip Fracture Care.* 24, 33

Arden, G.P. and Walley, G.J., 1950. *Treatment of Intertrochanteric Fractures of the Femur by Internal Fixation. British Medical Journal*, **2**(4688), pp. 1094 –1097. 15

ASTM, 2003. *ASTM D638-03: Standard Test Method for Tensile Properties of Plastics.* 64

ASTM, 2011. *ASTM F384 Standard Specifications and Test Methods for Metallic Angled Orthopedic Fracture Fixation Devices.* 33

Audigé, L., Hanson, B. and Swiontkowski, M.F., 2003. *Implant-related complications in the treatment of unstable intertrochanteric fractures: meta-analysis of dynamic screw-plate versus dynamic screw-intramedullary nail devices. International Orthopaedics*, **27**(4), pp. 197–203. 31, 32

Baca, V., Kachlk, D., Hork, Z. and Stingl, J., 2007. *The course of osteons in the compact bone of the human proximal femur with clinical and biomechanical significance. Surgical and radiologic anatomy: SRA*, **29**(3), pp. 201–207. 43

Bariteau, J.T., Fantry, A., Blankenhorn, B., Lareau, C., Paller, D. and DiGiovanni, C.W., 2014. *A biomechanical evaluation of locked plating for distal fibula fractures in an osteoporotic sawbone model. Foot and Ankle Surgery*, **20**(1), pp. 44–47. 44

Bartels, W.P., 1939. *The Treatment of Intertrochanteric Fractures. The Journal of Bone and Joint Surgery (American)*, **21**(3), pp. 773–775. 13

Baumgaertner, M., Curtain, S. and Lindskog, D., 1995. *The value of the tip-apex distance in predicting failure of fixation of peritrochanteric fractures of the hip. The Journal of Bone and Joint Surgery (American)*, **77**(7), pp. 1058–1064. 28

Bhandari, M., Schemitsch, E., Jnsson, A., Zlowodzki, M. and Haidukewych, G.J., 2009. *Gamma nails revisited: gamma nails versus compression hip screws in the management of intertrochanteric fractures of the hip: a meta-analysis. Journal of orthopaedic trauma*, **23**(6), pp. 460–464. 31, 32

Brandt, S., Lefever, S., Janzing, H., Broos, P., Pilot, P. and Houben, B., 2002. *Percutaneous compression plating (PCCP) versus the dynamic hip screw for pertrochanteric hip fractures: preliminary results. Injury*, **33**(5), pp. 413–418. 26, 178

British Standards Institute, 1990a. *BS 7251-6 Orthopaedic joint prostheses. Method for determination of endurance properties of stemmed femoral components of hip joint prostheses without application of torsion*, London: British Standards Institute. 39

British Standards Institute, 1990b. *BS 7254 Orthopaedic implants - Part 2: Specification for general requirements for materials and finish*, London: British Standards Institute. 182

British Standards Institute, 1998. *BS ISO 15374 Implants for Surgery. Requirements for the production of forgings.* 182

British Standards Institute, 2007. *BS ISO 5832 Implants for surgery - Metallic materials - Part 1: Wrought stainless steel*, London: British Standards Institute. 71, 143, 182

Charnley, J., Blockey, N.J. and Purser, D.W., 1957. *The Treatment of Displaced Fractures of the Neck of the Femur by Compression. The Journal of Bone and Joint Surgery (British)*, **39-B**(1), pp. 45–65. vii, 18, 19

Chirodian, N., Arch, B. and Parker, M.J., 2005. *Sliding hip screw fixation of trochanteric hip fractures: Outcome of 1024 procedures. Injury*, **36**(6), pp. 793–800. vii, 1, 10, 28, 106, 166

Chong, A.C.M., Miller, F., Buxton, M. and Friis, E.A., 2007. *Fracture Toughness and Fatigue Crack Propagation Rate of Short Fiber Reinforced Epoxy Composites for Analogue Cortical Bone. Journal of Biomechanical Engineering*, **129**(4), pp. 487–493. 64

Claes, L., Wilke, H.J., Augat, P., Rbenacker, S. and Margevicius, K., 1995. *Effect of dynamization on gap healing of diaphyseal fractures under external fixation. Clinical Biomechanics*, **10**(5), pp. 227–234. 12

Cleveland, M., Bosworth, D.M. and Thompson, F.R., 1947. *Intertrochanteric Fractures of the Femur: A Survey of Treatment in Traction and by Internal Fixation. The Journal of Bone and Joint Surgery (American)*, **29**(4), pp. 1049–1082. 14, 15, 16

Clyde, J., Kosmopoulos, V. and Carpenter, B., 2013. *A Biomechanical Investigation of a Knotless Tension Band in Medial Malleolar Fracture Models in Composite Sawbones. The Journal of Foot and Ankle Surgery*, **52**(2), pp. 192–194. 44

Cook, R.D., Malkus, D.S. and Plesha, M.E., 2001. *Concepts and Applications of Finite Element Analysis.* 4th edition. Wiley. 72

Cristofolini, L. and Viceconti, M., 2000. *Mechanical validation of whole bone composite tibia models. Journal of Biomechanics*, **33**(3), pp. 279–288. 43

Cristofolini, L., Viceconti, M., Cappello, A. and Toni, A., 1996. *Mechanical validation of whole bone composite femur models. Journal of Biomechanics*, **29**(4), pp. 525–535. 43

DiGioia, A.M., Plakseychuk, A.Y., Levison, T.J. and Jaramaz, B., 2003. *Mini-incision technique for total hip arthroplasty with navigation. The Journal of Arthroplasty*, **18**(2), pp. 123–128. 1, 24, 184

Eberle, S., Gerber, C., Oldenburg, G.v., Hgel, F. and Augat, P., 2010. *A Biomechanical Evaluation of Orthopaedic Implants for Hip Fractures by Finite Element Analysis and In-Vitro Tests. Proceedings of the Institution of Mechanical Engineers, Part H: Journal of Engineering in Medicine*, **224**(10), pp. 1141–1152. 42

Ender, J. and Ender, H.G., 1977. *US4055172 Patent.pdf. US Patent Office.* vii, 22

Esser, M., Kassab, J. and Jones, D., 1986. *Trochanteric fractures of the femur. A randomised prospective trial comparing the Jewett nail-plate with the dynamic hip screw. The Journal of Bone and Joint Surgery (British)*, **68-B**(4), pp. 557–560. 27

Evans, E.M., 1949. *The Treatment of Trochanteric Fractures of the Femur. The Journal of Bone and Joint Surgery (British)*, **31-B**(2), pp. 190–203. 8

Fielding, J.W., Wilson, S.A. and Ratzan, S., 1974. *A Continuing End-Result Study of Displaced Intracapsular Fractures of the Neck of the Femur Treated with the Pugh Nail. The Journal of Bone and Joint Surgery (American)*, **56**(7), pp. 1464–1472. 16, 17

Gardner, M.P., Chong, A.C.M., Pollock, A.G. and Wooley, P.H., 2010. *Mechanical Evaluation of Large-Size Fourth-Generation Composite Femur and Tibia Models. Annals of Biomedical Engineering*, **38**(3), pp. 613–620. 43

Goffin, J.M., Pankaj, P. and Simpson, A.H., 2014. *Are plasticity models required to predict relative risk of lag screw cut-out in finite element models of trochanteric fracture fixation? Journal of Biomechanics*, **47**(1), pp. 323–328. xi, 42, 172, 176

Gotfried, Y., 1994. *EP0617927A1.pdf.* 110, 178

Gotfried, Y., 2000. *Percutaneous Compression Plating of Intertrochanteric Hip Fractures. Journal of Orthopaedic Trauma*, **14**(7). 20, 26, 177

Greenbaum, M. and Kanat, I., 1993. *Current concepts in bone healing. Review of the literature. Journal of the American Podiatric Medical Association*, **83**(3), pp. 123 –129. 11, 12

Grundnes, O. and Reikers, O., 1993. *Effects of instability on bone healing: Femoral osteotomies studied in rats. Acta Orthop*, **64**(1), pp. 55–58. 13

Gullberg, B., Johnell, O. and Kanis, J., 1997. *World-wide Projections for Hip Fracture. Osteoporosis International*, **7**(5), pp. 407–413. 1, 9

Haentjens, P., Lamraski, G. and Boonen, S., 2005. *Costs and consequences of hip fracture occurrence in old age: An economic perspective. Disability & Rehabilitation*, **27**(18-19), pp. 1129–1141. 1, 9

Harrington, K.D. and Johnston, J.O., 1973. *The Management of Comminuted Unstable Intertrochanteric Fractures. The Journal of Bone and Joint Surgery (American)*, **55**(7), pp. 1367–1376. 34

Hata, Y., Saitoh, S., Murakami, N., Seki, H., Nakatsuchi, Y. and Takaoka, K., 2001. *A less invasive surgery for rotator cuff tear: Mini-open repair. Journal of Shoulder and Elbow Surgery*, **10**(1), pp. 11–16. 1, 24, 184

Health service Bergen, 2010. *National Arthroplasty, Cruciate Ligament and Hip Fracture Registry: Annual Report 2010.* 24, 32, 184

Heiner, A., 2008. *Structural properties of fourth-generation composite femurs and tibias. Journal of biomechanics*, **41**(15), pp. 3282–3284. 43, 44

Hoppenfeld, S. and Murthy, V.L., 2000. *Treatment and Rehabilitation of Fractures.* Lippincott Williams & Wilkins. 93

Hrubina, M., Hork, Z., Bartoka, R., Navrtil, L. and Rosina, J., 2013. *Computational modeling in the prediction of Dynamic Hip Screw failure in proximal femoral fractures. Journal of Applied Biomedicine*, **11**(3), pp. 143–151. xi, 42, 168, 171

IHFD, 2014. *Irish Hip Fracture Database - National Report 2014.* 24

Jensen, J.S., 1978a. *A Photoelastic Study of a Model of the Proximal Femur: A Biomechanical Study of Unstable Trochanteric Fractures. Acta Orthop*, **49**(1), pp. 54–59. 34

Jensen, J.S., 1978b. *A Photoelastic Study of the Hip Nail-Plate in Unstable Trochanteric Fractures: A Biomechanical Study of Unstable Trochanteric Fractures II. Acta Orthop*, **49**(1), pp. 60–64. 34

Jensen, J.S., 1980a. *Classification of Trochanteric Fractures. Acta Orthop*, **51**(1-6), pp. 803–810. 8

Jensen, J.S., 1980b. *Mechanical Strength of Jewett and McLaughlin hip Nail Plates Manufactured from Cobalt-Chromium-Molybdenum Alloy: A Biomechanical Study of Unstable Trochanteric Fractures. IV. Acta Orthop*, **51**(1-6), pp. 145–156. 34

Jensen, J.S., 1980c. *Mechanical Strength of McLaughlin hip NailPlates Manufactured from 316 Lvm Stainless Steel: A Biomechanical Study of Unstable Trochanteric Fractures. V. Acta Orthop*, **51**(1-6), pp. 439–444. 34

Jensen, J.S., 1980d. *Mechanical Strength of Sliding Screw-Plate hip Implants: A Biomechanical Study of Unstable Trochanteric Fractures. VI. Acta Orthop*, **51**(1-6), pp. 625–631. 34

Jensen, J.S., Sonne-Holm, S. and Tøbndevold, E., 1980a. *Unstable Trochanteric Fractures: A Comparative Analysis of Four Methods of Internal Fixation. Acta Orthop*, **51**(1-6), pp. 949–962. 27

Jensen, J.S., Tøndevold, E. and Mossing, N., 1978. *Unstable Trochanteric Fractures Treated with the Sliding Screw-Plate System: A Biomechanical Study of Unstable Trochanteric Fractures III. Acta Orthop*, **49**(4), pp. 392–397. 27, 34

Jensen, J.S., Tøndevold, E. and Sonne-Holm, S., 1980b. *Stable Trochanteric Fractures. A Comparative Analysis of four Methods of Internal Fixation. Acta Orthop*, **51**(1-6), pp. 811–816. 27

Jewett, E.L., 1941. *One-Piece Angle Nail for Trochanteric Fractures. The Journal of Bone and Joint Surgery (American)*, **23**(4), pp. 803–810. vii, 15

Keyak, J.H., Rossi, S.A., Jones, K.A., Les, C.M. and Skinner, H.B., 2001. *Prediction of fracture location in the proximal femur using finite element models. Medical Engineering & Physics*, **23**(9), pp. 657–664. 40

Kitchens, D.G., 2005. *US6916323.pdf*. 26

Koval, K.J., Sala, D.A., Kummer, F.J. and Zuckerman, J.D., 1998. *Postoperative Weight-Bearing after a Fracture of the Femoral Neck or an Intertrochanteric Fracture. The Journal of Bone & Joint Surgery*, **80**(3), pp. 352–6. 93, 156

Krischak, G., Augat, P., Beck, A., Arand, M., Baier, B., Blakytny, R., Gebhard, F. and Claes, L., 2007. *Biomechanical comparison of two side plate fixation techniques in an unstable intertrochanteric osteotomy model: Sliding Hip Screw and Percutaneous Compression Plate. Clinical Biomechanics*, **22**(10), pp. 1112–1118. viii, 34, 36

Kuntscher, G. and Maatz, R., 1945. *The Technique of Intramedullary Nailing*. Kiel University Hospital, Germany: Georg Thieme Publishers Leipzig. 18

Kyle, R.F., 1984. *US4438762.pdf*. 26, 110, 178

Leong, P. and Morgan, E., 2008. *Measurement of fracture callus material properties via nanoindentation. Acta Biomaterialia*, **4**(5), pp. 1569–1575. 67, 68

Markel, M.D., Wikenheiser, M.A. and Chao, E.Y.S., 1990. *A study of fracture callus material properties: Relationship to the torsional strength of bone. Journal of Orthopaedic Research*, **8**(6), pp. 843–850. 67, 68

Matre, K., Havelin, L.I., Gjertsen, J.E., Espehaug, B. and Fevang, J.M., 2013. *Intramedullary Nails Result in More Reoperations Than Sliding Hip Screws in Two-part Intertrochanteric Fractures. Clinical Orthopaedics and Related Research*, **471**(4), pp. 1379–1386. 31, 32, 39, 106

Morris, H.D., 1941. *Trochanteric Fractures. Southern Medical Journal*, **34**(6). 13

Murray, R.C. and Frew, J.F.M., 1949. *Trochanteric Fractures of the Femur: A Plea for Conservative Treatment. The Journal of Bone and Joint Surgery (British)*, **31-B**(2), pp. 204–219. 13

NICE, 2014. *Guideline 124: Hip fracture - The management of hip fracture in adults*. 24, 32

Oken, O.F., Soydan, Z., Yildirim, A.O., Gulcek, M., Ozlu, K. and Ucaner, A., 2011. *Performance of modified anatomic plates is comparable to proximal femoral nail, dynamic hip screw and anatomic plates: Finite element and biomechanical testing. Injury*, **42**(10), pp. 1077–1083. 40

Olsson, O., Kummer, F.J., Ceder, L., Koval, K.J., Larsson, S. and Zuckerman, J.D., 1998. *The Medoff sliding plate and a standard sliding hip screw for unstable intertrochanteric fractures: A mechanical comparison in cadaver femurs. Acta Orthop*, **69**(3), pp. 266–272. 20

Parker, M.J. and Handoll, H.H., 2009a. *Condylocephalic nails versus extramedullary implants for extracapsular hip fractures*. In *The Cochrane Library*. John Wiley & Sons, Ltd. 28, 30, 166

Parker, M.J. and Handoll, H.H., 2009b. *Extramedullary fixation implants and external fixators for extracapsular hip fractures in adults*. In *The Cochrane Library*. John Wiley & Sons, Ltd. 28, 29

Parker, M.J. and Handoll, H.H., 2010. *Gamma and other cephalocondylic intramedullary nails versus extramedullary implants for extracapsular hip fractures in adults*. In *The Cochrane Library*. John Wiley & Sons, Ltd. 28, 30, 31, 32

Paul, J.P., 1966. *Forces transmitted by joints in the human body. ARCHIVE: Proceedings of the Institution of Mechanical Engineers, Conference Proceedings 1964-1970 (vols 178-184), Various titles labelled Volumes A to S*, **181**(310), pp. 8–15. 74

Paul, J.P., 1967. *Forces at the human hip joint*. Ph.D. thesis, University of Glasgow, Glasgow. 34

Paul, J.P., 1976. *Force Actions Transmitted by Joints in the Human Body. Proceedings of the Royal Society of London. Series B. Biological Sciences*, **192**(1107), pp. 163 –172. 34

Peleg, E., Beek, M., Joskowicz, L., Liebergall, M., Mosheiff, R. and Whyne, C., 2010. *Patient specific quantitative analysis of fracture fixation in the proximal femur implementing principal strain ratios. Method and experimental validation. Journal of Biomechanics*, **43**(14), pp. 2684–2688. 41

Peleg, E., Mosheiff, R., Liebergall, M. and Mattan, Y., 2006. *A short plate compression screw with diagonal bolts: A biomechanical evaluation performed experimentally and by numerical computation. Clinical Biomechanics*, **21**(9), pp. 963–968. 38

Pugh, S., 1991. *Total Design: Integrated Methods for Successful Product Engineering*. Addison-Wesley Publishing Company. 45, 109

Pugh, W.L., 1955. *A Self-Adjusting Nail-Plate for Fractures About the Hip Joint. The Journal of Bone and Joint Surgery (American)*, **37**(5), pp. 1085–1093. vii, 16

Putti, V., 1940. *Cura operatoria delle fratture del collo del femore. Journal of the American Medical Association*, **115**(8), p. 640. vii, 14, 38

Rooppakhun, S., Chantarapanich, N., Chernchujit, B., Mahaisavariya, B., Sucharitpwatskul, S. and Sitthiseripratip, K., 2010. *Mechanical Evaluation of Stainless Steel and Titanium Dynamic Hip Screw (DHS) for Trochanteric Fracture. WASET*, (69), pp. 662–665. xi, 42, 68, 169, 173, 174

Ropars, M., Mitton, D. and Skalli, W., 2008. *Minimally invasive screw plates for surgery of unstable intertrochanteric femoral fractures: A biomechanical comparative study. Clinical Biomechanics*, **23**(8), pp. 1012–1017. viii, 23, 26, 178

Royal College of Physicians, 2013. *The National Hip Fracture Database annual report 2013*, London: RCP. 32, 184

Royal College of Physicians, 2014. *National Hip Fracture Database extended report 2014*, London: RCP. 24, 32, 184

Schipper, I., Marti, R. and van der Werken, C., 2004. *Unstable trochanteric femoral fractures: extramedullary or intramedullary fixation: Review of literature. Injury*, **35**(2), pp. 142–151. 32

Schumpelick, W. and Jantzen, 1955. *A New Principle in the Operative Treatment of Trochanteric Fractures of the Femur. The Journal of Bone and Joint Surgery (American)*, **37**(4), pp. 693–698. vii, 17, 18, 27

Sim, E., Freimller, W. and Reiter, T., 1995. *Finite element analysis of the stress distributions in the proximal end of the femur after stabilization of a pertrochanteric model fracture: a comparison of two implants. Injury*, **26**(7), pp. 445–449. 41, 42, 43

Strømsøe, K., Kok, W.L., Høiseth, A. and Alho, A., 1993. *Holding power of the 4.5 mm AO/ASIF cortex screw in cortical bone in relation to bone mineral. Injury*, **24**(10), pp. 656–659. 85

Taheri, N.S., Blicblau, A.S. and Singh, M., 2011. *Comparative study of two materials for dynamic hip screw during fall and gait loading: titanium alloy and stainless steel. Journal of Orthopaedic Science*, **16**(6), pp. 805–813. 39

Taheri, N.S., Blicblau, A.S. and Singh, M., 2012. *Effect of different load conditions on a DHS implanted human femur. Journal of Engineering Technology (JET)*, **1**(1). 40

Tan, C.K. and Wong, W.C., 1990. *Absence of the ligament of head of femur in the human hip joint. Singapore medical journal*, **31**(4), pp. 360–363. 4

Waddell, J., McMullan, J., Lo, N., O'Conner, M., Sheppard, L., Mensour, M., Palda, V. and McGlasson, R., 2010. *Improving Time to Surgery - Emergency Room, Preoperative and Immediate Postoperative Clinical Practice Guidelines for the Management of Hip Fracture Patients*, Bone and Joint Health Network, Canada. 24, 33

Willoughby, R., 2005. *Dynamic hip screw in the management of reverse obliquity intertrochanteric neck of femur fractures. Injury*, **36**(1), pp. 105–109. 1

Wong, T.C., Chiu, Y., Tsang, W.L., Leung, W.Y. and Yeung, S.H., 2009. *A double-blind, prospective, randomised, controlled clinical trial of minimally invasive dynamic hip screw fixation of intertrochanteric fractures. Injury*, **40**(4), pp. 422–427. viii, ix, 1, 24, 25, 112, 184

Wu, C.C. and Tai, C.L., 2009. *Reconstruction interlocking nails for ipsilateral femoral neck and shaft fractures: Biomechanical analysis of effect of supplementary cannulated screw on intracapsular femoral neck fracture. Clinical Biomechanics*, **24**(8), pp. 642–647. 44

Younge, A.M., 2011. *Computational and Experimental Modelling of the Femur*. Ph.D. thesis, Imperial College London, London. 52, 58

Zdero, R., Rose, S., Schemitsch, E.H. and Papini, M., 2006. *Cortical Screw Pullout Strength and Effective Shear Stress in Synthetic Third Generation Composite Femurs. Journal of Biomechanical Engineering*, **129**(2), pp. 289–293. 85